Characterisation and Modelling of a Fractured Crystalline Aquifer Contaminated with Hydrocarbons

2003-12-20

Department of Geology
Faculty of Natural and Agricultural Sciences
University of Pretoria
Pretoria

Michael David Sole

Abstract

A-1 Jet fuel leaked into the environment through a pipeline near Movements 2 in Louis Trichardt Air Force Base. The duration of fuel spillage continued for approximately 15 years resulting in a free phase pollution plume of approximately 750m in length and 250m in width. The free phase plume attained a maximum apparent thickness of 10.2m. This is currently the largest hydrocarbon pollution event in South African history. An investigation commenced during December 2000, which had the following broad objectives: determine the lateral extent of free phase and dissolved contaminants, prevent the spreading of contaminants and determine the most efficient method to rehabilitate the environment. A total of 67 boreholes were drilled in a phased approach following various geophysical surveys. A numerical model was developed to evaluate the extent and migration of dissolved contaminants. Monitoring of the plume though water quality samples indicate that low levels of pollution are present adjacent to the free phase plume. The available data and numerical model indicate that pollution is restricted to the air force base. Current remedial measures include the bailing of fuel from selected boreholes, which will be replaced by a pump-and-treat system.

Table of Contents

List of Figures

List of Tables

List of Appendices

Abbreviations

AFB	Air Force Base
BH	Prefix for boreholes drilled during this investigation
BR	Prefix for boreholes drilled during the Africon (1999) investigation
BTEX	Benzene, toluene, ethyl-benzene and xylene
COD	Chemical oxygen demand
DEAT	Department of Environmental Affairs and Tourism
DO	Dissolved oxygen
DWAF	Department of Water Affairs and Forestry
EC	Electrical conductivity
emrl	Environmental Modeling Research Laboratory
FDEM	Frequency Domain Electromagnetic geophysical survey
GMS	Groundwater Modeling System
h	Actual LNAPL thickness in adjacent aquifer
H	Apparent LNAPL thickness in borehole
IP	Induced Polarization
LNAPL	Light Non-Aqueous Phase Liquid
L.T.AFB	Louis Trichardt Air Force Base
mamsl	metres above mean sea level
MAP	Mean Annual Precipitation
mbgl	metres below ground level
PAH	Polycyclic aromatic hydrocarbons
RBCA	Risk Based Corrective Action
RMSE	Root Mean Square Error
SACS	South African Council for Stratigraphy
SMZ	Southern Marginal Zone of the Limpopo Belt
SWL	Static water level
SVOC	Semi-volatile organic compound
TDEM	Time Domain Electromagnetic geophysical survey
VOC	Volatile organic compound

Acknowledgements

I would like to thank the following people and institutions, for whom without this thesis would not have been possible:

- Dr. Louis van Rooy, from the University of Pretoria for his mentorship.
- Mr. Reynie Reyneke, from Geopollution Technologies for his time, guidance and expertise.
- The Department of Public Works for permitting the usage of information and data.
- The Department of Water Affairs and Forestry for allowing time off to complete the dissertation.
- Mr. Gert van Niekerk from VNM and Associates for making the data available.
- Mr. Anthony Erasmus from VNM and Associates for collecting and verifying data.

1. Introduction

1.1 Background

A-1 Jet fuel leaked into the environment from an underground pipeline at Louis Trichardt Air Force Base (L.T.AFB). The jet fuel is transported from Granite railway station to the Air Force Base (AFB) via a high-pressure pipeline. The leak occurred near Movements 2 due to a welding error at a joint in the pipeline used to transport fuel between reservoirs within the AFB. The leak had probably been in existence since the commissioning of the pipeline approximately 15 years ago.

The leak was detected once a system was installed to measure volumes of fuel at input and output points along the pipelines. The volume of fuel pumped into the pipeline that passes Movements 2 did not correspond with the volume of fuel that exited the pipeline, as well as pressure gauges indicated a decrease in pressure when fuel was not being pumped. An investigation was conducted by means of a soil vapour survey, which detected the location of the leak. The pipe was subsequently excavated and the hole repaired on the 25th July 2000.

The quantity of fuel present within the environment can only be estimated, however it is the largest hydrocarbon pollution event encountered to date within South Africa. Pressure tests were conducted prior to the leak being repaired to estimate the rate of fuel loss. For a leak of 3mm in diameter at 500kPa the fuel loss is estimated at 8ℓ/min. It is difficult to estimate the total volume of fuel leaked into the environment, as fuel was not pumped continuously through the pipeline.

The AFB and Makhado (Louis Trichardt) utilise ground water for domestic purposes. The water is abstracted primarily from aquifers adjacent to the Sand River. The AFB supplements this water supply with ground water from secondary aquifers on the base. A rural settlement located to the north of the AFB also utilises ground water for domestic purposes. A major concern was the risk associated with contaminants polluting the Sand River aquifer and secondary aquifers currently utilised within and north of the AFB.

VNM and Associates was awarded the contract to rehabilitate the environment following the contamination. The Department of Public Works was responsible for providing financing for the rehabilitation as owner of the property and the pollution was caused by faulty infrastructure. The Department of Environmental Affairs and Tourism (DEAT) and the Department of Water Affairs and Forestry (DWAF) were the regulators responsible for monitoring the progress of rehabilitation.

1.2 Location

The Air Force Base (AFB) is situated in the Limpopo Province of South Africa approximately 25km south west of Makhado (Louis Trichardt) and 80km north-northeast of Polokwane (Pietersburg) (Figure 1).

1.3 Objectives

The objective of the project is to rehabilitate the ground water in accordance with Section 19(2) of the National Water Act (Act No. 36 of 1998), thus to achieve the following relevant measures:

(a) cease, modify or control any act or process causing the pollution;
(b) comply with any prescribed waste standard or management practice;
(c) contain or prevent the movement of pollutants;
(d) eliminate any source of the pollution; and
(e) remedy the effects of the pollution.

The aim of the dissertation is to provide a documented account of the approach and methods adopted to rehabilitate the environment. At present there is no standard or guideline published with which to manage pollution occurrences of such magnitude, which is one of the measures mentioned in Section 19(2) point (b) of the National Water Act. The dissertation will hopefully be used as a guideline or for the development of a guideline for the efficient and economical remediation of ground water pollution.

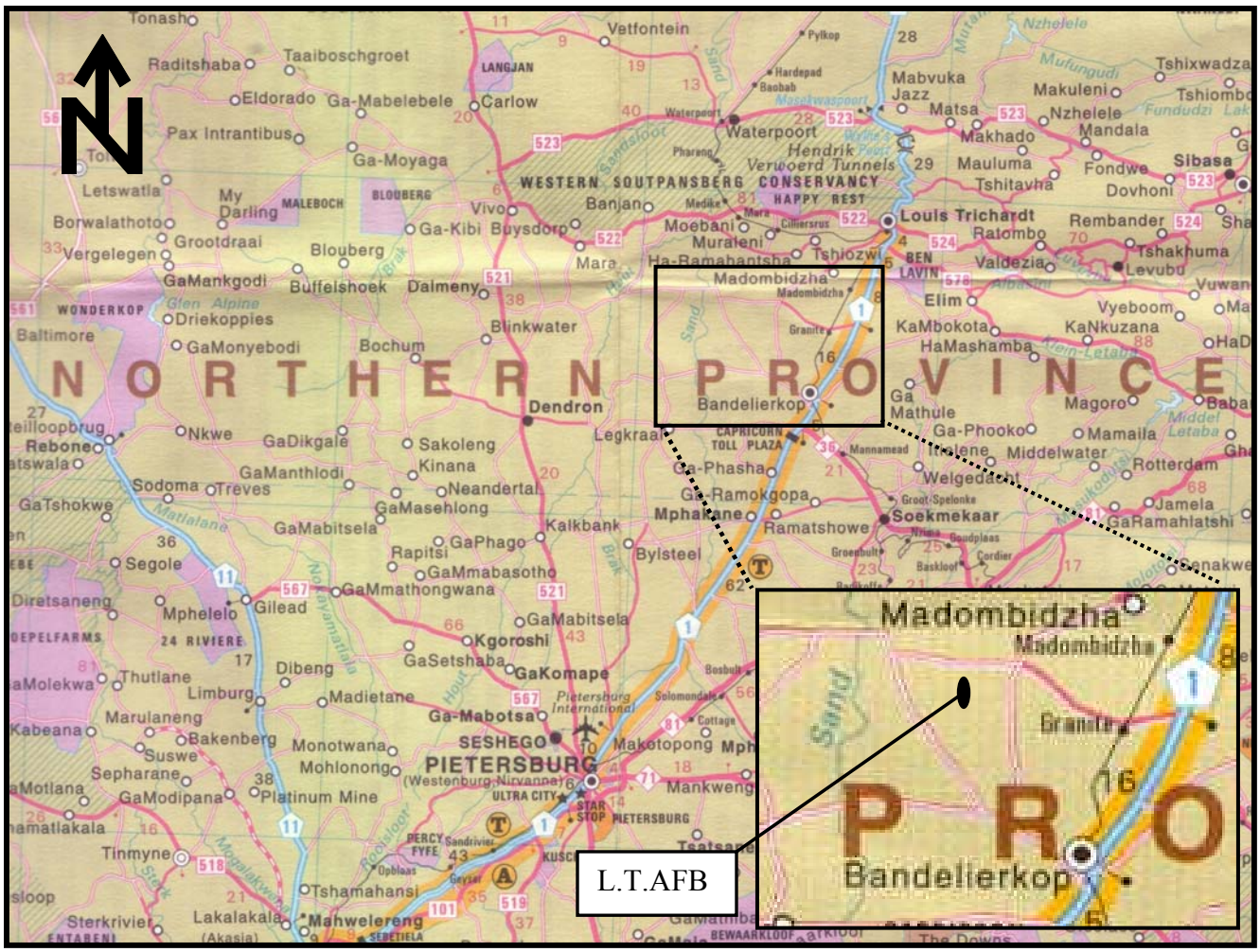

FIGURE 1: Locality map of the study area.

1.4 Scope

The following dissertation is a requirement for a Masters Degree in Engineering and Environmental Geology at the University of Pretoria. The dissertation provides an overview of the characterisation and remediation measures that were implemented to rehabilitate the contaminated aquifer. The data presented was collected between the commencement of the project in December 2000 and the finalisation of the dissertation in December 2003. The following aspects are covered in order to achieve the objectives mentioned:

1. Information on contaminant properties and method of transport.
2. Collection and evaluation of all applicable information and data.
3. Geophysical interpretation and drilling results.

4. Hydraulic testing of boreholes (slug and aquifer test results).
5. Aquifer classification and conceptualisation.
6. Plume monitoring through water quality analysis.
7. Numerical modelling: prospective evaluation of plume.
8. Emergency rehabilitation method and results.
9. Implementation of final remediation measures.

2. Literature Review

2.1 Introduction

The nature of the contaminant as well as the various modes of transport are discussed in this chapter. The properties of contaminants are important when modelling pollution plumes, as different transport mechanisms are more important than others for different pollutants.
The topics are discussed broadly and are intended for the reader with a limited knowledge of contaminant behaviour within an aquifer.

2.2 Contaminant Properties

A-1 Jet Fuel, also known as Aviation Kerosene, Aviation Turbine Fuel Jet A, Jet A, Jet A-1, JP-1 or Military Aviation Jet Fuel JP-1, is composed essentially of 100% by weight of kerosene and typically 0.04% naphthalene (Bucknam, 2000).

Jet fuel originates from "crude oil" pumped out of the ground, which is a black liquid known as petroleum. This liquid contains aliphatic hydrocarbons, or hydrocarbons composed of nothing but hydrogen and carbon. The carbon atoms link together in chains of different lengths that have different properties and behaviours. For example, a chain with just one carbon atom in it (CH4) is the lightest chain, known as methane. As the chains get longer, they get heavier.

The first four chains – CH4 (methane), C2H6 (ethane), C3H8 (propane) and C4H10 (butane) – are all gases, and they boil at –107, -67, -43 and –18 degrees C respectively. The chains through to C18H32 or so are all liquids at room temperature, and the chains above C19 are all solids at room temperature. The different chain lengths have progressively higher boiling points, so they can be separated by the distillation of crude oil at oil refineries by their different vaporisation temperatures.

Being kerosene-based, jet fuel consists primarily of hydrocarbon compounds ranging from 9 to 16 carbons in length that are either (McBride, 1999):

- volatile organic compounds (VOCs), or
- semi-volatile organic compounds (SVOCs).

The hydrocarbons present in jet fuel are essentially alkanes, cycloalkanes, alkenes and very low concentrations of aromatic hydrocarbons (e.g. BTEX: benzene, toluene, ethyl-benzene and xylene) and polycyclic aromatic hydrocarbons (PAHs, e.g. chrysene and benzo(a)pyrene). Additives such as metal deactivators, antioxidants and octane boosters are also added (McBride, 1999). Figure 2 shows a gas chromatogram for the individual hydrocarbon products.

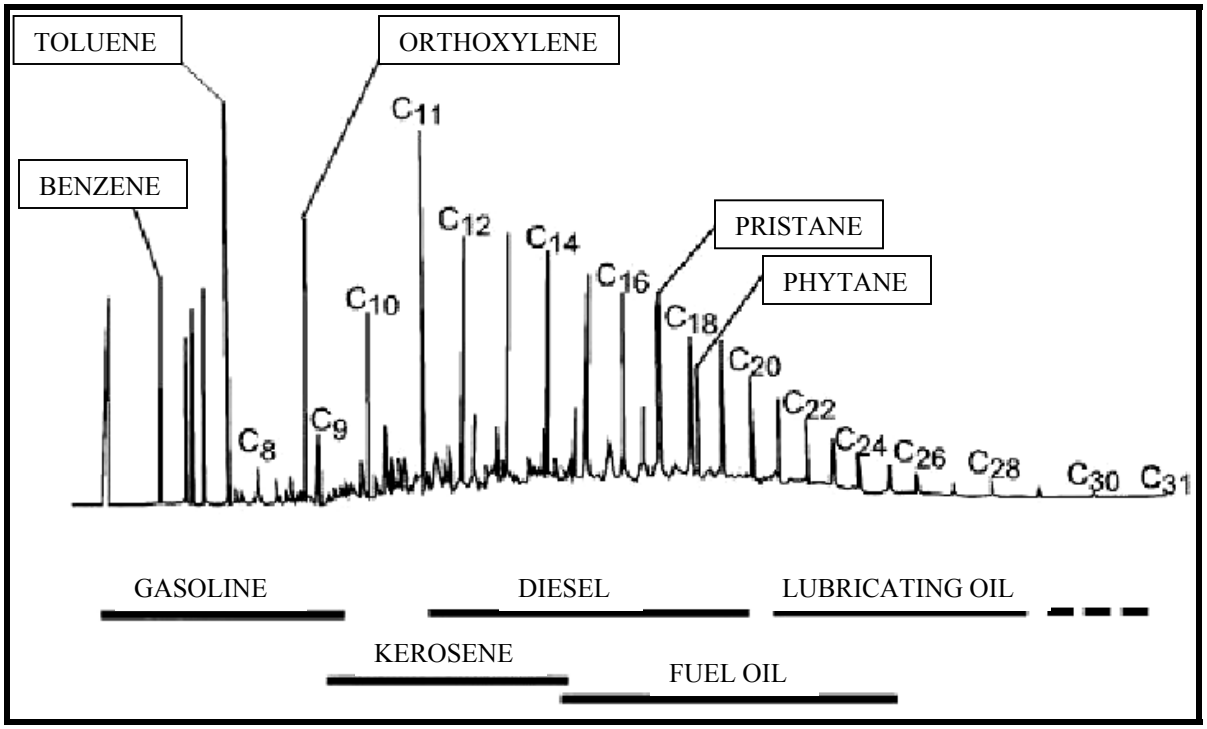

FIGURE 2: Gas chromatogram showing approximate ranges for individual hydrocarbon products. Jet A-1 Fuel is essentially kerosene (EPA, 1996).

A-1 Jet Fuel is less dense and generally more viscous, than water. It is immiscible and appears as a separate phase on top of water. Such liquids that are immiscible in water are referred to as light non-aqueous phase liquids or LNAPLs. They tend to "float" on the ground water and subsequent lateral migration depends on the hydraulic gradient as shown in Figure 3 (Testa *et al*, 1991 & Fetter, 1999).

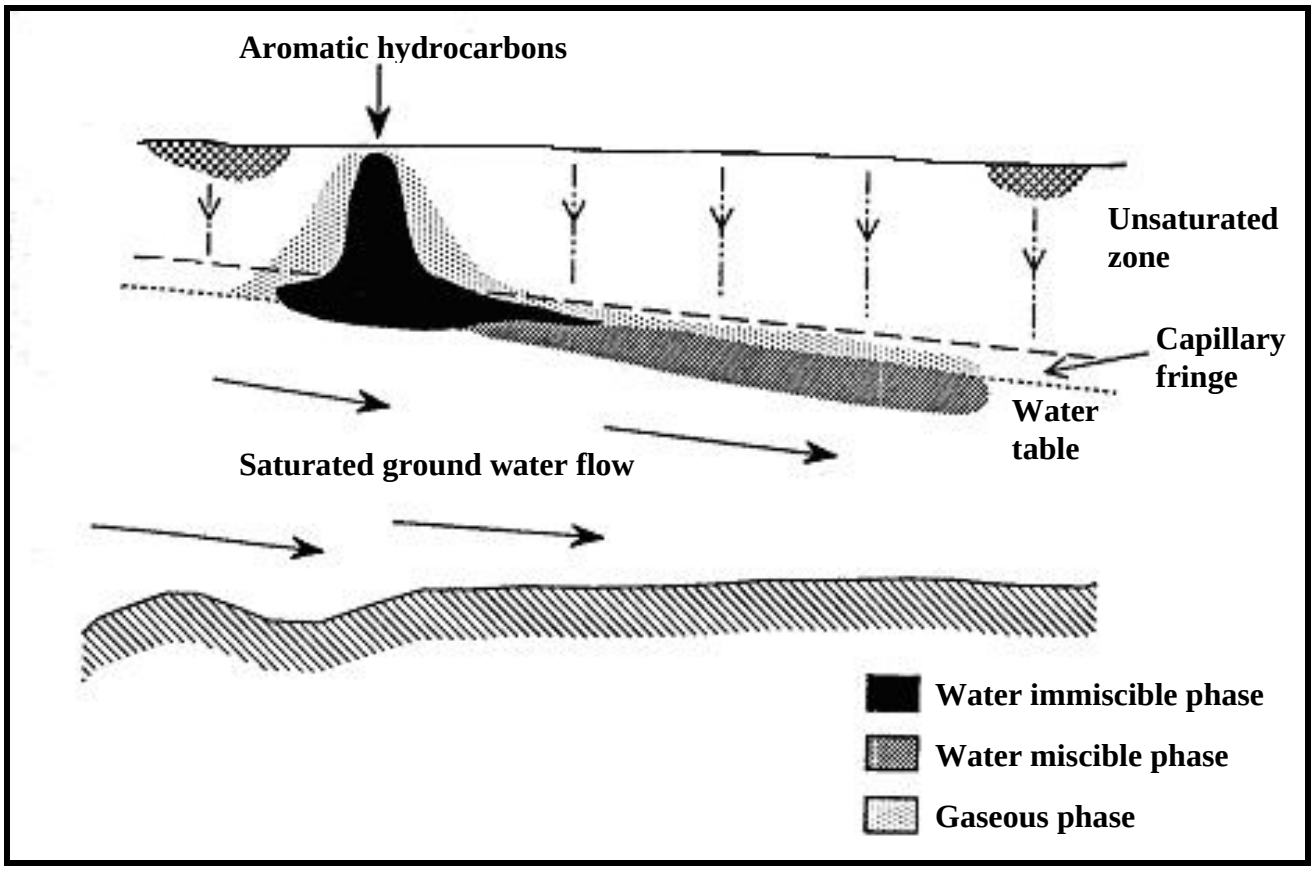

FIGURE 3: Generalised Distribution of hydrocarbon Phases down a Ground Water gradient following a surface spillage.

Table 1 indicates some physical and chemical properties of A-1 Jet Fuel and Table 2 compares the characteristics of the main pollutants found in the polluted ground water on the AFB.

TABLE 1: Typical values for some physical and chemical properties of A-1 Jet Fuel (Dippenaar, 2002).

Property	***Value***
Flash point	> 38°C
Auto-ignition point	210°C
Boiling range	140 – 300°C
Vapour pressure	0.029 psia
Specific gravity (H_2O = 1)	0.834 (for 100% kerosene)
Viscosity @ 20°C	4.47cSt
Percentage volatiles	~ 100%
Percentage aromatics	16.3% by volume
Evaporation rate	Slow

TABLE 2: Characteristics of priority pollutants found in the ground water at L.T.AFB (Sole, 2001).

Pollutant / Constituent	***Density ($g.cm^{-3}$)***	***Viscosity (cp)***	***Solubility***	***Vapour pressure (mmHg)***	***Henry coefficient ($atm.m^3.mol^{-1}$)***
Aromatic Compounds (BTEX)					
Benzene (benzol)	0.879	0.6028	820, 1750	60	$2.67E^{-3} – 5.3E^{-3}$
Toluene	0.867	0.552	470	10	$5.7E^{-3}$
Ethyl benzene	0.0866	0.678	140	7	$5.7E^{-3} – 6.6\ E^{-3}$
Polyaromatic hydrocarbons (PAH)					
Naphthalene	1.326	0.45	16,700;20,200	362	$2E^{-3} – 2.5E^{-3}$
Acenaphthalene			3.93	$1E^{-2}$	$1.9E^{-4}$, $1.45E^{-3}$
Fluorene	1.203		1.69 – 1.98	$1E^{-4}$	$2.1E^{-4}$, $6.4E^{-5}$
Phenanthrene	1.978		5	$1E^{-4}$	$2.1E^{-6} – 2.8E^{-6}$
Pyrene	1.07	4.076	82000	0.2 – 0.53	$2.7E^{-7} – 4.5E^{-7}$
Benz(a)anthracene			0.01 – 0.057	$5E^{-5}$	$1E^{-6}$
NOTE: THIS DOES NOT NECESSARILY REFLECT THE TRUE COMPOSITION OF A-1 JET FUEL AS NOT ALL ITS CONSTITUENTS ARE EQUALLY WATER-SOLUBLE.					

2.3 Distinguishing sources of ground water contamination

The contaminant source can be classified as either a point or diffuse source. Point sources are contamination from a single source, such as a waste disposal site. Diffuse sources refer to the cumulative contamination caused by regional activities, such as agricultural fertilisers or pesticides used by a community. The source geometry is useful as it influences the plume evolution, dilution of contaminants, exposure of pollutants to the aquifer, which influences biodegradation and remedial measures. Figure 4 illustrates different sources of ground water contamination (Deming, 2002; Fetter, 1994).

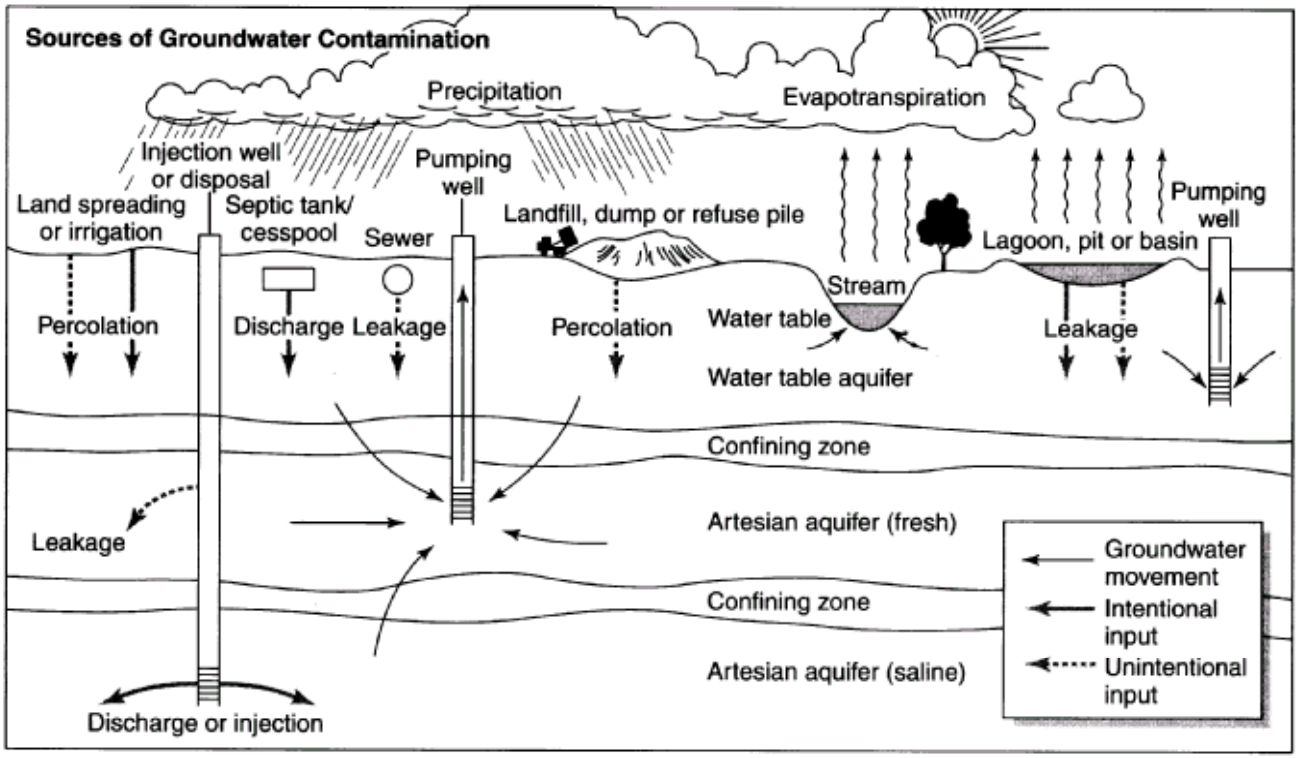

FIGURE 4: Sources of ground water contamination (EPA, 1984).

2.4 Classifying contaminants by transport behaviour

The density, viscosity, solubility, chemical stability and other characteristics of the contaminant influence the transport behaviour of contaminants in water. This is illustrated in Figure 5. The understanding of the properties of the contaminants is essential to modelling contaminant transport.

Contaminants may reach the ground water either dissolved in water (miscible) or as a liquid phase that may be immiscible in water. Miscible liquids (or dissolved contaminants) migrate through the aquifer as a single phase whereas immiscible liquids flow as a separate phase. Miscible fluids move through an aquifer according to Darcy's law (Spitz *et al*, 1996). The pollution at L.T.AFB is an example of both single and multiphase flow.

Solutes that remain stable in ground water and do not change due to physical, biological or chemical processes are described as conservative. Chloride is an example of a conservative solute and is often used as a tracer. The relationship between migration and degradation is important in classifying a contaminant as conservative or not. A contaminant that reacts and changes slowly,

but migrates in an aquifer with high transport velocities, may be considered conservative (Fetter, 1994; Spitz *et al*, 1996).

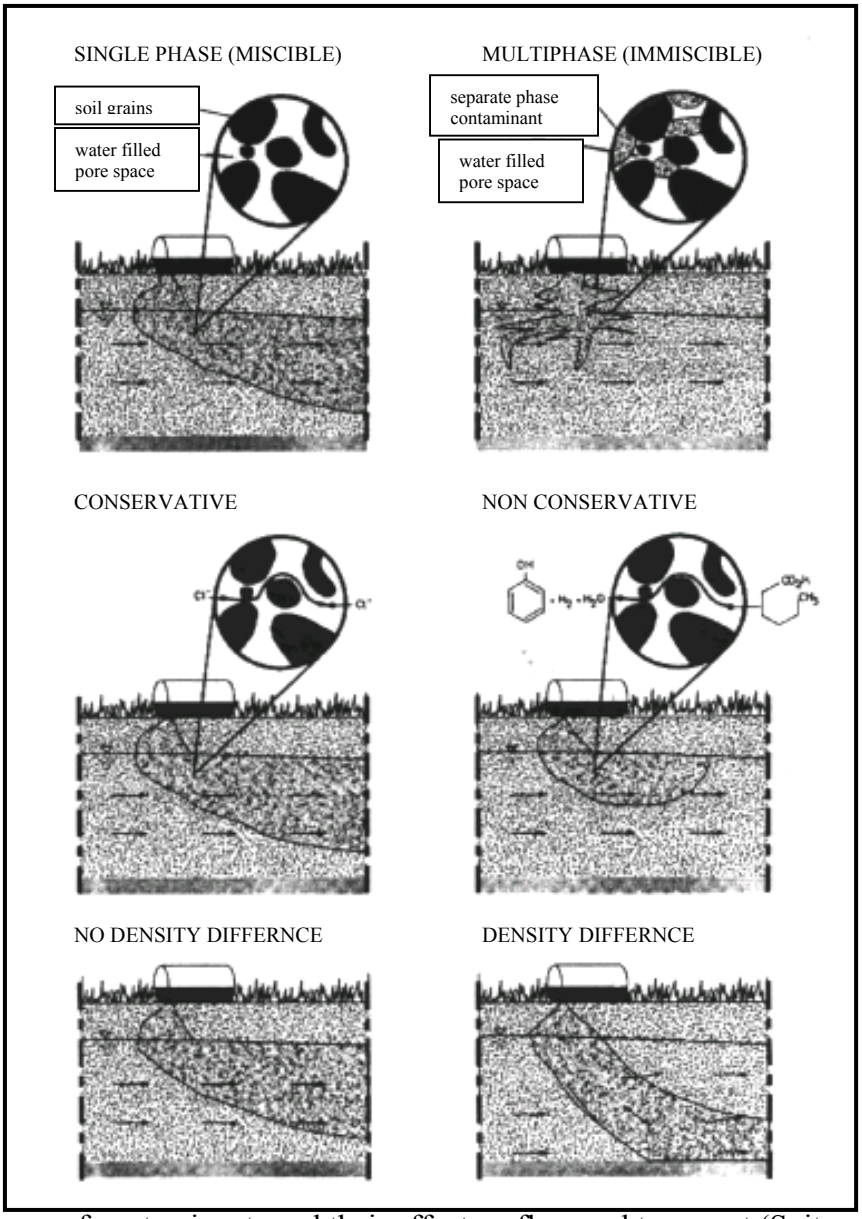

FIGURE 5: Groups of contaminants and their effect on flow and transport (Spitz *et al*, 1996).

2.5 Transport mechanisms

Contaminants are transported in ground water by three different physical processes, namely advection, dispersion and diffusion (Deming, 2002). Figure 6 illustrates the various transport mechanisms. A number of chemical and biological processes are responsible for retarding the

migration of pollutants in ground water. Sorption, decay and biodegradation are discussed briefly in the following section.

2.5.1 Advection

Advection is the movement of solutes due to the mass movement of ground water. The driving force is the hydraulic gradient. The following form of Darcy's equation determines the velocity of advective transport:

$$v = -\frac{k}{n_e}\frac{\partial h}{\partial l}$$

where v [L/T] is the linear ground water velocity, k [L/T] is the hydraulic conductivity, n_e is the effective porosity and $\partial h / \partial l$ [L/L] is the hydraulic gradient (Domenico, 1990).

2.5.2 Diffusion

Diffusion is the movement of solutes from a zone of high concentration to a zone of low concentration without fluid movement. The driving force is the random movement of ionic and molecular constituents under the influence of their kinetic activity called *Brownian motion*. Diffusion is irreversible. Once two solutions are mixed under natural conditions, they will form a single uniform solution. The global movement of solutes occurs in the direction of the concentration gradient according to Fick's Law. Fick's Law in one dimension is:

$$F = -D\frac{\partial C}{\partial x}$$

where F [M/L^2/T] is the mass flux of contaminant per unit area per time, D [L^2/T] is the diffusion coefficient and C [M/L^3] is the contaminant concentration (Deming, 2002). The negative sign indicates the movement is from greater to lesser concentrations (Fetter, 1994).

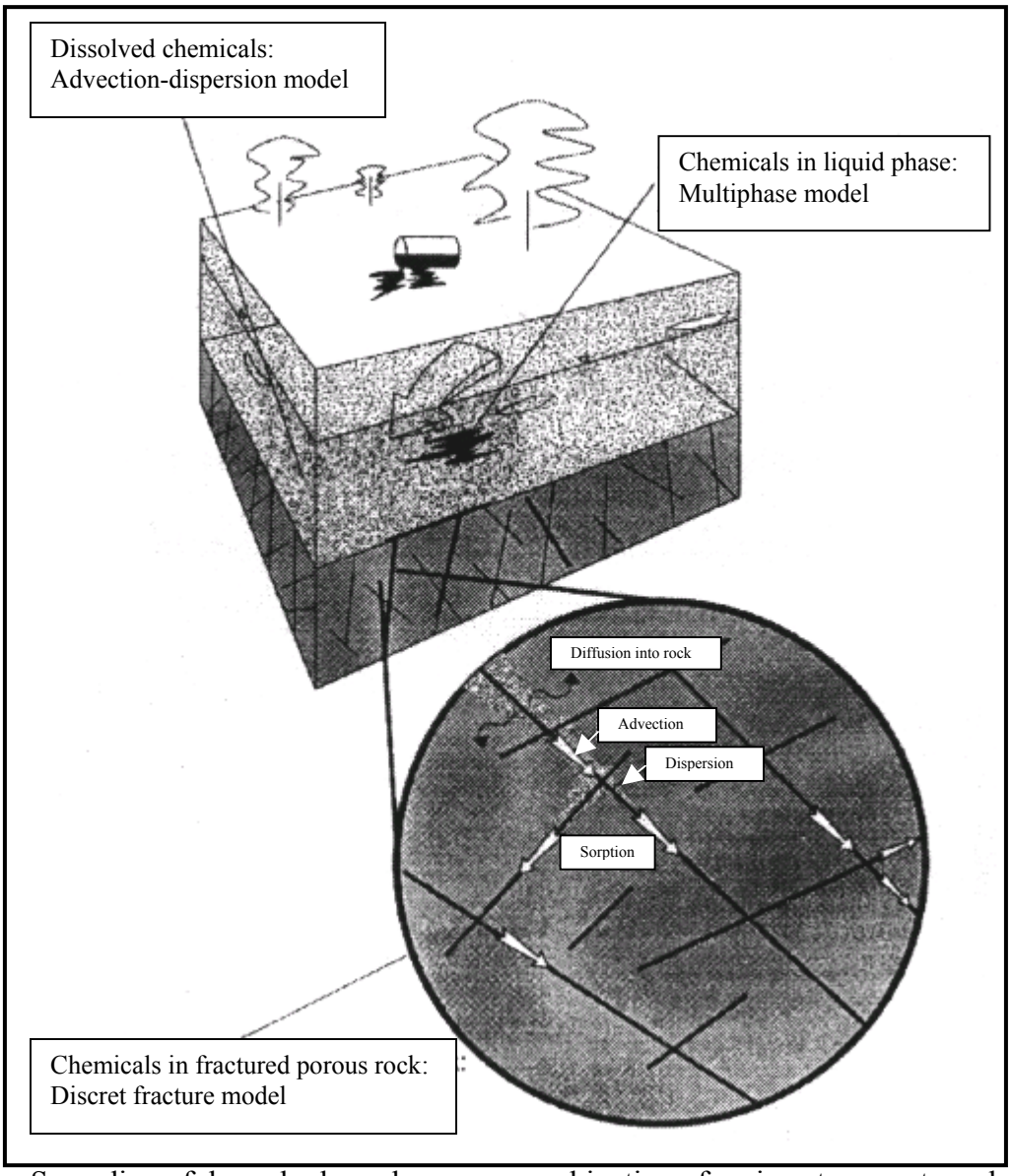

FIGURE 6: Spreading of dense hydrocarbons as a combination of various transport mechanisms (Spitz *et al*, 1996).

2.5.3 Dispersion

In dealing with contamination transport, one of the main tasks is the prediction of dispersive spreading. Dispersive spreading, within and transverse to, the main flow direction causes a gradual dilution of the contamination of the plume. In some situations when concentrations fall below the concentration values considered harmful to humans, dispersion may be a benefit. However dispersion is usually an undesirable effect due to the fast spreading of

contaminants, which increases the volume of contaminated water. Dispersion is superimposed on the average transport velocity, and it also transports contaminants into zones that do not participate directly in the advective plume evolution. Dispersion will lead to an increase in plume uniformity with travel distance (Fetter, 1994).

Mechanical dispersion in one dimension (x) can be defined mathematically as the product of the linear velocity v_x [L/T] and the longitudinal dispersivity α_L [L]. The process of diffusion and dispersion can be combined to define a longitudinal coefficient of hydrodynamic dispersion D_L [L^2/T].

$$D_L = \alpha_L v_x + D^*$$

where, D^* [L^2/T] is the effective diffusion coefficient and is defined as

$$D^* = WD$$

where, D [L^2/T] is the diffusion coefficient (Section 2.5.2) and W is a dimensionless constant determined empirically, and is usually between ≈0.01 and 0.5 for non-reactive species (Deming, 2002).

2.5.4 Sorption

Sorption refers to adsorption and desorption. Adsorption is the process when ions or molecules become attached to the surface of solid particles in the aquifer. The release from the solid phase is called *desorption*. Adsorption retards the movement of pollutants and causes a decrease of contaminant concentrations in the aqueous phase (Spitz *et al*, 1996).

The adsorption characteristics are typically plotted on a graph showing the mass of solute adsorbed per unit mass of soil as a function of the concentration of the solute. When an adsorption relationship can be plotted as a straight line on log-log paper, it is described by the Freundlich isotherm as:

$$\log C^* = b \log C + \log K_f \qquad \text{or} \qquad C^* = K_f C^j$$

where, C^* is the mass of solute sorbed per bulk unit dry mass of soil [M/ L^3]

C is the solute concentration [M/L^3]

K_f and j are coefficients

The slope of the curve plotted on log-log paper is represented by j. If a straight line is obtained when plotting C^* versus C, the relationship is linear and b has a value of one. Under these conditions, the derivative of C^* with respect to C yields the relationship

$$dC^* / dC = K_d$$

where K_d is known as the distribution coefficient (Fetter, 1994).

2.5.5 Decay

Not all contaminants that are absorbed or desorbed follow the principle of fast reactions. Reactions that are relatively slow in comparison to the average travel time of the contaminants are described by kinetics. Reactions of the first order follow the relationship:

$$\frac{\partial c}{\partial t} = -\lambda c$$

where c [M/L^3] is the concentration of contaminants and any time, t [T] is time and λ [T^{-1}] is the decay constant (Deming, 2002). Refer to Appendix A for the half-lifes of a number of organic pollutants found in the ground water at L.T.AFB.

2.5.6 Biodegradation

Biodegradation is the decomposition of organic materials by living organisms. Bacteria are the most common organisms responsible for biodegradation. The environmental conditions that influence the type and rate of reactions that take place include pH, temperature, state of oxidation or reduction, microorganisms present and types of other chemicals present. Biodegradation may be used as a remediation option depending on the nature of the contaminant as well as the aquifer. Biodegradation may however cause an increase in the concentration of other elements in the ground water (such as iron and manganese) particularly under anaerobic conditions (Deming, 2002; Fetter, 1994).

3. Site Description

3.1 Topography and Drainage

The area is characterised by flat undulating topography typical of basement complex lithologies. The topography generally decreases towards the northeast. The leakage site is situated on a localised topographic high, with the elevation decreasing at a gradient of 1:100, 1:50 and 1:70 in a northerly, north westerly and north easterly direction respectively. Due to the construction of Movements 2 and the taxiways the topography surrounding the leakage site was altered in such a way that the majority of the runoff over the leakage site is in a westerly direction towards Movements 2 as well as in a southerly direction towards drainage lines adjacent to the taxiway.

Drainage features within the AFB are poorly developed and consist mainly of shallow, narrow, non-perennial channels that drain in a northwesterly direction. Flow in these channels is of an intermittent nature and only occurs following high intensity precipitation. According to a report by Africon Inc. (1999) the area surrounding the base has a low potential for surface water storage due to a low average rainfall, relatively high infiltration rates, very low mean annual run-off, very high evaporation losses and an unsuitable topography for dam construction.

The AFB is located within the quaternary catchment A71H and is drained by the Sand River. The Sand River is situated approximately 10km west of the AFB and flows in a northerly direction into the Limpopo River.

3.2 Rainfall

Rainfall typically occurs as late afternoon thundershowers, with 91% of the rainfall occurring between September and March. The AFB receives an annual rainfall of between 181mm and 801mm, with an average of 390.9mm. The positive trend observed from Figure 7 is due to the abnormally high rainfall in 2000. Major floods occurred at the beginning of 2000, which surpassed the 1:100 year flood estimations. The average monthly rainfall for L.T.AFB and Makhado is indicated in Figure 8. The AFB receives on average 30mm less rainfall per month than Makhado.

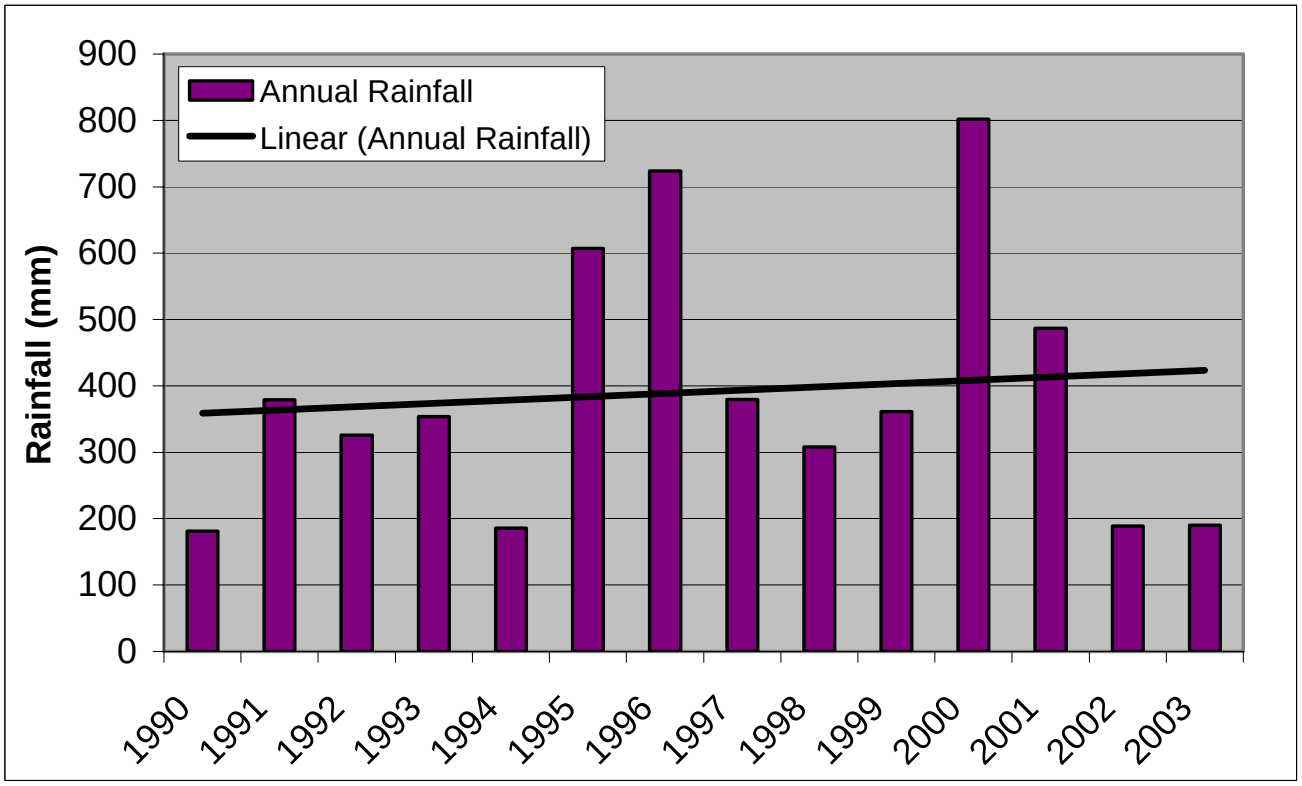

FIGURE 7: Annual rainfall for L.T.AFB (July 1990 - October 2003)

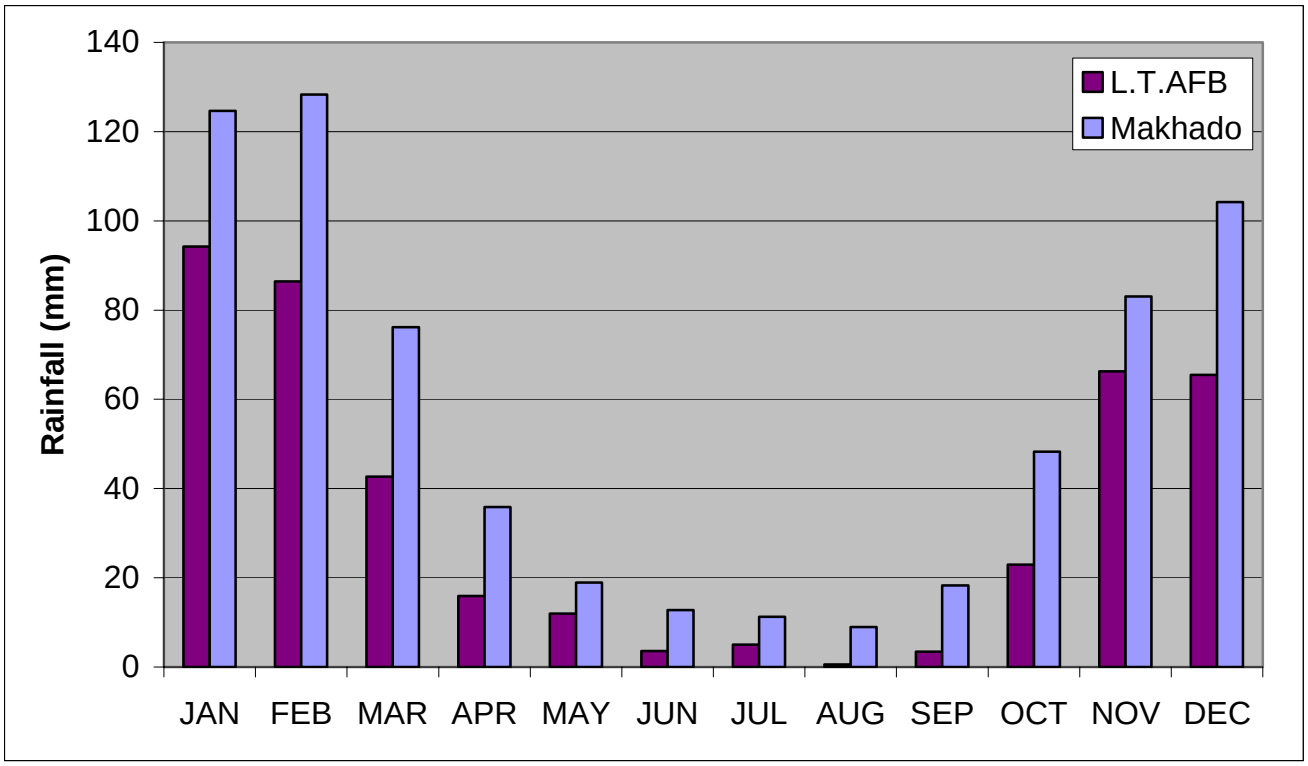

FIGURE 8: Average Monthly Rainfall for L.T.AFB and Makhado (1990-2003)

3.3 Temperature

The mean daily minimum and maximum temperatures for Makhado are illustrated in Figure 9. The readings were taken at 08:00 and the data presented is from September 1988 to July 1999.

3.4 Flora

3.4.1 Veld Type

The majority of the AFB is a nature reserve; thus the vegetation is generally undisturbed. The vegetation is described as type 14 Arid Sweet Bushveld (Acocks, 1975) and is a rather mixed shrubby type with *acacia* species dominating.

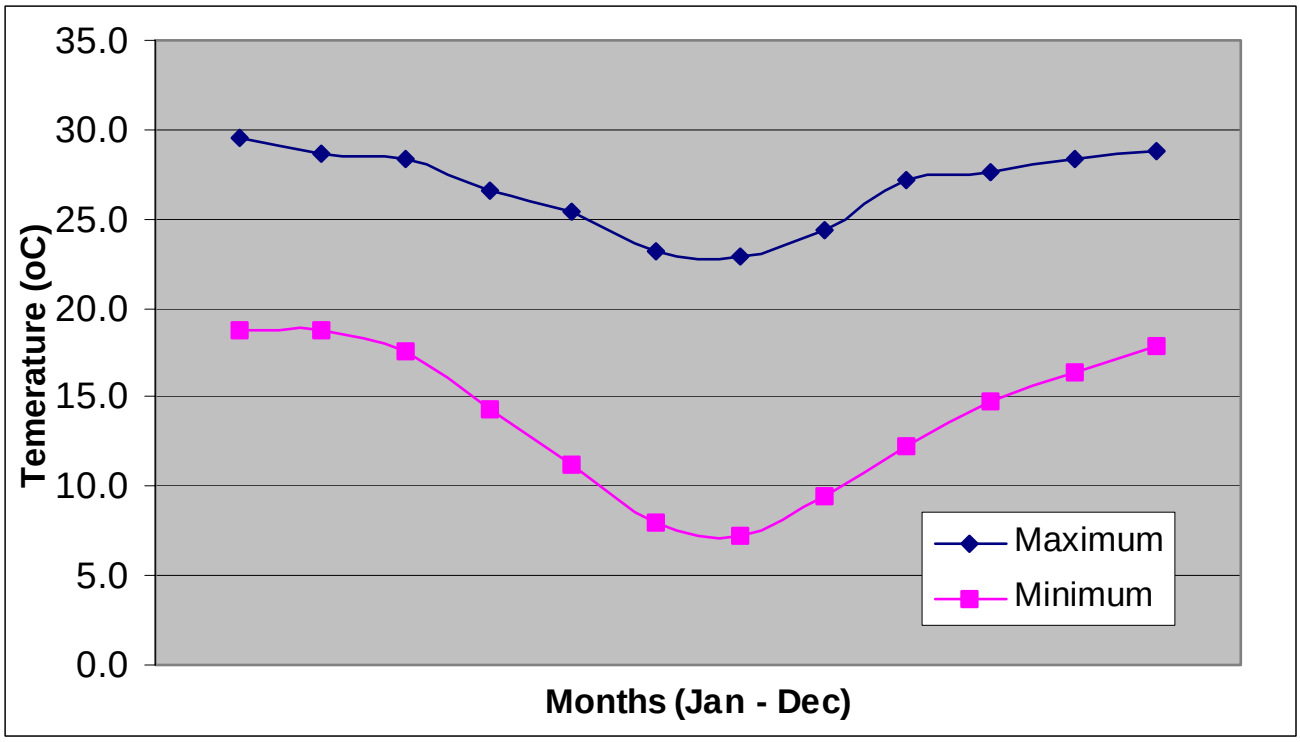

FIGURE 9: Mean daily temperatures for Makhado [station 07233387] (South African Weather Service).

3.5 Fauna

The following list of birds and mammals covers those that were observed within the AFB by the author during field visits. The names of aves and mammals were obtained from Maclean (1993) and Smithers (1986) respectively.

3.5.1 Class: Aves

Family Struthionidae	
Ostrich	*Struthio camelus*
Family Ardeidae	
Blackheaded Heron	*Ardea melanocephala*
Family Accipitridae	
Blackshouldered Kite	*Elanus caeruleus*
Pale Chanting Goshawk	*Melierax canorus*
Family Falconidae	
Greater Kestrel	*Falco rupicoloides*
Lanner Falcon	*Falco biarmicus*
Family Phasianidae	
Swainson's Francolin	*Francolinus swainsonii*
Family Columbiformes	
Cape Turtle Dove	*Streptopelia capicola*
Laughing Dove	*Streptopelia senegalensis*
Family Musophagidae	
Grey Lourie	*Corythaixoides concolor*
Family Cuculiformes	
Diederik Cuckoo	*Chrysococcyx caprius*
Family Apodidae	
Little Swift	*Apus affinis*
Family Meropidae	
Whitefronted Bee-eater	*Merops bullockoides*
Little Bee-eater	*Merops pusillus*
Family Coraciidae	
Lilacbreasted Roller	*Coracias caudate*

Family Coraciidae (cont.)	
Purple Roller	*Coracias naevia*
Family Hirundinidae	
European Swallow	*Hirundo rustica*
Family Orioidae	
Blackheaded Oriole	*Oriolus larvatus*
Family Corvidae	
Pied Crow	*Corvus albus*
Family Turdidae	
Kurrichane Thrush	*Turdus libonyana*
Whitethroated Robin	*Cossypha humeralis*
Family Sylviidae	
Barthroated Apalis	*Apalis thoracica*
Rattling Cisticola	*Cisticola chiniana*
Blackchested Prinia	*Prinia flavicans*
Family Muscicapidae	
Marico Flycatcher	*Melaenornis mariquesis*
Paradise Flycatcher	*Terpsiphone virdis*
Family Laniidae	
Fiscal Shrike	*Lanius collaris*
Redbacked Shrike	*Lanius collurio*
Chrimsonbreasted Shrike	*Laniarius atrococcineus*
Whitecrowned Shrike	*Eurocephalus anguitimens*
Family Nectariniidae	
Black Sunbird	Nectarinia amethystine
Family Ploceidae	
House Sparrow	*Passer domesticus*
Cape Sparrow	*Passer melanurus*
Family Estrildidae	
Scalyfeathered Finch	*Sporopipes squamifrons*
Blue Waxbill	*Uraeginthus angolensis*
Blackthroated Canary	*Serinus atrogularis*
Family Viduidae	
Paradise Whydah	*Vidua paradisaea*

BREEDING SPECIES

A pair of Pied Crows *Corvus albus* built a number of nests within the hanger roof at Movements 2. There was however no indication of breeding activity. An active Cape Turtle Dove *Streptopelia capicola* nest was noted approximately 100m north of Movements 2. A number of active Scalyfeathered Finch *Sporopipes squanifrons* nests were present in the veld surrounding Movements 2 and the taxiways. Blackthroated Canary *Serinus atrogularis* bred near pump station B.

RED DATA SPECIES

No red data species were noted.

3.5.2 Class: Mammalia

Kudu	*Tragelaphus strepsiceros*
Warthog	*Phacochoerus aethiopicus*
Impala	*Aepyceros melampus*
Scrub Rabbit	*Lepus saxatillus*
Vervet Monkey	*Cercopithecus aethiops*

RED DATA SPECIES

No red data or endangered species were noted.

3.6 Geology

3.6.1 Regional Geology

The study area lies within the Southern Marginal Zone (SMZ) of the Limpopo Belt and consists of high-grade equivalents of a granite-greenstone terrane (Smit *et al*., 1992). Typical lithologies include banded gneiss, mafic and ultramafic gneiss, migmatite and leucogranite, which formed during the Swazian erathum. These have been intruded by a number of younger granites of the Randian erathem with the major intrusions being the Matok granite to the south and Hugomond biotite granite to the south west. The Soutpansberg Group forms a younger cover to the north of the SMZ and was deposited during the Mokolian erathem. The Soutpansberg Group consists of sedimentary and volcanic rocks, which are represented by

sandstones, conglomerates, basalt and tuff. The above-mentioned lithologies have been intruded by younger diabase dykes, which have a general northwest – southeast strike direction (1:250 000 Geological Series, 2328 Pietersburg).

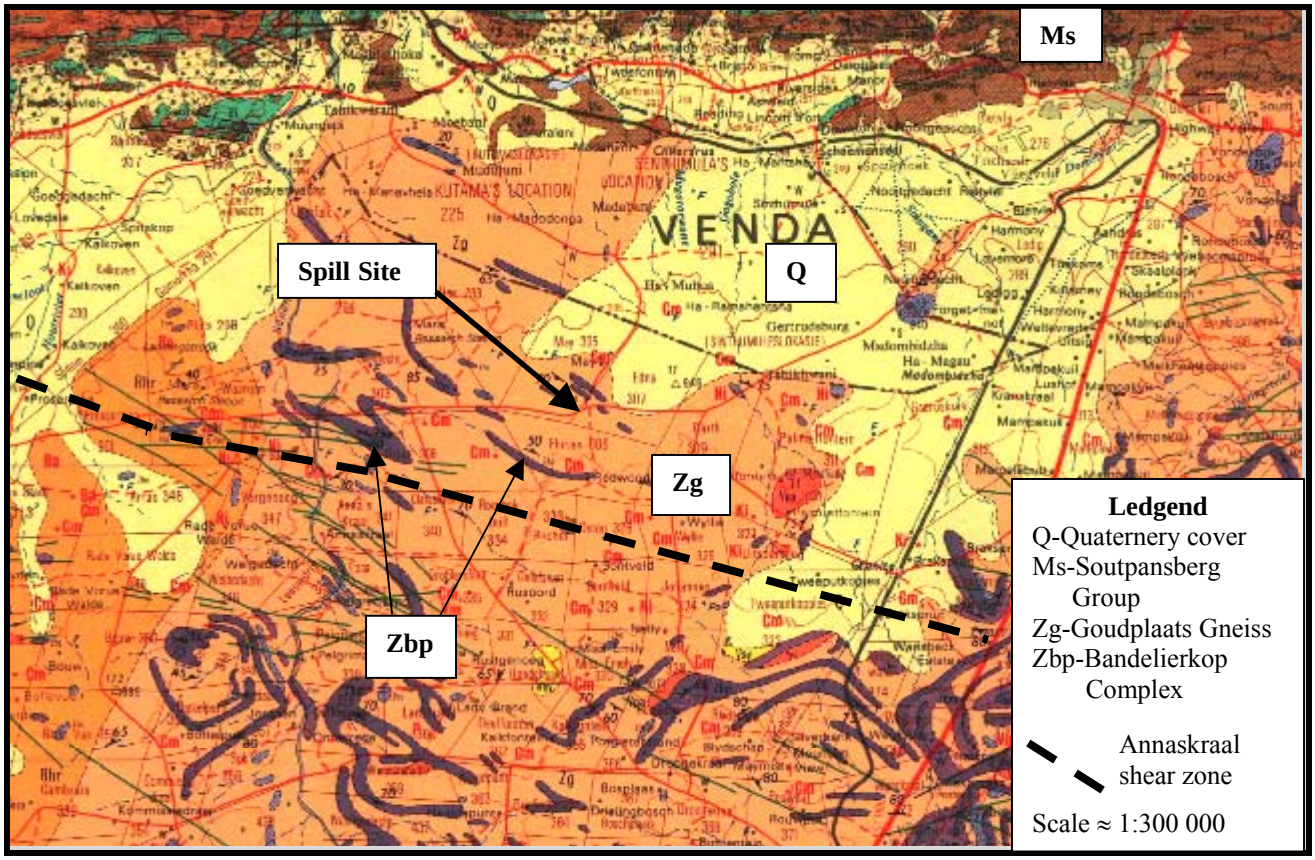

FIGURE 10: Regional geology of the study area (1:250000 Geological Series, 2328 Pietersburg).

3.6.2 Local Geology

The AFB is located on lithology from the Goudplaats Gneiss[†], which consists locally of intercalated dark amphibolite and light leucogneiss layers. The foliation has an average dip direction of 346° and dip of 20°. The orientation of the foliation and joint sets are indicated in Figures 11 and 12 respectively. The restricted data set is due to the limited number of outcrops present.

[†] Name not yet approved by SACS

Number	*Dip (°)*	*Dip direction (°)*
1	14°	316 °
2	20 °	329 °
3	20 °	356 °
4	10 °	329 °
5	20 °	23 °
6	10 °	337 °
7	20 °	334 °
8	33 °	12 °
9	30 °	355 °

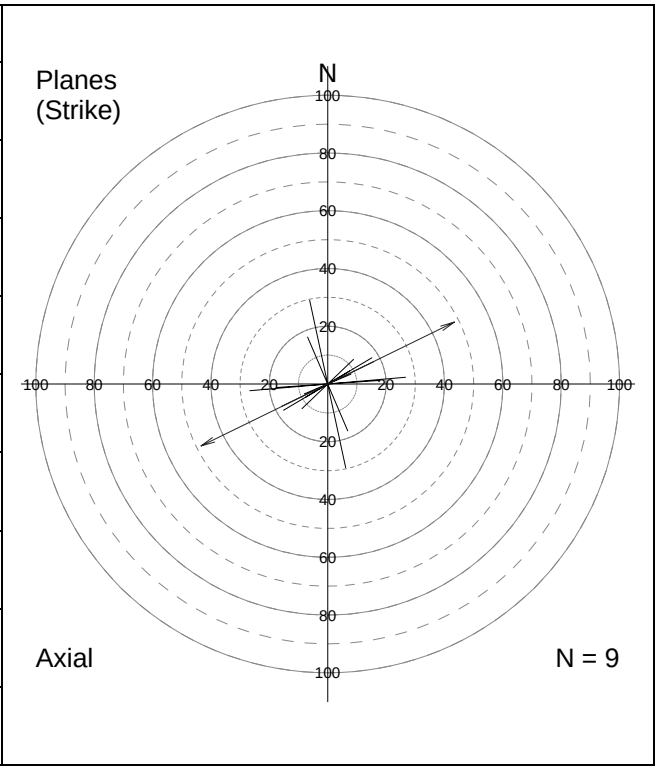

FIGURE 11: Rose diagram indicating the orientation of the gneiss foliation (Dippenaar, 2002).

Number	*Dip (°)*	*Dip direction (°)*
1	85°	285 °
2	85 °	300 °
3	83 °	120 °
4	78 °	65 °
5	80 °	270 °
6	67 °	315 °

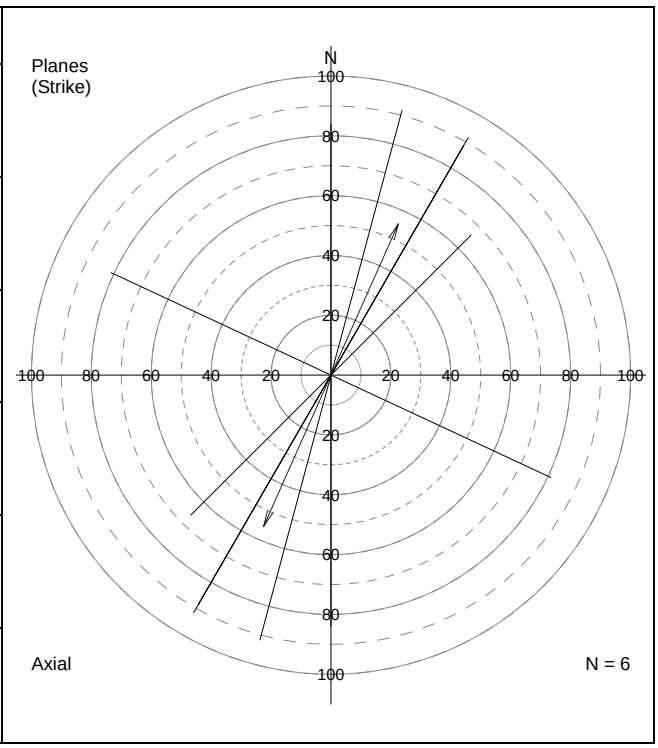

FIGURE 12: Rose diagram indicating the orientation of joints within the gneiss (Dippenaar, 2002).

Two diabase dykes are present within the study area and are indicated in Figure 15. The northern dyke strikes in a northeasterly direction and has been displaced by an inferred fault (aeromagnetic data interpretation). The southern dyke consists of two sub-parallel intrusions which strike in an east-northeast direction.

3.6.3 Structural Geology

Deformation in the SMZ was polyphase, widespread, intense and resulted in complex fold geometry in rocks under granulite conditions. Two prominent regional structural features characterise the SMZ, namely massive crustal wedges (20km x 50km), with large oval shaped closed folds associated with an early phase of deformation (D_1), and which are bounded by major ductile shear zones with a broad ENE-WSW structural trend.

Structural maps of the SMZ indicate linear zones separating the large crustal wedges with their characteristic large-scale D_1 folds. Air photo interpretation and regional structural mapping indicates steeply dipping crustal sheets separated by younger shear deformation (D_2). The majority of strain generated during D_2 deformation was partitioned into the shear zones. On a regional scale these shear zones form an anastomosing network and are many tens of kilometres in length and several kilometres in width (Figure 13).

The presence of high-grade shear zones is difficult to detect in the field due to the lack of marker lithologies. Their presence can however be established from, large-scale deformation into straightening zones, a change from coarse grained, folded and banded migmatitic gneisses to finer grained thinly banded straight gneisses where transposition parallel to the shear zone has occurred and the presence of mineral stretching lineations, boudins, rods and occasional sheath folds which all have the same orientation direction (Smit *et al*, 1992).

The spill site is situated 5km north of the Annaskraal shear zone. The approximate location of the shear zone is illustrated in Figure 10.

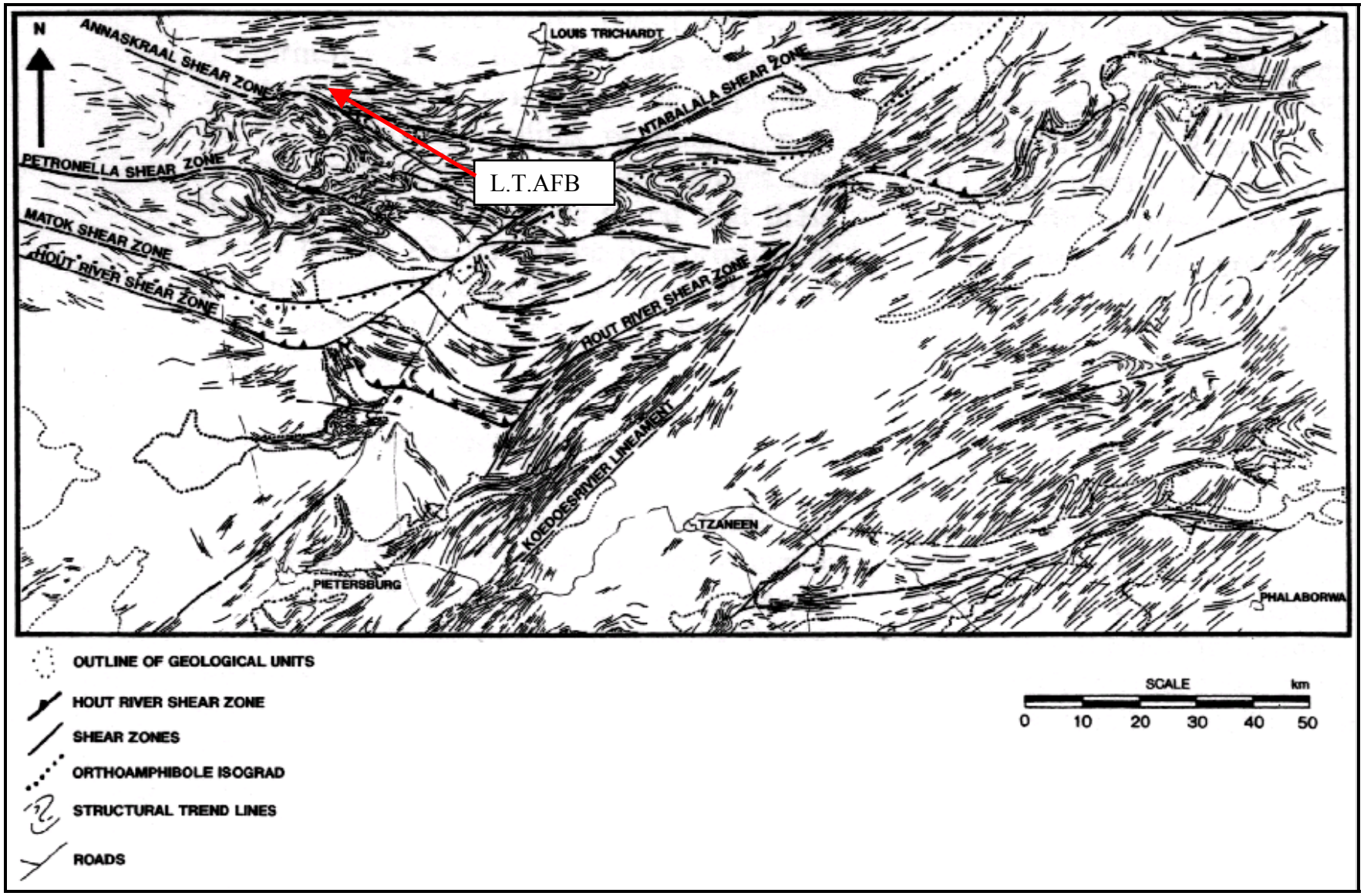

FIGURE 13: The regional structural framework of the Southern Marginal Zone of the Limpopo Belt (Smit *et al*, 1992).

3.7 Regional Hydrogeology

Two types of aquifers are present in the region, namely primary and secondary aquifers. Primary aquifers are restricted to alluvial deposits adjacent to major rivers, such as the Sand River. Secondary aquifers cover the majority of the area and are developed in the form of faults, shear zones and contact zones between different lithologies.

Alluvial deposits along the Sand and Blood River channels are approximately 250m to 300m wide and 5m to 25m thick (Wilken, 1997). Boreholes drilled in the primary aquifer along the Sand River during an investigation by Pretorius *et al* (1994) had a recommended yield of between 6ℓ/s and 20ℓ/s for nine hours per day (Pretorius *et al*, 1994). According to an investigation by Africon Inc. (1999), secondary aquifers with a very high transmissivity exist in the area. Some of these occur on the AFB and boreholes with high yields can be located on them. Two high yielding boreholes were drilled in the AFB during this investigation, namely BR06 and BR11. The recommended abstraction rates for these boreholes are 15ℓ/s and 5ℓ/s respectively for twelve hours per day.

According to Parsons *et al* (1998) aquifer classification map of South Africa the AFB is located within a major aquifer region. The vulnerability of the aquifer is classified as least vulnerable with a medium susceptibility. This is a regional aquifer classification. The leak occurred in a minor aquifer, however major aquifers are present in the area and are represented by fracture zones.

Definitions (from Parsons *et al*, 1998):

Major aquifer region – A high yielding aquifer system of good quality water.

Vulnerability – The tendency or likelihood for contamination to reach a specified position in the ground water system after introduction at some location above the uppermost aquifer.

Susceptibility – A qualitative measure of the relative ease with which a ground water body can be potentially contaminated by anthropogenic activities and includes both aquifer vulnerability and the relative importance of the aquifer in terms of its classification.

4. Site Characterisation

4.1 General

The desk study consisted of obtaining information on the hydrogeology, geology, topography, rainfall and nature of the pollutants. Information of the pollutants was obtained from the manufacturer of the fuel, namely Sasol/Total Supply Group. This information is important in understanding the method of transport as well as the process of natural degradation of the pollutants in the vadose and saturated zones. Africon Inc. (1999) conducted a large-scale investigation in 1999 into the ground water potential of the AFB and surrounds. Information was also obtained from an investigation conducted by Wilken (1997) into the Sand/Blood River groundwater development for the Polokwane Transitional Council.

To completely understand the following section it is imperative to mention the order in which the events took place, particularly between the geophysical investigations and drilling phases.

4.2 Geophysical Investigation

Geophysical investigations were conducted to map subsurface geological features in order to obtain a better understanding of their influence on the hydrogeology. These features are detected due to a difference in physical properties to the environmental/regional rocks. Different techniques are adopted to delineate the change of different physical properties.

4.2.1 Electrical Resistivity

A survey was conducted by GeoCon (Pty) Ltd during the initial phases of the investigation. The results were however inconclusive due to high levels of background noise caused by services. The results are not presented or discussed any further.

4.2.2 Magnetic Survey

4.2.2.1 Magnetic Traverses

Two magnetic surveys were conducted and consisted of 15 traverses covering a distance of 5.8km. The first survey consisted of 11 traverses (2.3km in length), covering the immediate area surrounding the leak. The results of this survey was inconclusive as the anomalies detected were from underground services (eg. pipes, cables etc.) and not a variation in subsurface geology. The results are not included in this dissertation.

The second survey consisted of both electromagnetic and magnetic profiles along five traverses. The survey is discussed in more detail under Section 4.2.3.1 - Frequency Domain Electromagnetics. The result of this survey is illustrated in Appendix B.

4.2.2.2 Airborne geophysics

Stettler *et al* (2002) conducted an airborne magnetic survey with an ultra-light aircraft. A grid of 5km by 5km was covered with the leakage site located in the centre. The aim of the survey was to detect the presence of structures which may influence the movement of contaminants. The survey was flown at a line spacing of 100m and flying height of 50m. Magnetic data was recorded at a 4m interval along the flight lines. The flight line direction was north-south. Gamma-ray spectrometer data was collected simultaneously at a 40m interval along flight lines.

The magnetic data was more useful than the gamma-ray spectrometry. The magnetic data collected is illustrated in Figure 14. The warm colours signify magnetic highs and the cold colours magnetic lows. The data has also been artificially shaded to give a false topography to the magnetic anomalies, so that highs appear as elevated areas and lows as valleys (Stettler *et al*, 2002).

The magnetic highs are interpreted as intrusive mafic bodies, either diabase or dolerite. The northern intrusive body is displaced by a possible northwest striking fault as indicated

in Figure 15. The magnetic lows are interpreted as inferred dykes which are remanantely magnetised. Minor east west striking inferred faults and dykes are illustrated (Stettler *et al*, 2002).

4.2.3 Electromagnetic Survey

4.2.3.1 Frequency Domain Electromagnetics (FDEMs)

Two EM34 surveys were conducted and consisted of nine profiles with a total length of 6km. The first survey was conducted prior to phase 4 drilling and the second survey prior to phase 5. The results of the FDEM surveys are presented in Appendix B.

SURVEY 1

Combrink (2001) a geophysicist from the Department of Geology, University of Pretoria surveyed the first four profiles, which had a total length of 2.5km. A Geonics EM34 system was used. The profiles were surveyed at 10m station spacing with 20m coil separation. The aim of the survey was to target a north-south striking feature identified from aeromagnetic data during the Africon Inc. (1999) investigation.

Profiles 1 and 2 intersected the north-south striking feature. The EM data shows two distinct geological zones, namely a zone characterised by low conductivities (5-20mS/m) and another with high conductivities (>40mS/m). The high conductive anomaly extends for approximately 400m and is interpreted as either a mafic intrusion into the granite-gneiss basement or a very broad zone of weathering (Combrink, 2001). Two boreholes, BH45 and BH46 were sited on line 1 and drilling confirmed the anomaly as a zone of higher weathering (e.g. shear or fracture zone).

Profiles 3 and 4 were done close to existing boreholes in order to search for possible structures influencing the contamination distribution. Profile 3 indicated a negligible lateral variation in geology, while profile 4 indicated a deeper weathering zone to the south. The above two profiles are not illustrated in Appendix B.

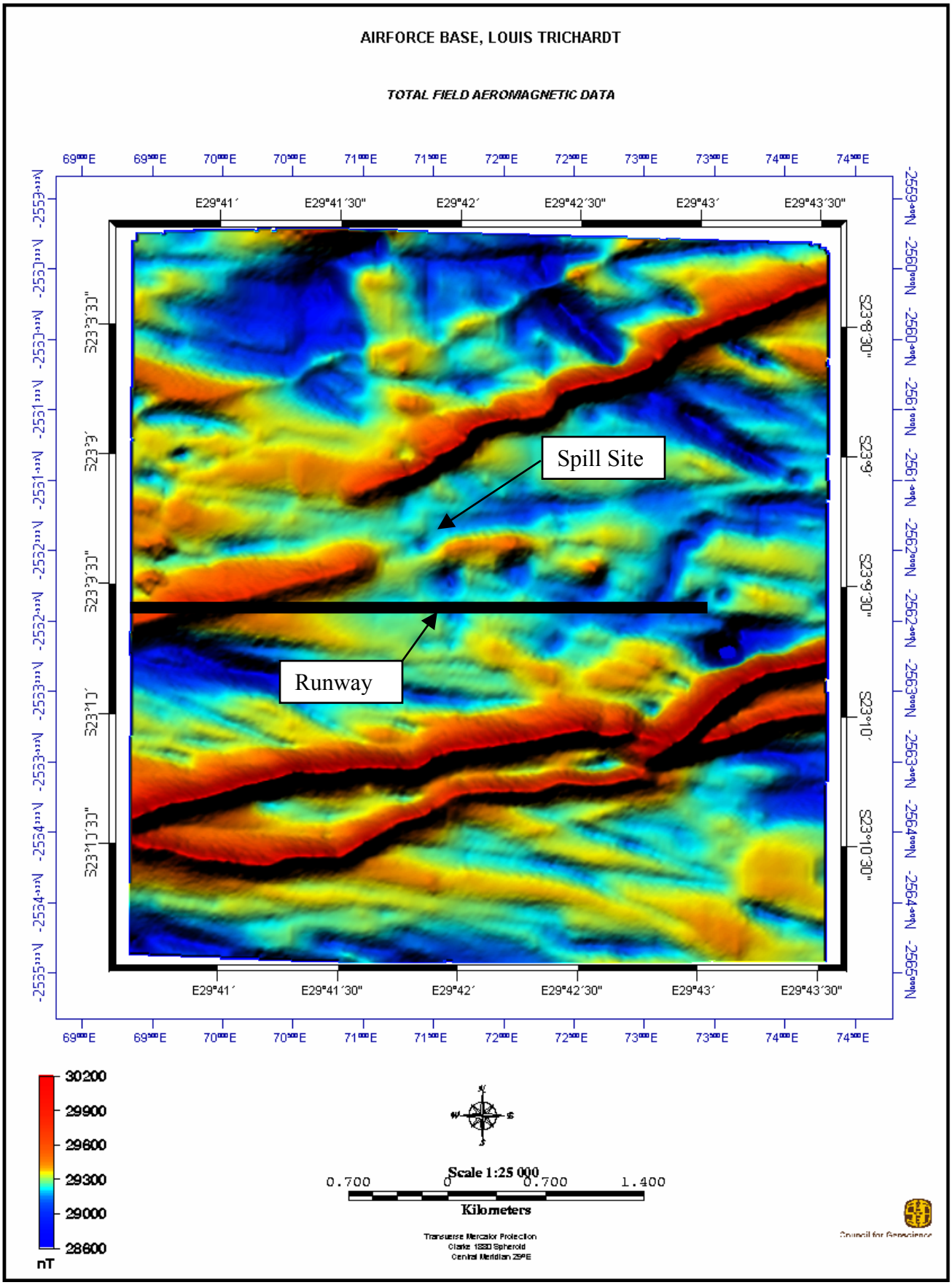

FIGURE 14: Total Field Magnetic Intensity Map (Stettler *et al*, 2002).

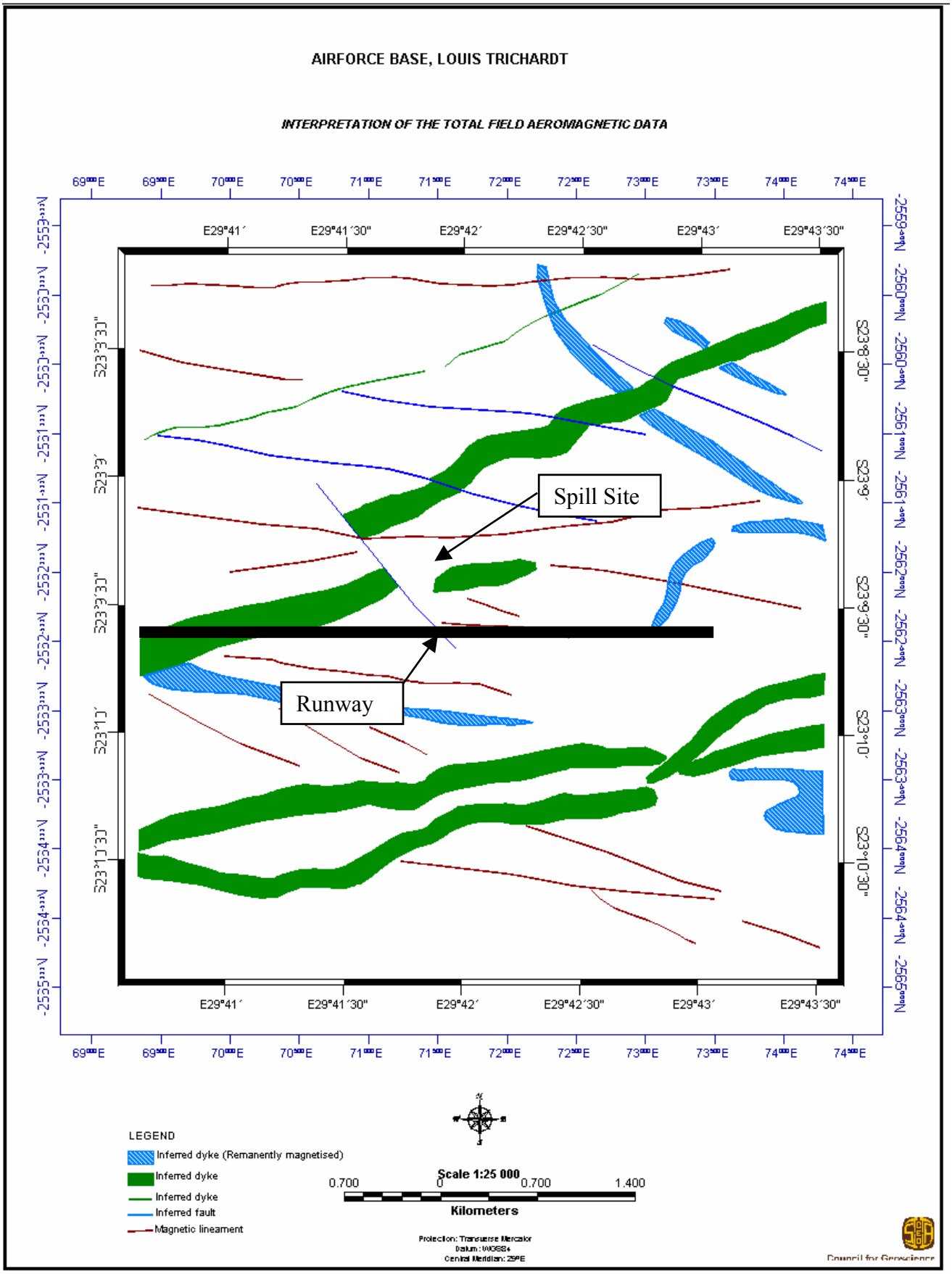

FIGURE 15: Interpretation of the Total Field Intensity map (Stettler *et al*, 2002).

SURVEY 2

The second survey was conducted by P. Badenhorst from GeoPollution Technologies (Pty) Ltd during March 2002 and consisted of five EM34 profiles with a total length of 3.5km. Appendix C indicates the location of target areas where the following traverses were conducted. The results of the survey are illustrated in Appendix B.

The first profile was 350m in length and was conducted in target area D in a southwest to northeast direction. Boreholes BH58 and BH57 were drilled along this profile at 46m and 227m respectively.

The second and third profiles were conducted in target area F with a length 800m and 805m respectively. Both the traverses were from west to east. The aim of the traverses was to detect the north south structure north of BH45 and BH46 to determine the extent of pollution within the structure. Boreholes BH47, BH48, BH49, BH50 and BH51 were sited along the two profiles.

The fourth traverse was conducted in target area D and had a length of 300m in a direction from west to east.

The fifth traverse was 1335m in length and was conducted in target area E with a profile direction of west to east. Boreholes BH59, BH60 and BH61 were sited along this profile.

4.2.3.2 Time Domain Electromagnetics (TDEMs)

A TDEM survey was conducted by Stettler *et al* (2002) from the Council for Geoscience between November 2001 and February 2002. The aim of the survey was to determine the extent of free phase pollution. The detection of free phase on the ground water is achieved by the analysis of the Induced Polarisation (IP) response in transient soundings. According to Zadorozhnaya *et al* (2002) two types of polarisation occur in sediments without metallic particles, namely the membrane and electro-osmosis polarisation effects.

Hallbauer-Zadorozhnaya *et al* (2002) ascribed the IP phenomena observed during shallow soundings for the detection of hydrocarbons to the electro-osmosis effect since the time window used during data acquisition is too short to detect the membrane IP effect.

A total of 84 TDEM soundings were completed between November 2001 and February 2002. The extent of the inferred pollution plume and results of the survey are illustrated in Appendix C. The inferred plume from this survey is larger than what was confirmed by drilling results. This is either due to some types of geology that give a false electro-osmosis effect or an electrically very noisy environment (Stettler *et al*, 2002).

4.2.4 Soil Vapour Survey

A soil vapour survey was conducted by GeoPollution Technologies (Pty) Ltd in 2000 prior to the repair of the leak. The survey was conducted along the faulty pipeline to determine the exact location of the leak. The survey did not include oxygen and CO_2 concentrations, as the equipment used could not measure these parameters.

A second soil vapour survey was conducted in 2001 in an attempt to delineate the boundary of the free phase plume as well as the extent of contamination at pump station B. A number of profiles were traversed where the presence of free phase was confirmed by drilling. The survey was unsuccessful due to the free phase being situated approximately 30 metres below ground level (mbgl) and the concentration of hydrocarbon vapours on the surface was below the detection limits of the equipment. Surface contamination was detected at pump station B surrounding the fuel storage tanks. The pollution is presumably caused by spillages during the filling of vehicles and/or the tanks. Borehole BH65 was subsequently drilled north of pump station B to quantify the extent of ground water pollution (discussed in more detail under Section 4.3 - Drilling Program, Phase 5).

4.3 Drilling Program

A total of sixty-seven (67) 165mm percussion boreholes were drilled in a phased approach for the pollution investigation. The following section deals with the conceptual ideas behind siting the boreholes, aims of the drilling phases and drilling results.

PHASE 1: The first phase consisted of drilling five boreholes (BH01 to BH05) over the period 8-9 December 2000 (Figure 16). These boreholes were drilled to the west and northwest of the leakage site. This was the presumed direction of ground water flow, if one assumes the piezometric surface follows topography. BH04 and BH05 were drilled next to the back filled trench housing the pipeline as it was thought that the majority of fuel would have followed the back filled trench before infiltrating into the vadose zone.

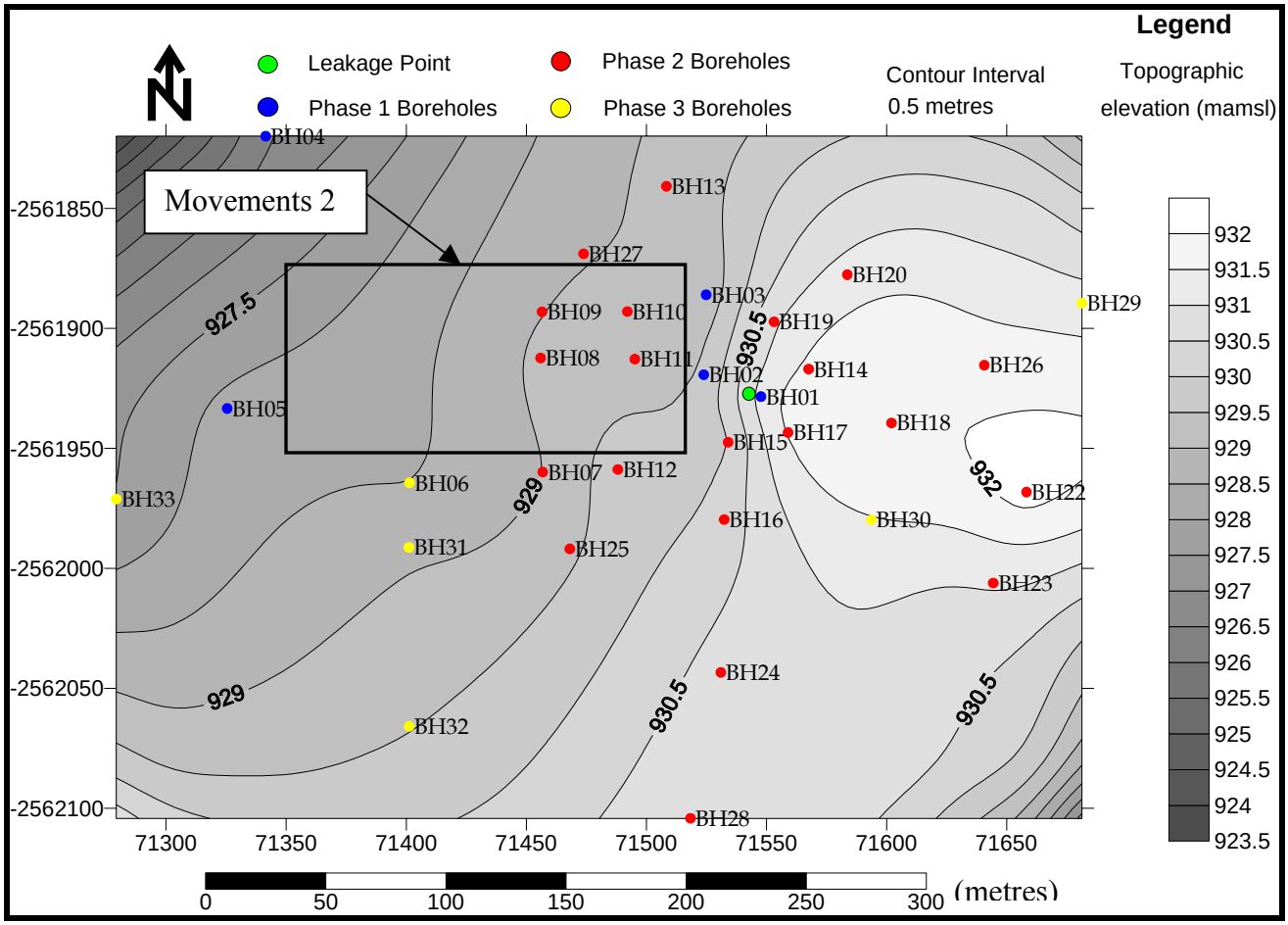

FIGURE 16: Location of Boreholes Drilled during Phase 1, 2 and 3 (excl. BH21).

PHASE 2: The aim of this phase was to delineate the extent of the free phase pollution plume. Twenty-two boreholes (BH07 to BH28) were drilled from the 19th to 23rd March 2001 (Figure 16). Due to no significant anomalies in the electrical resistivity and magnetic traverses a total of 12 boreholes were sited along the circumference of two concentric circles with the leakage site in the centre. The inner and outer circles had a radius of 25m and 60m respectively. Both circles had six boreholes spaced at equal distances along their circumference. A number of the outer boreholes (especially BH10, BH16 and BH18) contained large amounts of free phase, which lead to the drilling of a further nine boreholes. Due to the aquifers low hydraulic conductivity a number of the outer boreholes only showed unacceptable free phase levels approximately two weeks after they were drilled. BH21 was drilled between the leakage site and BR06 and BR11, which at that stage were still being used for water supply to the AFB. The borehole is approximately 500m north of the leakage site (Figure 17).

PHASE 3: Six boreholes were drilled during this phase (BH06 and BH29 to BH33) from 30th April to 3rd May 2001 (Figure 16). This phase was still unsuccessful in delineating the free phase plume as BH29 yielded an apparent free phase thickness of 9.7m. This lead to a forth phase of drilling which investigated the area to the east of the previous drilling phases.

PHASE 4: A total of thirteen boreholes were drilled during this phase (BH34 to BH46) from 10th to 13th September 2001 (Figure 17). Boreholes BH34 to BH44 were drilled to the east of the previous boreholes due to the fact that BH29 had 9.7m of free phase. The aim of the close spacing of boreholes was to facilitate the removal of free phase in as short a time as possible. The two boreholes BH45 and BH46 were drilled as monitoring boreholes on an electromagnetic anomaly. The anomaly is a north-south striking feature that is the same feature on which BR06 is located.

PHASE 5: Twenty-one boreholes were drilled during this phase (BH47 to BH67) from the 1st to 8th April 2002 (Figure 18). A regional approach was adopted for this drilling phase following the completion of the Time Domain and Frequency Domain Electromagnetic geophysical surveys. The aim of this phase was to determine the extent of pollution within the AFB as previous fuel spills had occurred. A number of target areas (A to F) were identified where pollution had or may have occurred. The target areas are illustrated in Appendix C.

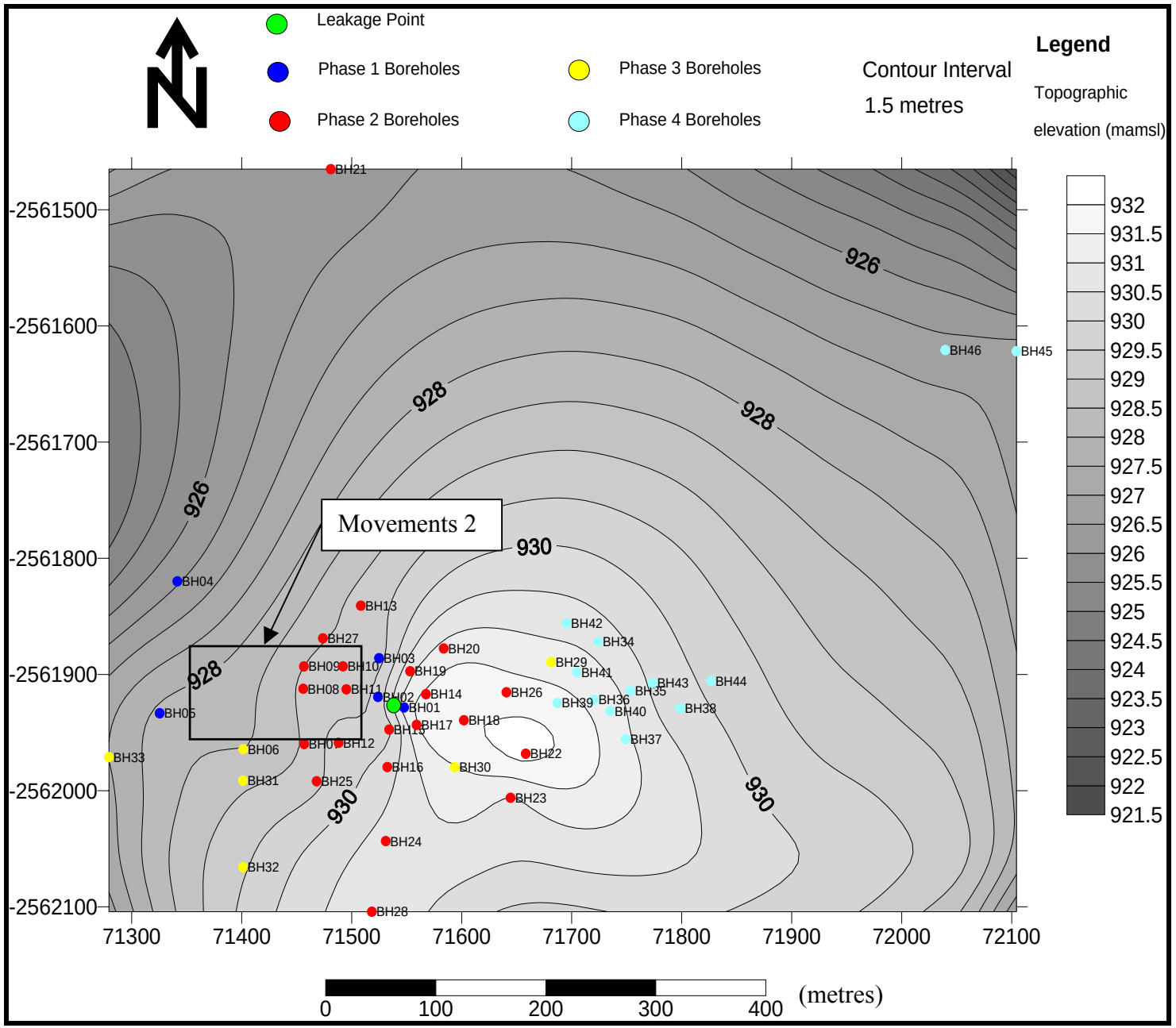

FIGURE 17: Location of Boreholes Drilled during Phases 1 to 4.

Target area A was identified due to the TDEM readings S62, S64 and S65 that showed the IP effect as well as an inferred fault from the aeromagnetic survey and a surface spill at pump station B. Boreholes BH52 and BH53 were drilled to the south and north of the inferred fault. Borehole BH65 was drilled following a soil vapour survey which indicated surface pollution and a subsequent surface spill due to the over filling of a fuel reservoir.

Target area B is the location of the storm water drain outlet from the jet refuelling area. The TDEM reading S83 showed the IP effect and an area of possible contamination was outlined. An inferred east-northeast striking dyke and west-northwest striking fault were also included into the area. The presence of the inferred structures was investigated with boreholes BH66 and BH67.

Target area C is situated to the north of a spill that occurred in the past. Borehole BH62 was drilled down gradient of the spill to investigate the presence of pollution.

Target area D was located around TDEM readings S70 and S56, which show an IP effect. The area also includes an inferred dyke and fault from the aeromagnetic survey. Boreholes BH56, BH57 and BH58 were drilled in this area.

Target area E is situated along the southern margin of the interpreted contaminated area. The aim of the five boreholes drilled in this area is to delineate the southern margin of the inferred plume and to ensure that the plume is not migrating in a southerly direction.

Target area F was identified to determine the extent of pollution in a north-south structure identified by Africon Inc. (1999) following an aeromagnetic survey. Boreholes BH47, BH48, BH49, BH50 and BH51 were drilled following two FDEM traverses.

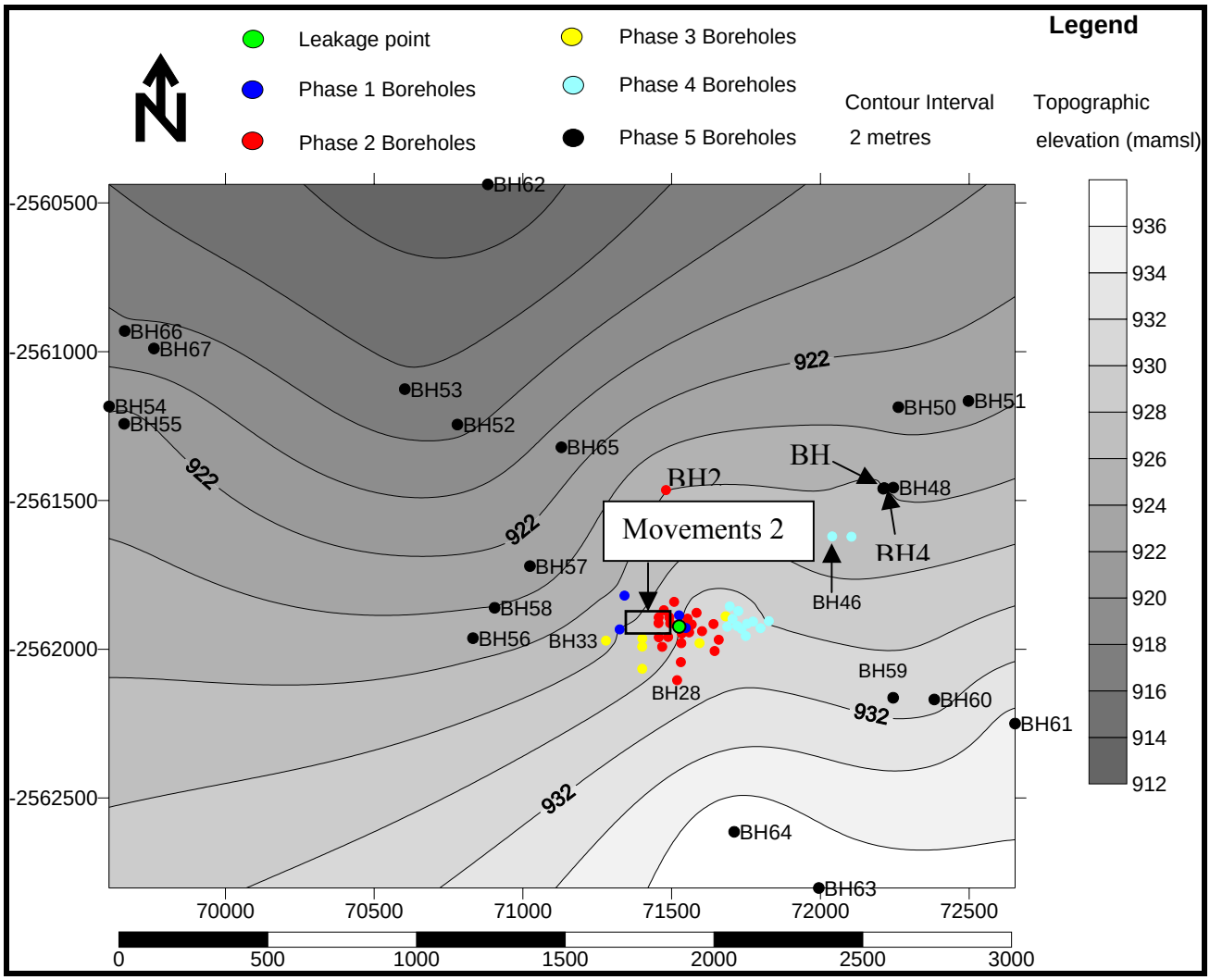

FIGURE 18: Location of Boreholes Drilled during Phases 1 to 5.

4.3.1 Drilling Results

All the boreholes were geologically logged by describing the percussion drill chips brought to the surface by compressed air. Borehole logs are located in Appendix D. Chips were collected for each metre of borehole drilled and laid in piles. The piles were washed using a sieve and water to remove dust. The boreholes were logged with special reference to colour, grain size, weathering, lithology, water strikes and blow yield. Water strikes were noted where possible however due to low yielding boreholes and the use of water during drilling to reduce dust emissions and assist with sample recovery all the water strikes were not obtained. The odour of hydrocarbons was checked for each pile and noted in the logs.

The boreholes varied in depth from 43m (BH56) to 76m (BH03) with an average depth of 56m. Casing was inserted to a depth where the material was competent. Solid steel casing was used and was seldom seated deeper than 12mbgl. The casing protruded above the ground and was supported with a $0.5m^2$ concrete block surrounding the casing and was fitted with a cap and locking bolt to prevent vandalism and precipitation from entering the borehole. The casing of boreholes drilled through asphalt surfaces and those next to the taxiway were cut flush with the ground surface. A special cap was used for these boreholes, which fits inside the borehole and has a protruding lip around the casing. No grouting was used between the casing and side of the borehole as the casing was never seated below the free phase or water level. The vertical migration of pollutants along the borehole was not a concern, as the solid casing never intersected the free phase.

The lithology intersected by the boreholes consists of alternate leucocratic (light coloured) and melanocratic (dark coloured) bands as well as diabase/dolerite intrusions. The leucocratic bands consist of leucogneiss with a mineralogy of predominantly quartz and feldspar. The melanocratic bands consist of amphibolite, which has a mineral assemblage of predominantly mica (biotite) and amphibole.

The weathering was generally very shallow with a thin layer of scree overlying the bedrock (usually less than 1m). At similar depths the amphibolite showed a higher degree of weathering than the leucogneiss, which is expected due to the mineralogy.

Diabase/dolerite intrusions are intersected between 1mbgl and 56mbgl in the following boreholes BH21, BH25, BH27, BH40, BH43, BH54, BH58 and BH66. The diabase is less weathered than the surrounding bedrock and varies from fresh to slightly weathered.

4.4 Hydrogeology

Granite-gneiss is generally classified as a poor aquifer except where fractures are developed in the form of faults, shear zones and contact zones between different lithologies. Dykes are usually targets for siting boreholes, as they tend to intrude into weaker zones of bedrock (faults, shear zones etc.) and contract during cooling, thus leaving adjacent open fractures. In this area it is

however not the case, as a previous investigation by the Department of Water Affairs and Forestry had little success in siting high yielding boreholes on dykes (Africon Inc., 1999).

According to the Africon Inc. (1999) report secondary aquifers with very high transmissivity values exist in the area. Anderson and Less (1992) stressed the importance of targeting fractures that formed under tensile rather than compressive stresses. They identified the most favourable structure orientation as between 340° and 350° while the second most favourable orientation is between 0° and 40°. This is confirmed by the highest yielding borehole on the base (BR06) being located on a structure with an orientation of 345°. The safe yield of production boreholes drilled on the AFB during the Africon Inc. (1999) investigation was 15ℓ/s (BR06) and 5ℓ/s (BR11) for 12 hours/day and 2ℓ/s (BR02) for 8 hours/day.

The behaviour of fractured rock aquifers is similar to porous media on a large scale, however on a small-scale anisotropic features become more important. The regional ground water flow is in a northwesterly direction and follows the general topography. The ground water flow on the AFB does not follow the topography (Figure 19) and moves in a northeasterly direction.

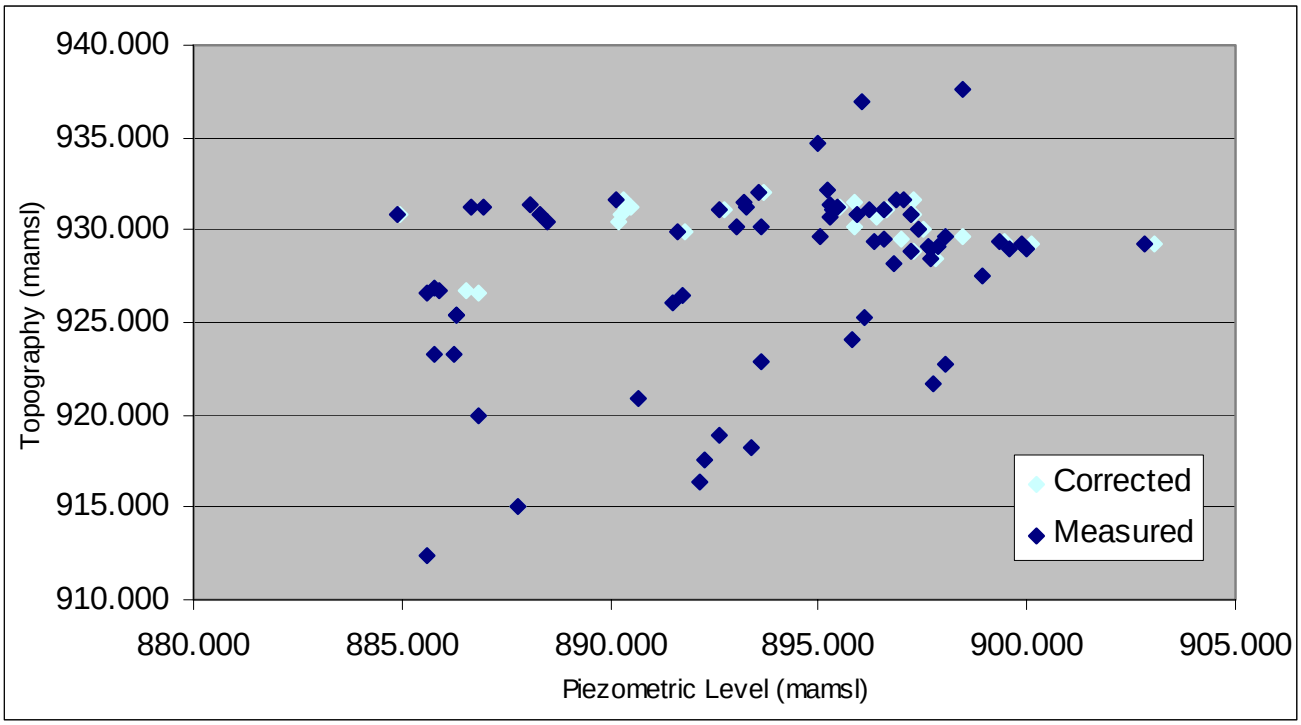

FIGURE 19: Topography versus Corrected and Observed Piezometric Levels measured on the 15th January 2003.

The majority (55%) of water strikes were intersected at a depth of between 41 to 50mbgl (Figure 20). The aperture of the fractures decreases with depth and no water strikes were obtained below 60mbgl.

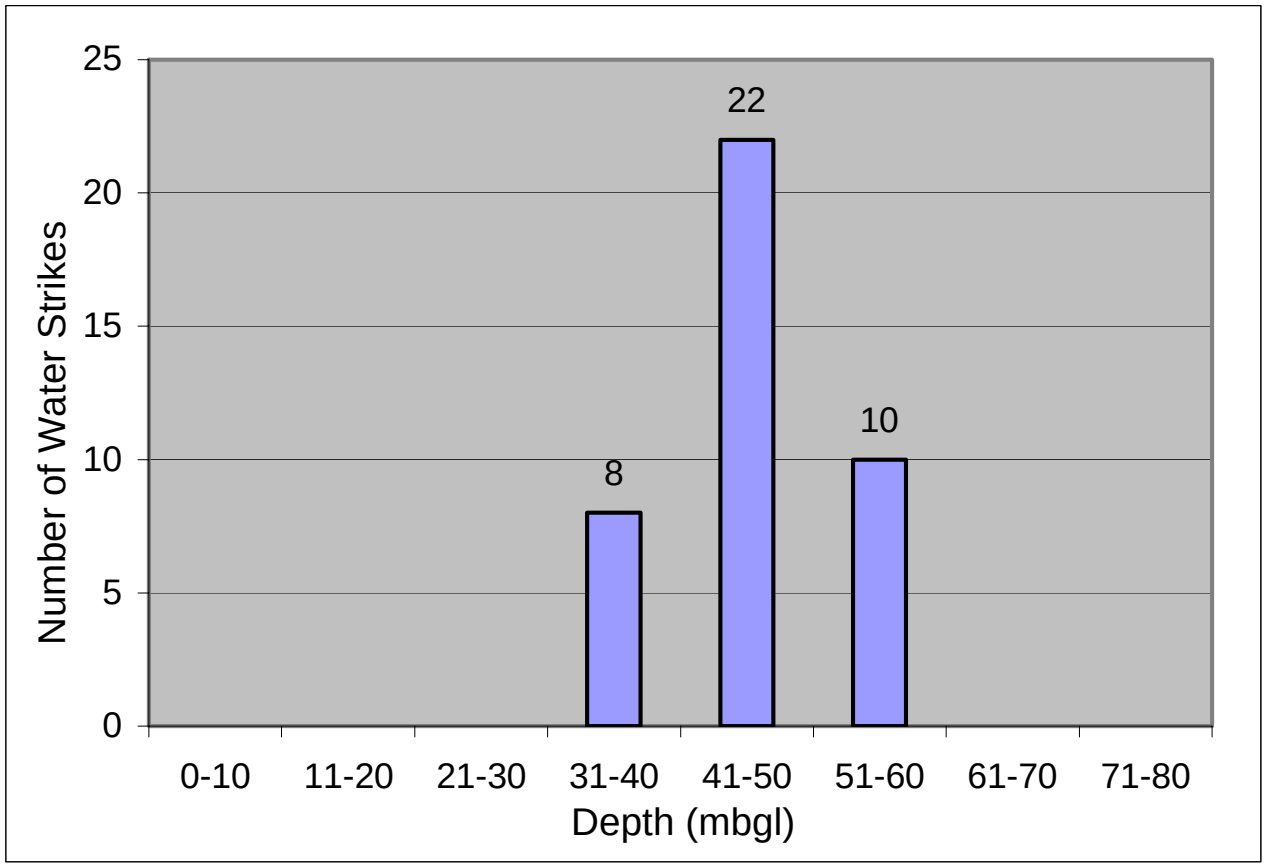

FIGURE 20: Number of Water Strikes vs. Depth (mbgl).

The response of the ground water level to precipitation for boreholes BH11 and BH19 is indicated in Figure 21. Due to a lack of data the immediate response is difficult to determine, however general trends can be obtained from the graphs. BH11 is below the asphalt layer of Movements 2 however large season fluctuations in water level are noticed. BH19 is situated to the east of BH11 and is not covered by asphalt. The seasonal fluctuations of BH19 are significantly less than BH11. A number of boreholes were analysed for ground water level response following precipitation, however only boreholes that have negligible amounts of free phase present showed a response following precipitation.

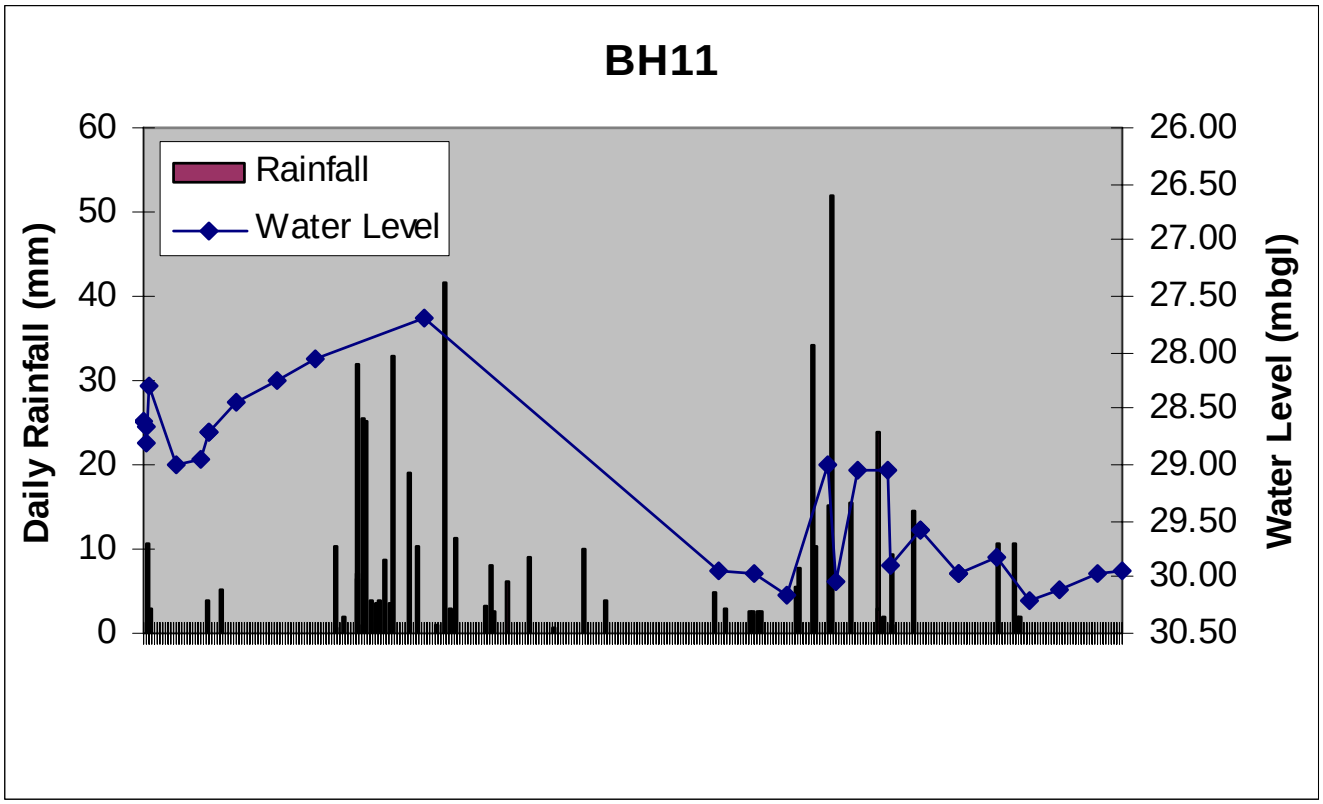

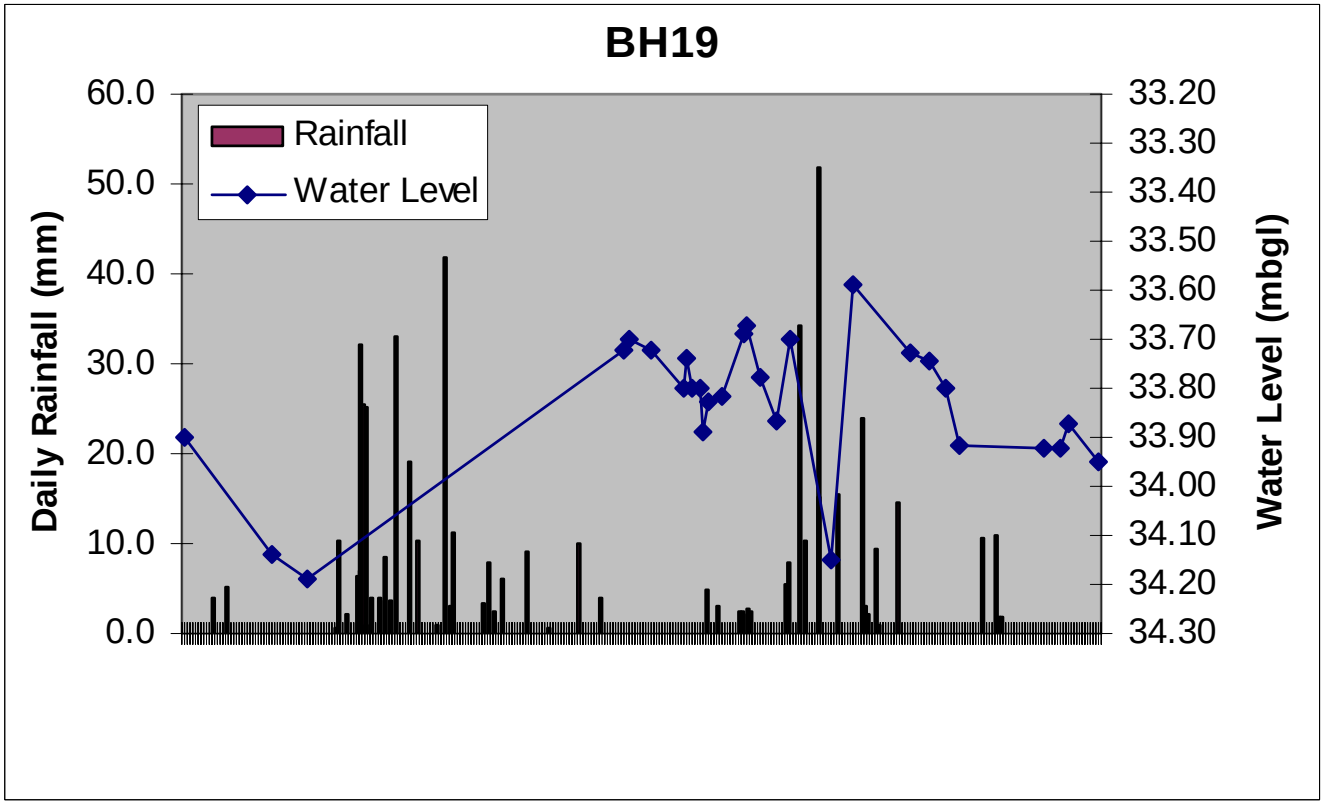

FIGURE 21: Comparison of ground water response following precipitation for BH11 and BH19 (30th April 2001 to 29th September 2003).

The northward dipping leucocratic and melanocratic bands may theoretically have resulted in the pollution migrating in a northerly direction while in the vadose zone. The melanocratic bands are generally more weathered and have a higher clay content than the leucocratic bands at the same depth. Therefore the melanocratic bands probably have a lower hydraulic conductivity than the leucocratic bands. Figure 22 is a schematic illustration of the theoretical migration of pollutants in the vadose zone. The fluid (Jet fuel) moves vertically and 'rapidly' through the zone of high hydraulic conductivity (leucogneiss) until it reaches a zone of lower hydraulic conductivity (amphibolite). The fluid gradually infiltrates the zone of lower hydraulic conductivity and accumulates at the contact with the zone of higher hydraulic conductivity (under dry conditions). The fluid must build up sufficient pore pressure before it moves into the zone of higher hydraulic conductivity. The fluid may move laterally down the zone of lower hydraulic conductivity under gravity, however this will require a positive gage pressure. A positive gage pressure will also allow the fluid to pass into the zone of higher hydraulic conductivity. The deflection under these conditions will be small and possibly negligible. This process is typically called a capillary effect of a liquid (jet fuel).

However under wet conditions the zones of lower hydraulic conductivity may have water in the small spaces, for example 2000, which had an annual rainfall of 801mm. This will result in the fluid accumulating on the top of the zone of lower hydraulic conductivity and result in subsequent lateral migration. Under these conditions the lateral migration of the fluid will be much larger than under dry conditions.

It is important to determine the effect these different layers have on the geohydrology in order to develop an effective remediation strategy. Packer tests would have to be conducted to quantify the effect that changes in lithology have on the hydraulic conductivity.

The pollutants will initially reach the ground water level as dissolved phase, however with time free phase will start to accumulate. The dissolved phase initially originates from rainwater, which has come into contact with contaminants in the vadose zone and infiltrated to the ground water. The free phase forms a 'pancake' in the capillary zone of the ground water and spreads laterally. If sufficient free phase accumulates interfacial forces may be overcome and the free phase migrates under gravity until buoyant forces reach equilibrium. No capillary fringe will be present

under these conditions. This will be true where the pore sizes are moderate to large and where the free phase is thickest.

The majority of pollution has migrated in an east-northeast direction, which corresponds to the regional structural framework and local orientation of the foliation in the bedrock.

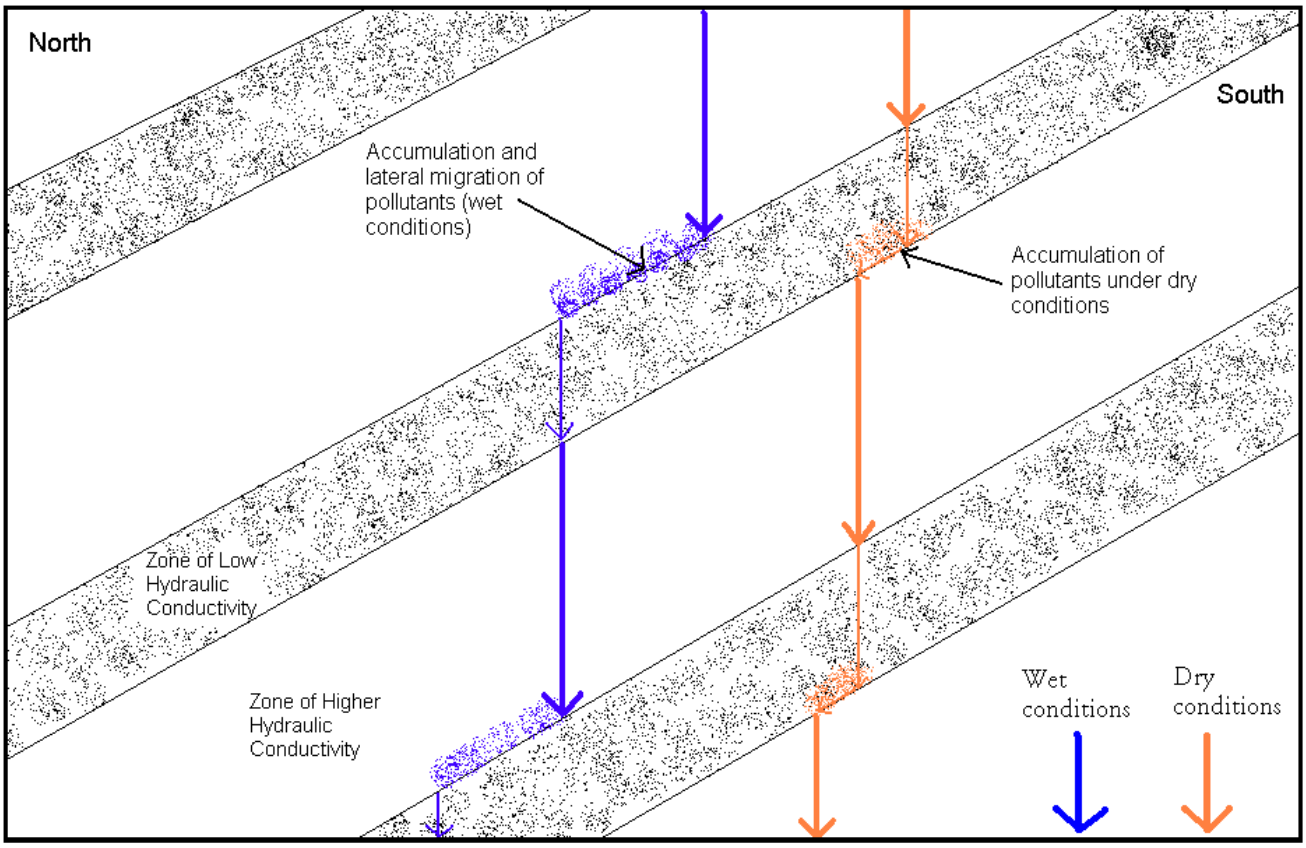

FIGURE 22: Schematic representation of theoretical migration of pollutants in the vadose zone.

4.4.1 Hydrogeological Parameters

4.4.1.1 Slug Tests

A slug is lowered into a borehole resulting in a sudden rise of the water level. This causes an increase in piezometric pressure throughout the entire borehole. Sufficient water should be displaced in order to raise the water level by approximately 10cm to 50cm. The rate at which the water level subsides is measured and gives an indication of the hydraulic conductivity of the aquifer adjacent to the borehole.

The slug test results were analysed using the Bouwer and Rice (1976) method. The borehole can be either partially or fully penetrating. The Bouwer and Rice equation is:

$$K = \frac{(r_c)^2 \ln(R_e/R)}{2L_e} \frac{1}{t} ln \frac{H_0}{H_t}$$

where, K is hydraulic conductivity [L/T]

r_c is the radius of the well casing [L]

R is the radius of the gravel envelope [L]

R_e is the effective radial distance over which head is dissipated [L]

L_e is the length of the screen or open section of the well through which water can enter [L]

H_0 is the drawdown at time t = 0 [L]

H_t is the drawdown at time t = t [L]

t is the time since H = H_0

The effective distance over which the induced head is dissipated, R_e, is also the distance away from the borehole that the average value of K is being measured. There is no way to know what the value of R_e is for a given borehole (Fetter, 1994).

A total of 53 slug tests were conducted for this investigation. The hydraulic conductivity (m/day) varied between 0.001 and 1.20 with an average of 0.143. The results for the slug tests are indicated in Table 3.

4.4.1.2 Aquifer Tests

Aquifer tests are important tools in providing information on the hydraulic and physical properties of an aquifer. The general objectives of an aquifer test are:

⇒ To obtain an understanding of the aquifer,

⇒ To quantify the aquifer's hydraulic and physical properties and

⇒ To determine the sustainable yield and efficiency of a borehole.

TABLE 3: Piezometric and fuel levels as measured on 15th January 2003 and slug test results.

BH No.	X	Y	Altitude (mamsl)	Collar Height (m)	Free Phase Level (mamsl)	Observed Piezometric Level (mamsl)	Corrected Piezometric Level (mamsl) – see pg 61	Apparent Free Phase Thickness (m)	Actual Free Phase Thickness (m)-see pg 61	Hydraulic Conductivity (m/day)
BH01	71547.67	-2561928.39	931.140	0.220	896.67	896.550	896.646	0.120	0.024	0.014
BH02	71523.86	-2561919.30	929.590	0.210	899.34	895.040	898.480	4.300	0.850	0.001
BH03	71524.85	-2561885.96	929.195	0.315	900.16	899.860	900.100	0.300	0.059	0.018
BH04	71341.49	-2561819.87	926.405	0.205	NO FUEL	891.740	891.740			0.254
BH05	71325.44	-2561933.37	928.120	0.220	NO FUEL	896.810	896.810			0.002
BH06	71401.36	-2561964.31	928.515	0.145	897.87	897.670	897.830	0.200	0.040	0.038
BH07	71456.81	-2561959.86	929.020	0.150	897.87	897.680	897.832	0.190	0.038	0.016
BH08	71455.93	-2561912.30	929.100	0.000	NO FUEL	897.870	897.870			0.015
BH09	71456.52	-2561893.07	928.980	0.000	900.02	900.000	900.016	0.020	0.004	0.005
BH10	71492.06	-2561892.97	929.240	0.000	903.10	902.840	903.048	0.260	0.051	0.018
BH11	71495.18	-2561912.77	929.390	0.000	899.47	899.340	899.444	0.130	0.026	0.018
BH12	71488.09	-2561958.79	929.705	0.125	898.04	898.020	898.036	0.020	0.004	0.013
BH13	71508.31	-2561840.75	929.145	0.355	NO FUEL	897.640	897.640			0.005
BH14	71567.52	-2561916.95	931.585	0.315	897.33	897.022	897.268	0.308	0.061	0.040
BH15	71534.04	-2561947.40	930.060	0.140	897.53	897.390	897.502	0.140	0.028	0.033
BH16	71532.37	-2561979.65	930.230	0.120	896.58	893.020	895.868	3.560	0.704	0.012
BH17	71558.97	-2561943.37	931.575	0.065	NO FUEL	896.870	896.870			0.025
BH18	71602.02	-2561939.38	931.970	0.370	893.71	893.570	893.682	0.140	0.028	0.045
BH19	71553.11	-2561897.21	930.850	0.120	897.26	897.210	897.250	0.050	0.010	0.274
BH20	71583.63	-2561877.59	931.185	0.305	895.52	895.450	895.506	0.070	0.014	0.010
BH21	71480.95	-2561465.05	926.015	0.275	NO FUEL	891.510	891.510			
BH22	71658.23	-2561968.21	932.125	0.365	NO FUEL	895.190	895.190			
BH23	71644.39	-2562006.12	931.050	0.000	NO FUEL	896.220	896.220			
BH24	71530.95	-2562043.39	930.670	0.000	896.66	895.300	896.388	1.360	0.269	
BH25	71468.11	-2561991.88	929.420	0.000	NO FUEL	896.310	896.310			
BH26	71640.66	-2561915.30	931.735	0.195	BOREHOLE DAMAGED					
BH27	71473.81	-2561868.90	928.950	0.000	899.57	899.555	899.563	0.010	0.002	
BH28	71518.33	-2562104.19	930.830	0.000	NO FUEL	895.940	895.940			
BH29	71681.31	-2561889.42	931.255	0.095	891.30	886.980	890.436	4.320	0.854	
BH30	71593.68	-2561979.76	931.520	0.130	896.51	893.200	895.848	3.310	0.654	0.018
BH31	71401.15	-2561991.29	928.890	0.000	897.27	897.200	897.256	0.070	0.014	0.006
BH32	71401.24	-2562065.85	929.485	0.365	897.09	896.590	896.990	0.500	0.099	0.041
BH33	71279.27	-2561971.07	927.540	0.000	NO FUEL	898.940	898.940			0.001
BH34	71723.99	-2561871.80	930.835	0.225	884.93	884.910	884.926	0.020	0.004	
BH35	71753.41	-2561914.19	930.835	0.255	890.75	888.310	890.262	2.440	0.482	0.076
BH36	71720.12	-2561921.79	931.340	0.300	890.85	888.090	890.298	2.760	0.545	
BH37	71749.10	-2561955.62	931.170	0.200	892.77	892.590	892.734	0.180	0.036	0.002
BH38	71798.71	-2561929.17	930.220	0.170	NO FUEL	893.610	893.610			0.002
BH39	71686.81	-2561924.53	931.665	0.345	890.40	890.120	890.344	0.280	0.055	0.005
BH40	71735.05	-2561931.57	931.225	0.285	NO FUEL	893.260	893.260			0.025
BH41	71704.52	-2561897.99	931.290	0.180	891.45	886.670	890.494	4.780	0.945	0.023
BH42	71695.29	-2561855.93	930.785	0.405	PROBE TOO SHORT					
BH43	71773.57	-2561907.17	930.440	0.190	890.64	888.490	890.210	2.150	0.425	0.115
BH44	71826.50	-2561905.49	929.930	0.100	891.82	891.610	891.778	0.210	0.042	0.003
BH45	72104.29	-2561621.81	926.695	0.225	886.73	885.870	886.558	0.860	0.170	0.092
BH46	72039.59	-2561620.76	926.655	0.245	887.17	885.580	886.852	1.590	0.314	0.017
BH47	72214.67	-2561458.44	925.350	0.360	NO FUEL	886.320	886.320			0.507
BH48	72245.00	-2561457.00	925.405	0.225	NO FUEL	886.280	886.280			0.270
BH49	72211.12	-2561460.47	926.915	0.375	NO FUEL	885.780	885.780			1.200
BH50	72262.04	-2561186.57	923.260	0.230	NO FUEL	886.230	886.230			
BH51	72497.56	-2561165.66	923.320	0.500	NO FUEL	885.780	885.780			

TABLE 3 (cont.)

BH No.	X	Y	Altitude (mamsl)	Collar Height (m)	Free Phase Level (mamsl)	Observed Piezometric Level (mamsl)	Corrected Piezometric Level (mamsl) – see pg 61	Apparent Free Phase Thickness (m)	Actual Free Phase Thickness (m)-see pg 61	Hydraulic Conductivity (m/day)
BH52	70779.85	-2561244.95	917.523	0.495	NO FUEL	892.268	892.268			0.201
BH53	70603.04	-2561125.92	916.385	0.455	NO FUEL	892.150	892.150			0.012
BH54	69609.04	-2561184.01	921.710	0.550	NO FUEL	897.770	897.770			0.066
BH55	69659.86	-2561242.50	922.705	0.555	NO FUEL	898.030	898.030			0.062
BH56	70832.22	-2561962.95	925.200	0.440	NO FUEL	896.110	896.110			0.803
BH57	71023.71	-2561720.65	922.870	0.410	NO FUEL	893.630	893.630			0.124
BH58	70904.93	-2561860.84	924.060	0.430	NO FUEL	895.780	895.780			0.103
BH59	72244.54	-2562163.20	931.165	0.335	NO FUEL	895.340	895.340			0.709
BH60	72382.85	-2562168.91	931.355	0.495	NO FUEL	895.270	895.270			0.846
BH61	72654.23	-2562249.89	934.745	0.475	NO FUEL	894.960	894.960			0.148
BH62	70882.08	-2560437.66	912.450	0.490	NO FUEL	885.620	885.620			0.114
BH63	71994.63	-2562802.51	936.900	0.490	NO FUEL	896.060	896.060			0.303
BH64	71710.18	-2562613.72	937.620	0.460	NO FUEL	898.480	898.480			0.218
BH65	71129.42	-2561321.31	920.865	0.415	NO FUEL	890.690	890.690			0.611
BH66	69661.59	-2560930.39	918.270	0.350	NO FUEL	893.400	893.400			0.002
BH67	69759.92	-2560989.32	918.945	0.415	NO FUEL	892.630	892.630			0.003
BRO6	72234.89	-2560125.52	920.000	0.000	NO FUEL	886.860	886.860			
BR11	71183.20	-2559905.18	915.000	0.000	NO FUEL	887.760	887.760			

Aquifer test data is interpreted by mathematical models that relate drawdown response to discharge in the abstraction borehole. The results obtained from short duration tests can then be extrapolated to predict the long-term performance of a borehole. In fractured rock aquifers, the geometry and permeability of the system may be large in relation to the scale of the test. Therefore conventional models developed for homogeneous porous aquifers might not be viable in fractured rock systems. For this reason a software program, FC_EXCEL was developed to analyse aquifer tests conducted in fractured rock systems (van Tonder *et al*, 2002).

The FC_EXCEL program consists of two software packages:

⇒ FC (Flow Characteristics method) and

⇒ TPA (Test Pumping Analysis).

FC software consists of the following procedures:

⇒ Porous aquifer solutions (Theis, Cooper-Jacob I and II and Hantush methods and a solution for water-table aquifers),

⇒ Step drawdown and multirate analysis,

⇒ Fractional pumping test analysis (Barker's Generalised Radial Flow Model),
⇒ Slug Test Analysis (Bouwer and Rice method),
⇒ Estimation of a risk-based sustainable yield of a borehole by using drawdown derivatives, boundary information and error propagation,
⇒ Different diagnostic plots for flow regime identification (eg. Derivatives, second derivatives, LogLog (Theis) plot, LinLog (Cooper-Jacob) plot, square root of time plot, fourth root of time plot, spherical and recovery plot and
⇒ Delineation of borehole protection zones in fractured aquifers.

TPA is a windows program and was written by Ingo Bardenhagen as part of his Ph.D. study. It was developed to fit pumping test in fractured aquifers and includes the following fractured aquifer methods:

⇒ Double porosity aquifer (Moench method),
⇒ Solutions for single vertical and horizontal fractures (Gringarten, Kazemi, Warren and Root, Stallman, including uniform flux, finite conductive and infinite conductive fractures as well as boundary conditions and a solution for a dyke aquifer),
⇒ Porous solutions and
⇒ Diagnostic plots.

TPA was specially designed as a curve fitting procedure for aquifer tests conducted in fractured aquifers (van Tonder *et al*, 2002).

The boreholes were assumed to be fully penetrating. Aquifer tests were conducted in the following boreholes, BH01, BH35, BH45 and BH55. The aim of the aquifer tests were:

⇒ Quantify possible abstraction rates for a pump and treat remediation system,
⇒ Determine the anisotropic orientation/s of the fractured aquifer system and
⇒ Determine the relationship between different fracture networks.

The results of the aquifer tests are listed in Appendix E.

Borehole BH01

A step test was conducted for a total time of 120min and consisted of 3 steps. The borehole was pumped at 0.2ℓ/s for 15min, 0.26ℓ/s for 50min and 0.38ℓ/s for 55min. The total drawdown after 120min was 11.34m.

The constant discharge test on this borehole was carried out for 482min at a pump rate of 0.42ℓ/s. The total drawdown of the water level during this period was 14.95m. Figure 23 illustrates drawdown versus time for BH01 during the constant rate test. The water level recovered to within 88% of the static water level within 360min after stopping the pump.

Throughout the duration of the constant discharge test water levels were observed in a number of observation boreholes. The drawdown measured in the observation boreholes is illustrated in Figure 24.

The measured static water level prior to the test was 35.2mbgl (896.16mamsl). Observation boreholes that had a SWL above the pumped borehole were relatively unaffected, whereas those that had a SWL below the pumped borehole showed a rise in water levels. This is possibly due to a multi fracture network where abstraction from one fracture network may result in pressure release in another and the subsequent rising of water levels.

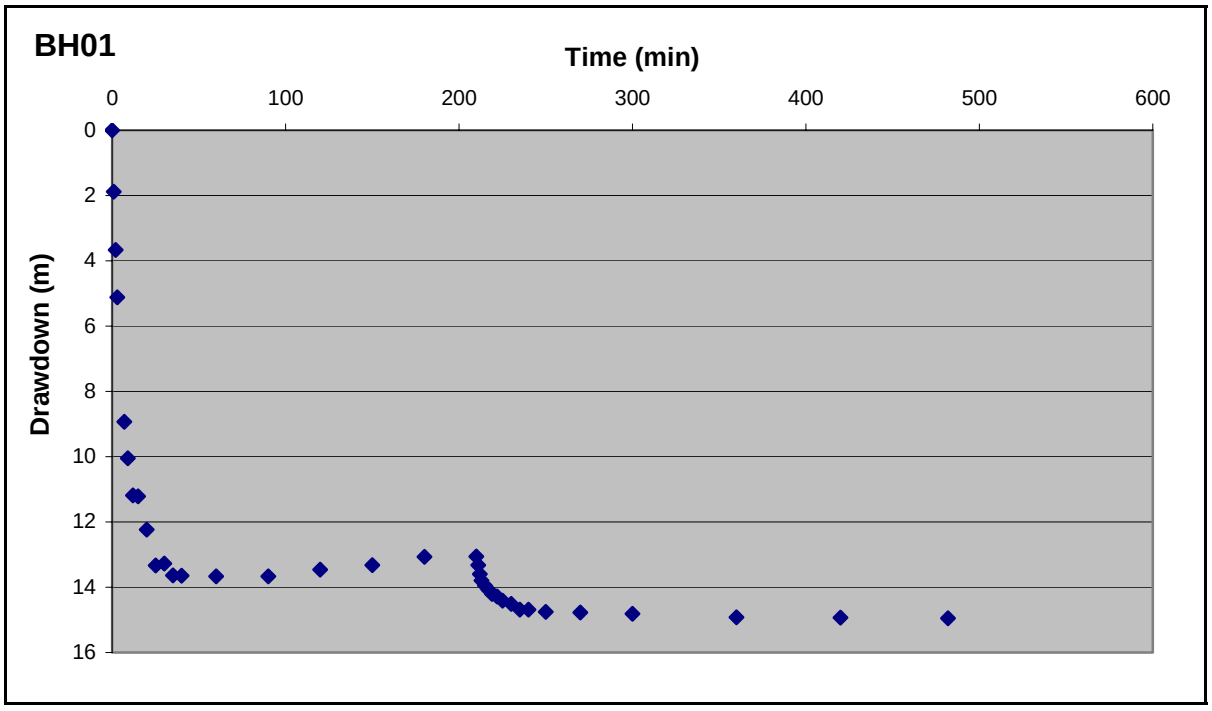

FIGURE 23: Drawdown versus time for BH01 during constant rate aquifer test.

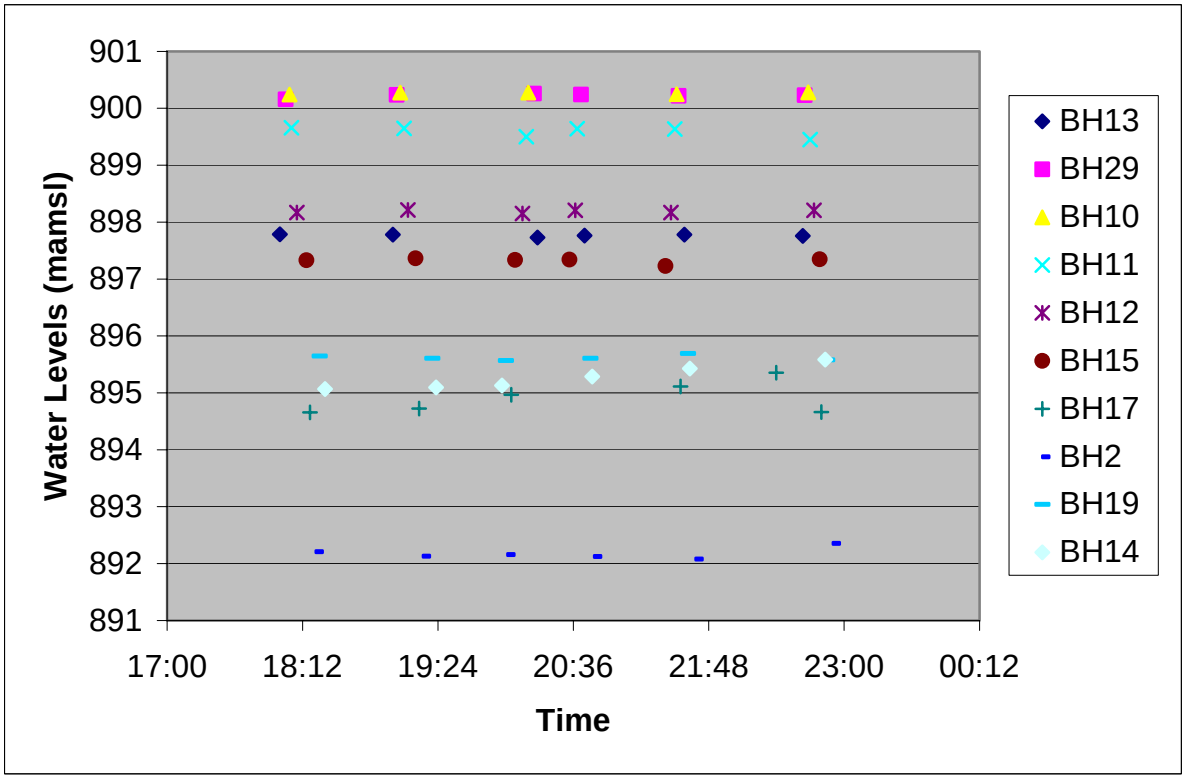

FIGURE 24: Measured water levels versus time for observation boreholes during a constant discharge test conducted on borehole BH01.

Borehole BH35

The step test was conducted for a total time of 169min and consisted of 5 steps. The borehole was pumped at 0.02ℓ/s for 63min, 0.88ℓ/s for 12min, 0.5ℓ/s for 37min, 0.22ℓ/s for 19min and 1ℓ/s for 38min. The total drawdown after 169min was 4.41m.

The constant discharge test was conducted for 480min at a pump rate of 0.3ℓ/s. The total drawdown of the water level during this period was 1.46m. Figure 25 illustrates drawdown versus time for BH35 during the constant rate test. The water level recovered to within 73% of the static water level within 420min after stopping the pump.

Throughout the duration of the constant discharge test water levels were measured in a number of observation boreholes. The water levels measured in observation boreholes are illustrated in Figure 26.

The measured static water level prior to the test was 42.76mbgl (888.33mamsl). The measured drawdown (value in brackets) for observation boreholes is listed in descending order of magnitude, BH36(0.98m), BH41(0.56m), BH40(0.16m), BH38(0.16m), BH44(0.14m) and BH37(0.09m). The most drawdown was observed in BH41 and BH36 which both had static water levels with a similar elevation to the pumped borehole prior to the pump test. Observation boreholes with shallower water levels showed the least change.

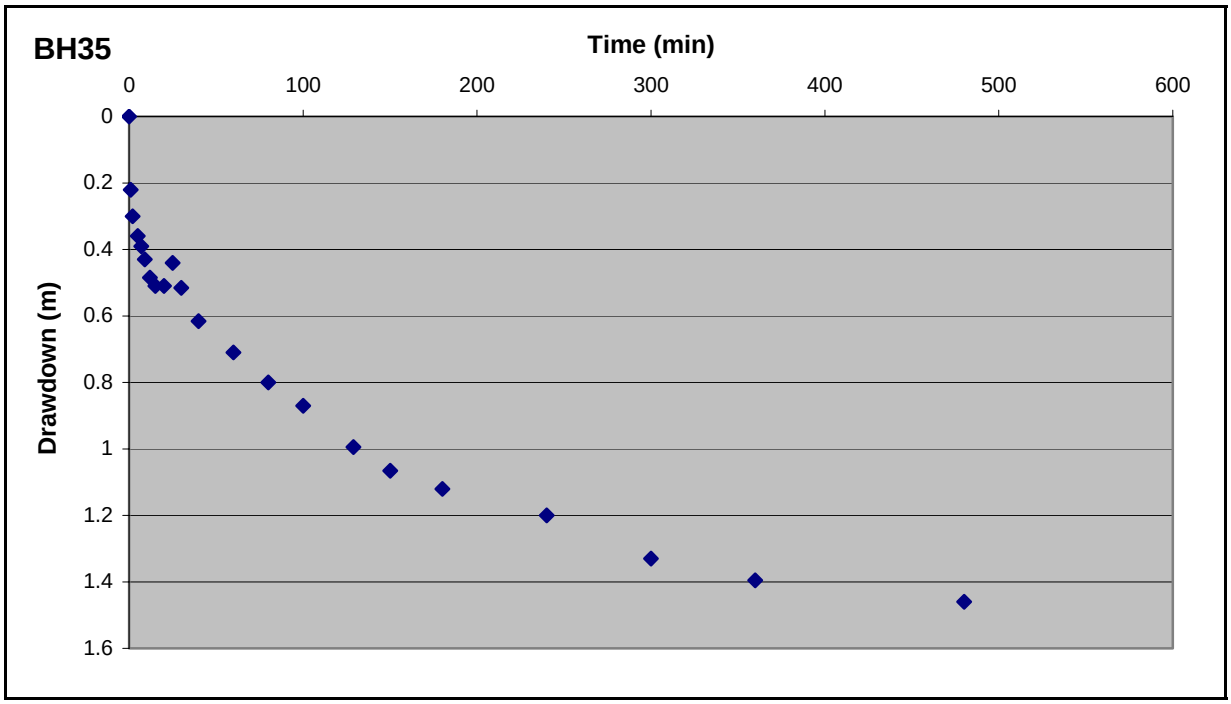

FIGURE 25: Drawdown versus time for BH35 during constant rate aquifer test.

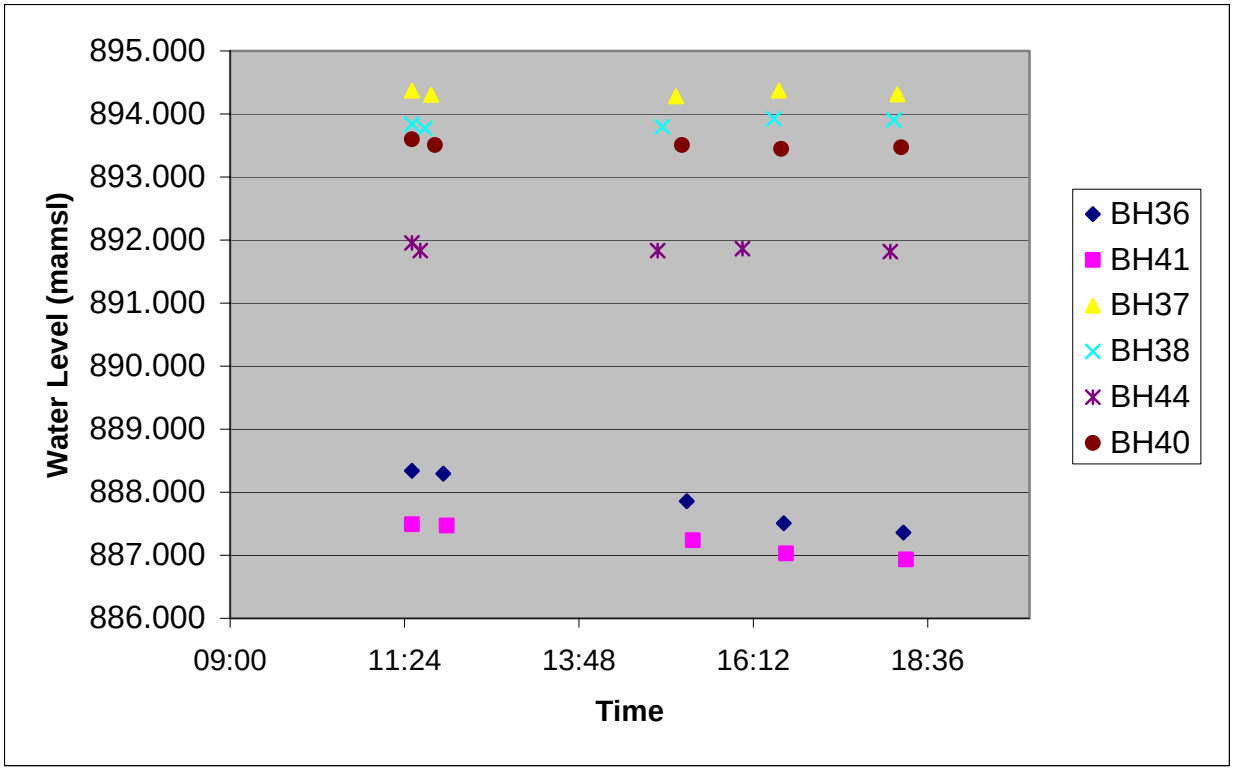

FIGURE 26: Measured water levels versus time for observation boreholes during a constant discharge test conducted on borehole BH35.

Borehole 45

The step test consisted of four abstraction rates and was conducted for a total time of 175min. The borehole was pumped at 0.4ℓ/s for 30min, 0.6ℓ/s for 25min, 1ℓ/s for 60min and 1.5ℓ/s for 60min. The total drawdown after the duration of the test was 2.41m.

The borehole was pumped at a constant rate of 0.27ℓ/s over a period of 480min. The total drawdown of the water level over this period was 2.92m. Figure 27 illustrates drawdown versus time for BH45 during the constant rate test. The water level recovered to within 97% of the original water level after 60min of the pump being stopped.

The static water level prior to the test was 41.84mbgl (885.08mamsl). Observation borehole BH46 had the most drawdown of 0.62m while the remaining boreholes remained relatively constant through out the duration of the test (Figure 28).

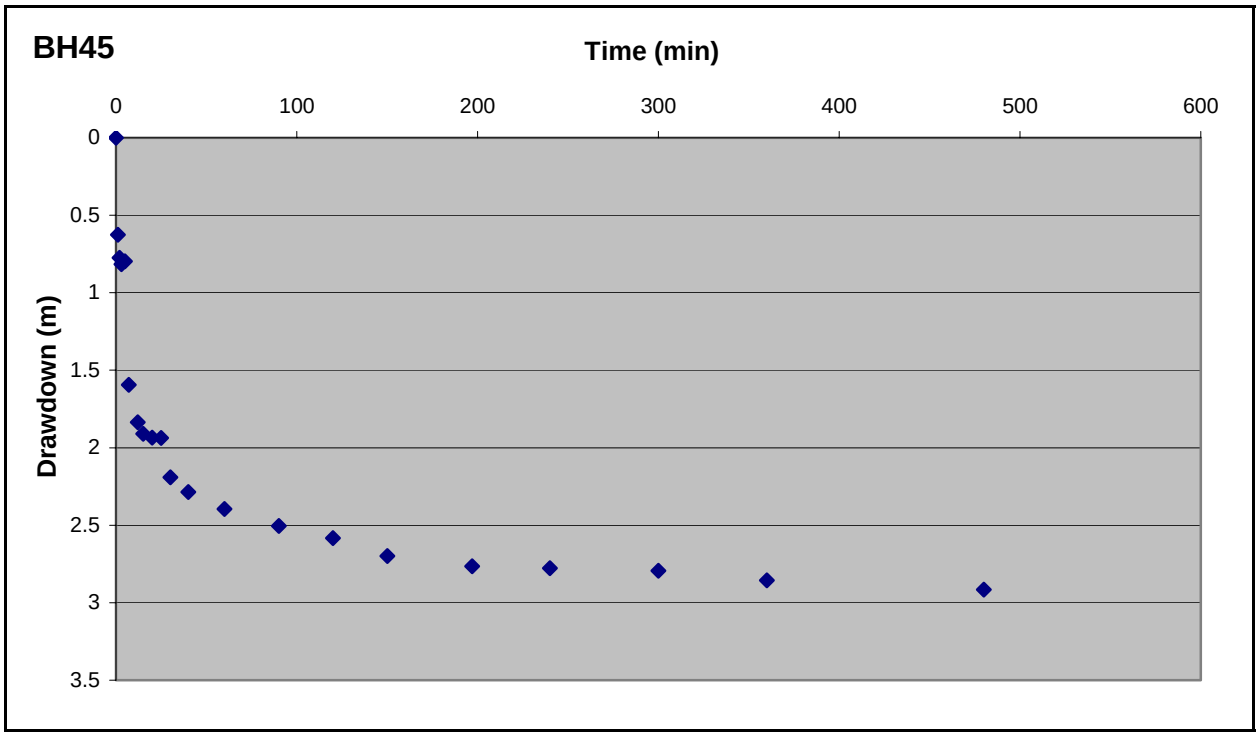

FIGURE 27: Drawdown versus time for BH45 during constant rate aquifer test.

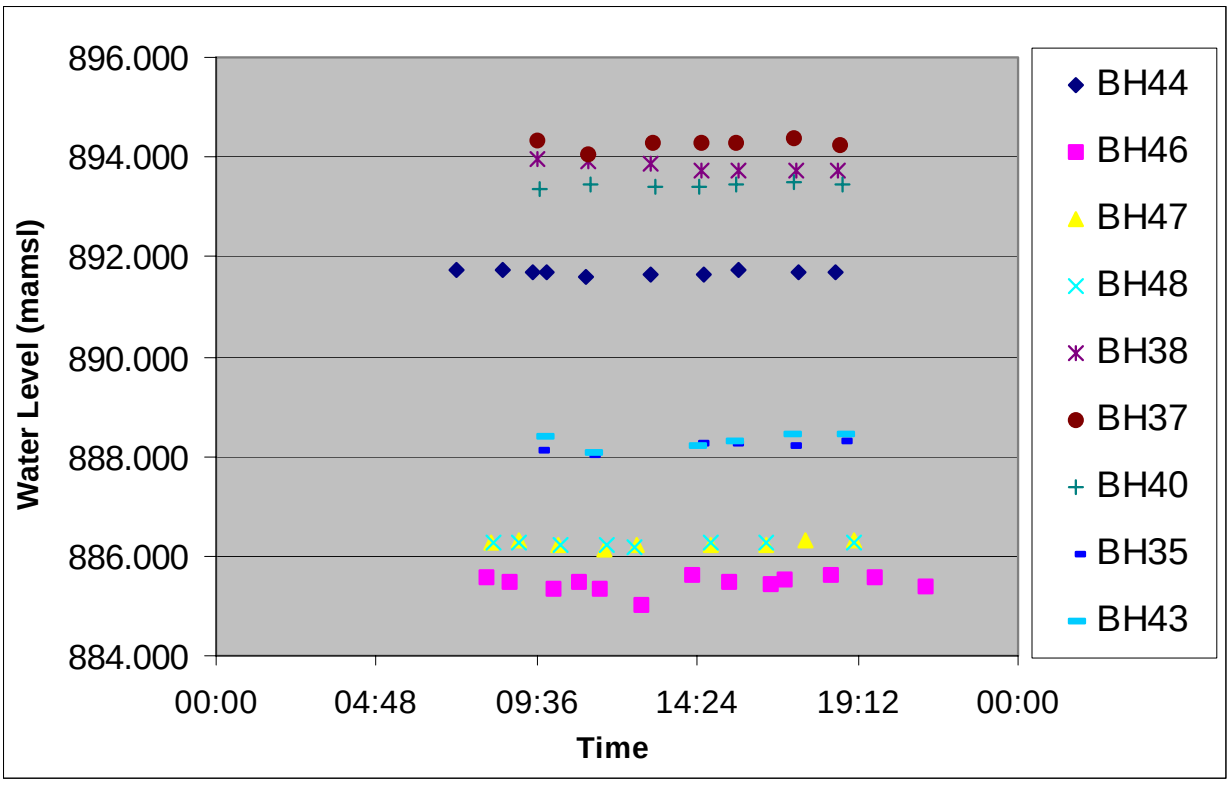

FIGURE 28: Measured water levels versus time for observation boreholes during a constant discharge test conducted on borehole BH45.

Borehole 55

The pumping rate varied significantly during the duration of the step test. No definite steps could be determined from the pumping rates. The average pump rate over a period of 184min was 0.31ℓ/s. The total drawdown over this period was 25.54m.

The constant discharge test consisted of pumping the borehole at a rate of 0.27ℓ/s over a period of 450min. The total drawdown of the water level was 23.24m. Figure 29 illustrates drawdown versus time for BH55 during the constant rate test. The water level recovered to within 94% after 240min of stopping the pump.

The static water level prior to the test was 26.95mbgl (896.31mamsl). Observation borehole BH54 showed the largest drawdown of 0.20m, borehole Bh66 remained constant. The water level in BH67 rose by 0.17m over the duration of the test (Figure 30).

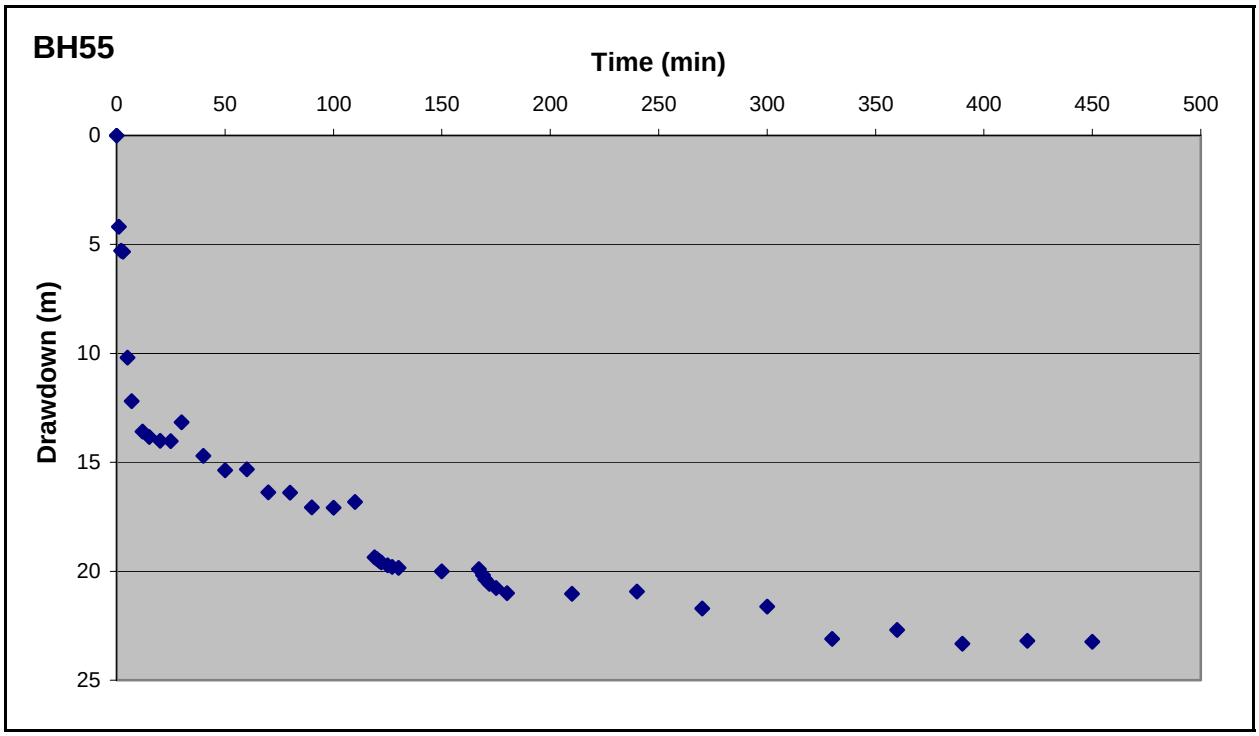

FIGURE 29: Drawdown versus time for BH55 during constant rate aquifer test.

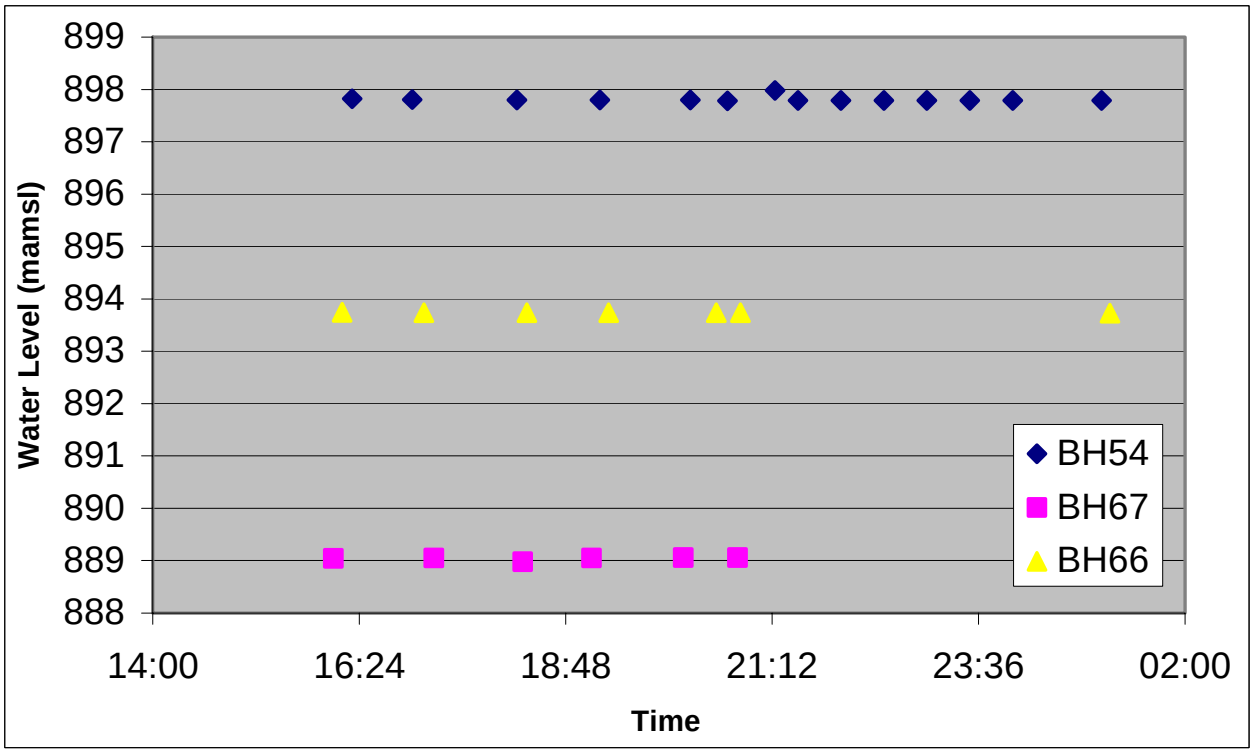

FIGURE 30: Measured water levels versus time for observation boreholes during a constant discharge test conducted on borehole BH55.

4.4.1.3 Aquifer test results

The recommended abstraction rate of water for the boreholes is 0.01ℓ/s (BH01), 0.02ℓ/s (BH55), 0.17ℓ/s (BH35) and 0.20ℓ/s (BH45). The rise of water levels in observation boreholes during the aquifer test in borehole BH01 illustrates the complexity of fractured rock aquifers. The aquifer test conducted on BH35 illustrated a preferential drawdown in a west-southwest (BH36) direction followed by an east-northeast (BH41) direction. This illustrates a preferential flow direction in an ENE-WSW direction, which corresponds to the orientation of the foliation as well as the migration of pollutants.

4.4.2 Recharge

A study was conducted by Bredenkamp *et al* (1995) at Dendron, which lies approximately 35km south west of the AFB (Figure 1). The method used to determine recharge was the comparison of measured chloride concentrations in rainwater with that in the ground water. The climate, lithology and structural history of this site is similar to that of the AFB. Recharge inferred from chloride profiles was 6.78mm/a or 2% of the mean annual precipitation (MAP). A recharge of 2% of the MAP for L.T.AFB equates to 7.8mm/a.

A ground water recharge study conducted by Beekman *et al* (1996) explored the relationship between recharge and annual rainfall. The relationship is according to the following function:

$$y = 148(x) - 880$$

where y is recharge (mm/a) and x the annual rainfall. A recharge of 2.99mm/a or 0.77% of the MAP is obtained when using the above method for L.T.AFB.

4.4.3 Piezometric and Free Phase Levels

Water and free phase levels were measured using an interface probe. The free phase level is detected by a sensor located at the front of the probe, which sets off an alarm when within close proximity to the free phase. A second alarm sounds once the probe has passed through

the free phase and enters water. The second alarm sounds when current is conducted between two brass rings. The different electrical conductive properties of the free phase and water allow the use of such a probe. If no free phase is present both alarms sound simultaneously.

Water and free phase levels were taken on a daily basis for the boreholes that were bailed (see Section 6.2.1). The levels were taken on a monthly basis for all the boreholes. The bailing operation was discontinued prior to the monthly water and free phase levels being measured. This ensured that the aquifer system was in a relative state of equilibrium during the monthly measurements. Water and free phase levels measured on the 15th January 2003 are presented in Table 3.

4.4.3.1 Piezometric Levels

The measured piezometric levels varied between 24 and 46mbgl, with an average of 34mbgl. A profile from west to east through the pollution plume is illustrated in Figure 31. The localised peak in the graph is due to elevated water levels measured in boreholes drilled through the asphalt layer at Movements 2. An analysis of the inorganic chemical data from these boreholes, indicate elevated concentrations of Na, Mg and Cl which do not correspond to background aquifer values (Figure 44 and 45). This is discussed further under Section 4.5.2.1.

The water level measured in boreholes with free phase is lower than the actual static water level (SWL). The free phase thickness measured in the borehole is an apparent free phase thickness and does not represent the actual free phase thickness in the adjacent aquifer (Figure 32). This is due to the absence of capillary forces in the borehole, which exist in the adjacent aquifer. The degree of water level suppression is governed by the difference in densities between the jet fuel and water.

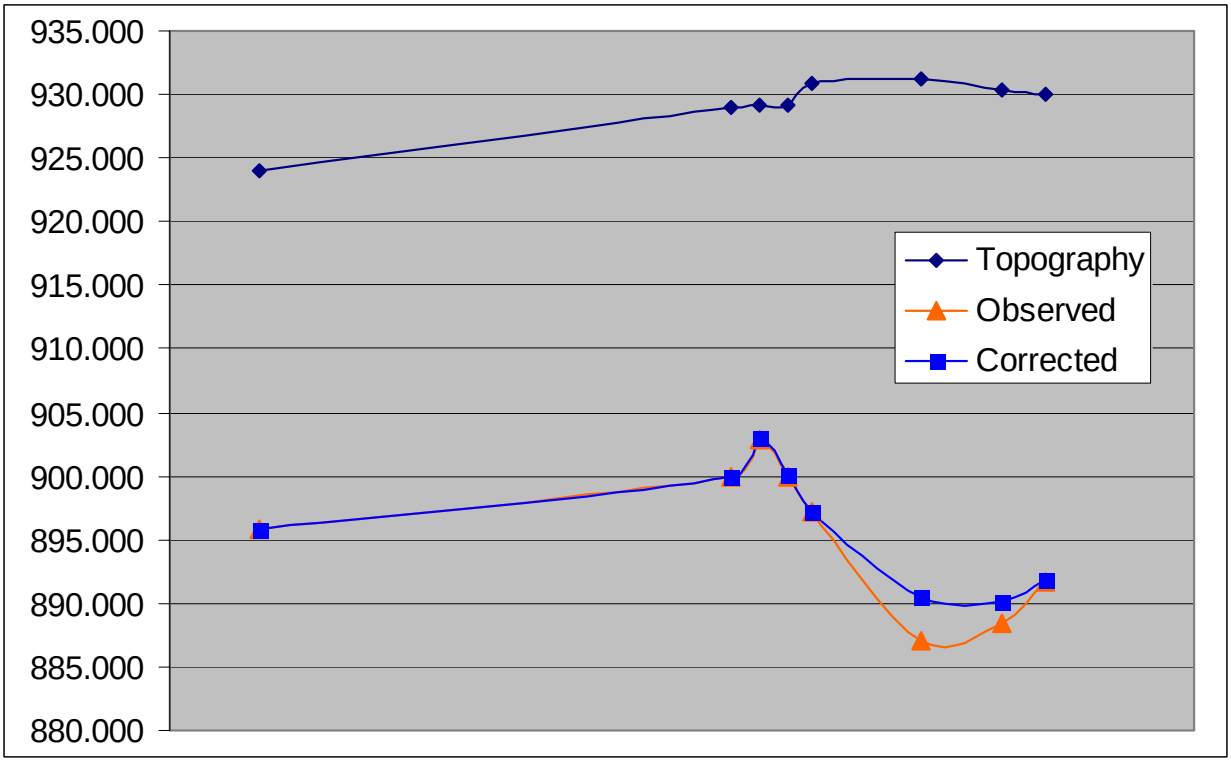

FIGURE 31: Profile of piezometric levels from west to east (from left to right BH58, BH09, BH10, BH03, BH19, BH29, BH43 and BH44).

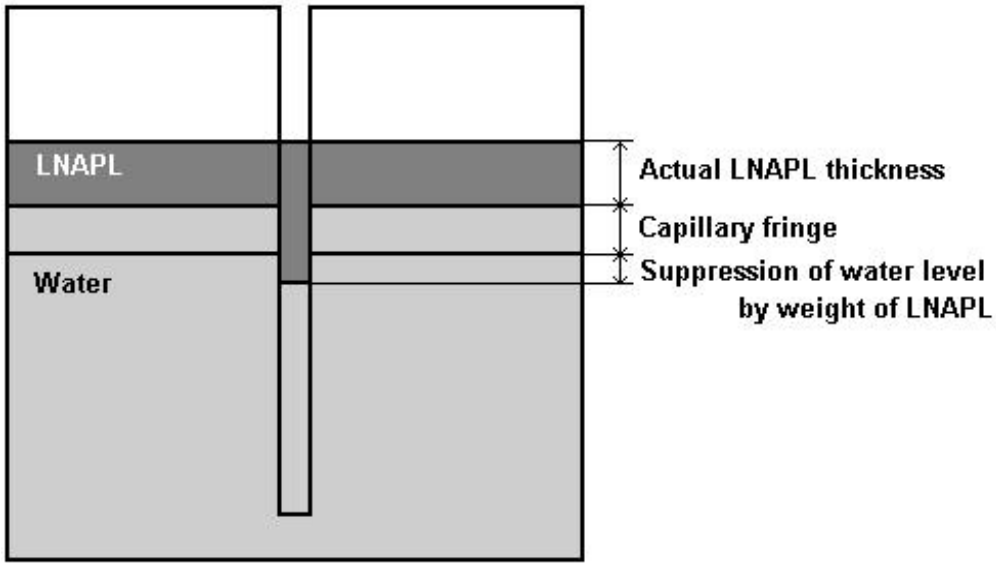

FIGURE 32: Schematic diagram of the factors determining apparent free phase thickness (Dippenaar, 2002).

A substantial amount of data was collected during the bailing operation. The data analysed below was collected over the period 30th April 2001 to 23rd May 2003. The boreholes listed in Table 4 had the largest number of available measurements. This is due to the fact that 84% of the total volume of fuel removed was bailed from these boreholes.

The apparent free phase thickness in the boreholes reduced on a daily basis as fuel was bailed. When plotting apparent free phase thickness in metres versus depth of the water and free phase level in metres below ground level (mbgl), the points plotted on two lines which intersect the X-axis where the apparent free phase thickness is zero (Figure 33). The free phase level and water level converged to a single point as the apparent free phase thickness tends towards zero. The point where the two lines intersect is the static water level (SWL) as there is no free phase in the borehole suppressing the water. If the SWL and the maximum free phase level is obtained from the graph, then the maximum true free phase thickness of the pollution plume in the adjacent aquifer can be calculated by subtracting the maximum free phase level from the SWL. The maximum free phase level is the shallowest measured free phase level, which corresponded with the maximum apparent thickness value in Table 4. The results obtained from the graphs for boreholes where the data follows the above-mentioned trends are indicated in Table 4.

The best results were obtained from boreholes that were bailed regularly and had an apparent free phase thickness of more than 1.6m. The volume of fuel bailed from boreholes that were analysed varied between 1300 to 92800 litres over the two and a half year period.

The above analysis does not take into account the capillary fringe, as illustrated in Figure 32. Capillary forces may however be overcome where the pore spaces in the aquifer are of medium to large size and where the free phase LNAPL plume is very thick. The LNAPL plume will migrate under the force of gravity until buoyant forces hold the plume up. Under these conditions Figure 34 will be more realistic and is used to determine the actual LNAPL thickness for a number of boreholes.

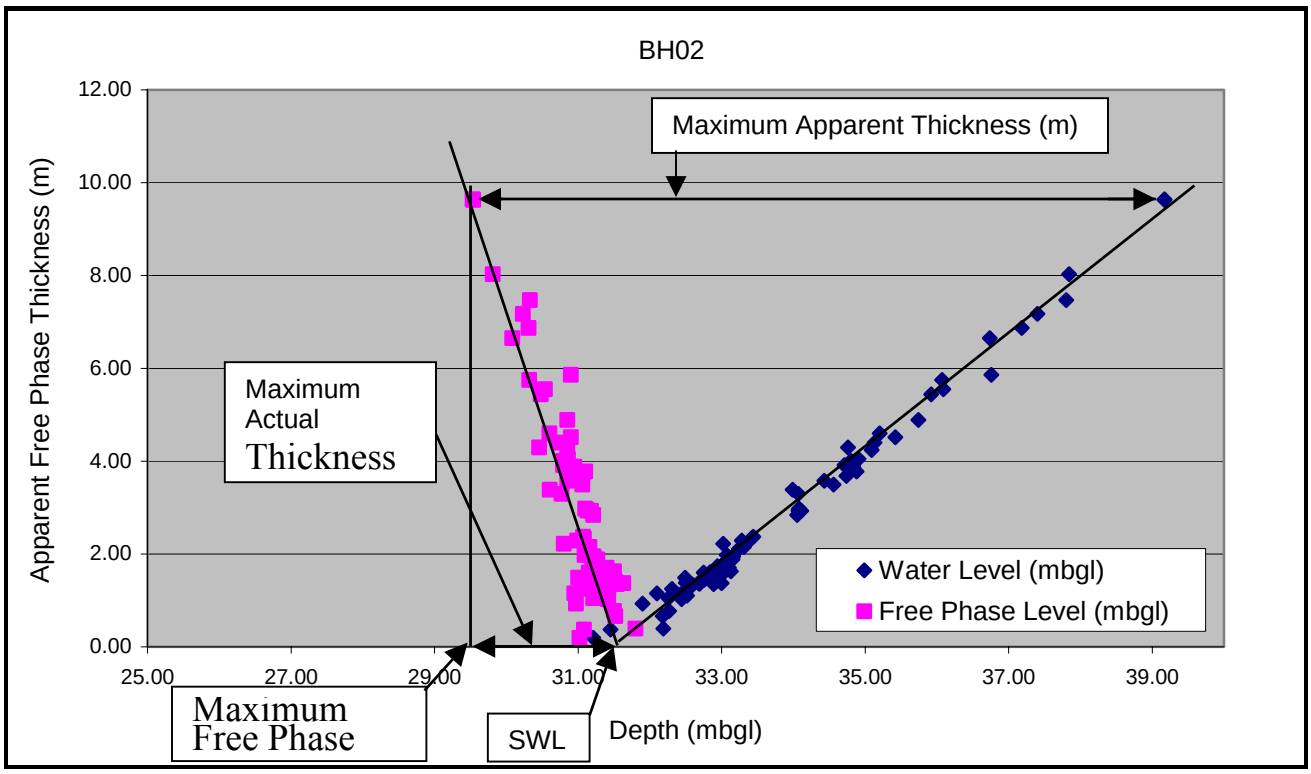

FIGURE 33: Analysis of bailing data for BH02 collected over the period 30th April 2001 to 5th May 2003.

TABLE 4: Results obtained from plotting apparent free phase thickness versus free phase and water levels.

Borehole Number	Maximum Free Phase Level (mbgl)	Static Water Level (mbgl)	Maximum Apparent Thickness (m)	Maximum Actual Thickness (m)	Ratio of Apparent to Actual Thickness	Gradient of Free Phase Level	Gradient of Water Level	Ratio of Free Phase to Water Level Gradient
BH02	29.54	31.50	9.63	1.96	4.91	-5.15	1.25	4.12
BH06	29.69	30.60	3.72	0.91	4.09	-3.98	1.29	3.09
BH10	27.11	28.16	7.45	1.05	7.10	-6.54	1.21	5.40
BH16	33.21	33.95	3.56	0.74	4.80	-4.94	1.29	3.84
BH24	33.52	33.92	1.43	0.40	3.59	-3.48	1.25	2.78
BH29	38.48	40.61	9.80	2.13	4.60	-4.69	1.18	3.99
BH30	34.72	35.38	3.16	0.66	4.77	-4.63	1.27	3.65
BH35	39.42	40.65	6.20	1.23	5.02	-4.98	1.25	3.97
BH36	39.95	41.04	6.38	1.09	5.87	-5.59	1.21	4.63
BH41	39.19	40.96	8.42	1.77	4.76	-4.51	1.29	3.50
BH43	39.07	40.07	6.20	1.00	6.19	-6.10	1.22	4.98
				Average	5.06	-4.96	1.25	4.00

The ratio of h to H is primarily dependant upon the different densities of the two immiscible fluids. The mass of the fuel in the borehole should equal the mass of water it has displaced. This leads to the following equation:

$\Rightarrow$ H x Area x Density of fuel (ρ_F) = (H - h) x Area x Density of water (ρ_w)

The areas are identical, therefore:

$\Rightarrow$ $H \times \rho_F = (H - h) \times \rho_w$

Which can be rewritten as:

$$\Rightarrow \frac{H - h}{H} = \frac{\rho_F}{\rho_W} \qquad \text{OR} \qquad \frac{h}{H} = 1 - \frac{\rho_F}{\rho_W}$$

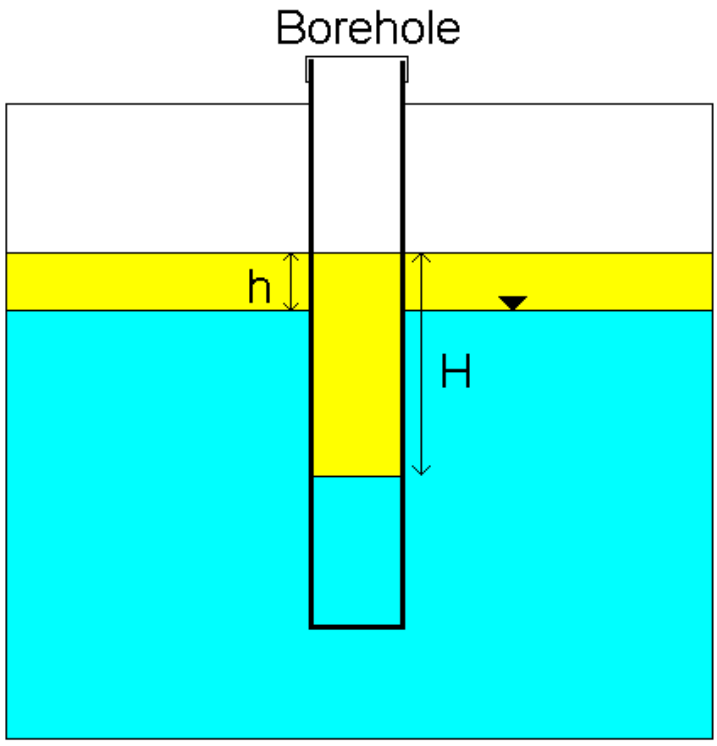

FIGURE 34: Simplified schematic representation of apparent free phase thickness (H) and true free phase thickness (h).

If a value of 0.834 (density of 100% kerosene) is used for the density of fuel and 1 for the density of water, then:

$$\Rightarrow \frac{h}{H} = 1 - \frac{0.834}{1} = 0.166$$

However when using the results obtained in Table 4 the density of fuel can be calculated as the ratio of actual thickness to apparent thickness, therefore:

$$\Rightarrow \frac{h}{H} = \frac{1}{5.06} = 0.198$$

$$\Rightarrow \frac{h}{H} = 1 - \frac{\rho_F}{\rho_W} = 0.198$$

$$\Rightarrow 1 - \frac{\rho_F}{1} = 0.198$$

$$\Rightarrow \rho_F = 1 - 0.198 = 0.802$$

The difference between the theoretical and calculated value is probably due to the interaction of the fuel with the lithology and ground water of the aquifer. The actual free phase thickness values represented in Table 3 are calculated according the following expression:

$$\Rightarrow h = \frac{H}{5.06}$$

Dippenaar (2002) compared both direct field approaches and empirical techniques to determine the actual LNAPL thickness at L.T.AFB. The results of the study are listed in Appendix F. The above expression was used to determine the actual LNAPL thickness

and corrected water levels and not those obtained by Dippenaar (2002) for the following reasons:

- The corrected water levels used to calibrate the numerical model (Section 5) were measured on the 15th January 2003 whereas those used by Dippenaar (2002) were measured on the 2nd February 2002.
- According to Dippenaar (2002) the best results were obtained when using the Huges bail test and the Empirical method (After CONCAVE). These results are listed in Appendix F. The results obtained in Table 3 and 4 on page 46 and 60 respectively are comparable to these results and
- The Huges bail test was only conducted on selected boreholes that had significant free phase, i.e. the largest apparent free phase values.

4.4.3.2 Free Phase Levels

The free phase levels varied between 26 to 46mbgl over the site. The apparent free phase thickness varied from 0m to 10.2m. The apparent free phase thickness in boreholes has decreased due the bailing operation (Figure 56 see Emergency Measures of page 98). The distribution of apparent free phase thickness (m) and free phase levels (mamsl) are illustrated in Figure 35 and 36 respectively.

The free phase plume extents in an ENE-WSW direction. In Figure 35 the plume is illustrated as very broad in a northeasterly direction. This is however only the case due to a lack of observation points adjacent to BH45 and BH46 as well as the relatively high free phase values in these boreholes. The plume would more realistically be a narrow zone of free phase restricted to fracture zones.

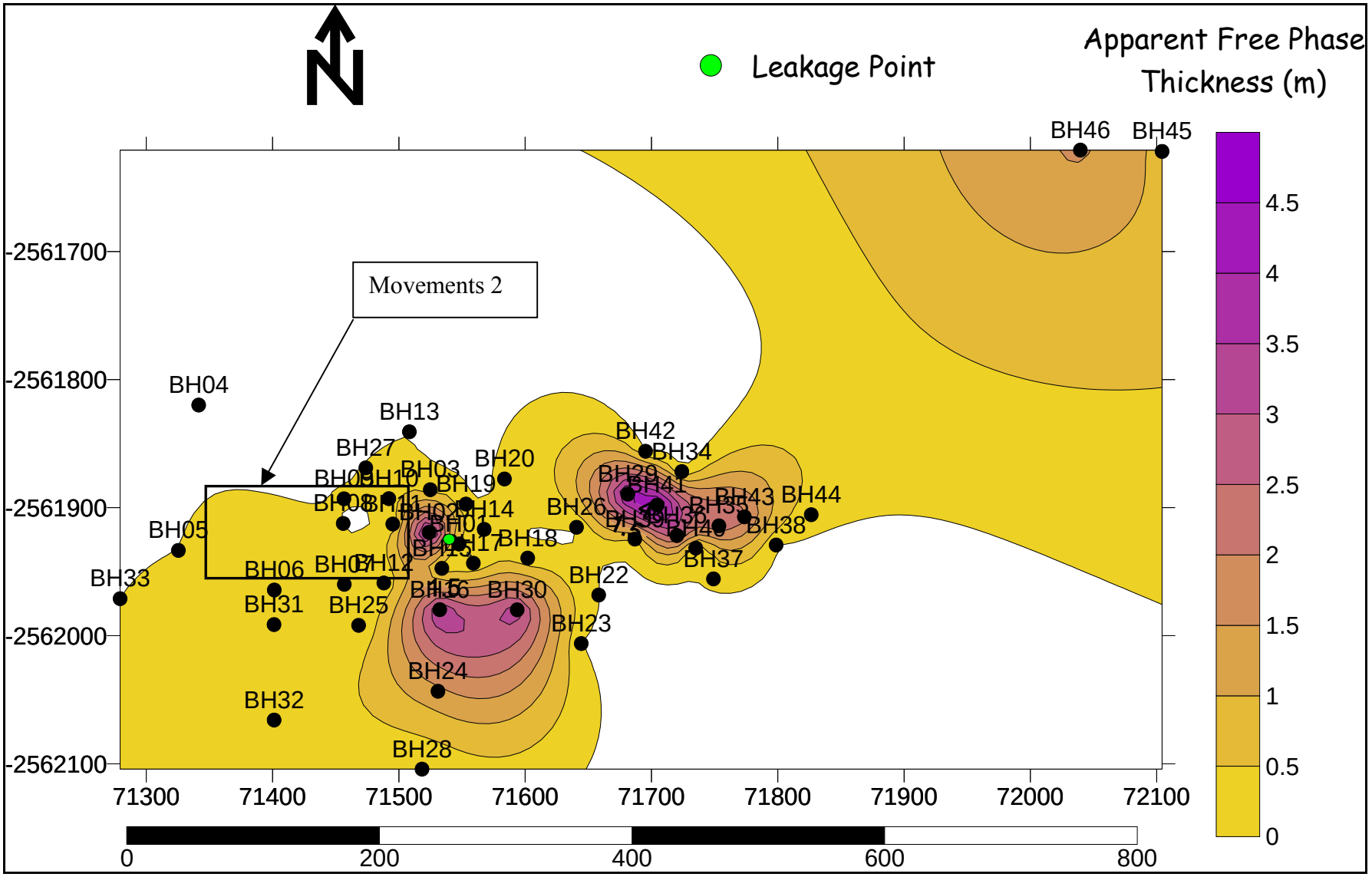

FIGURE 35: Apparent free phase thickness (m) as measured on the 15th January 2003.

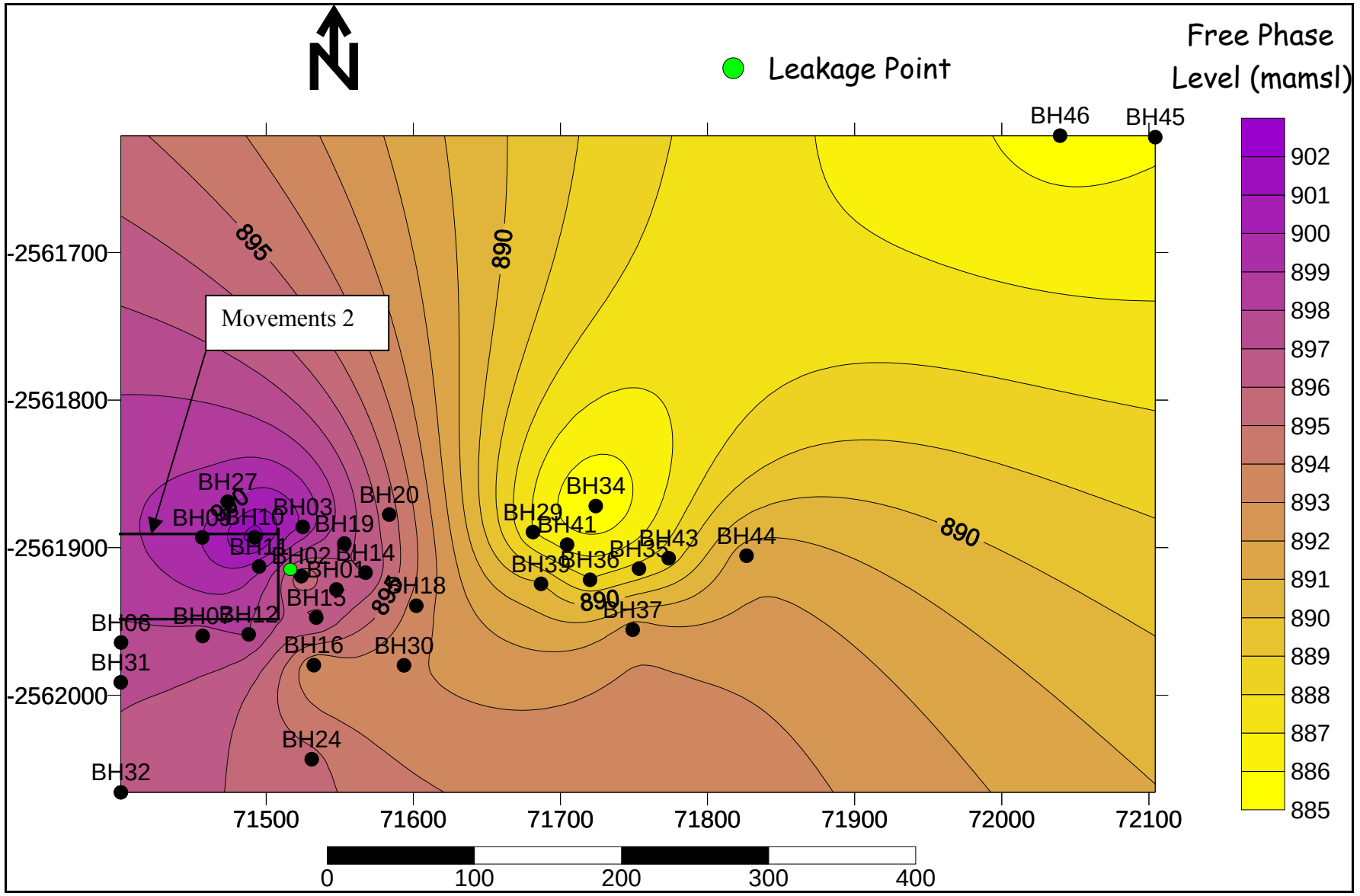

FIGURE 36: Free phase level (mamsl) as measured on the 15th January 2003.

4.5 Water Chemistry

4.5.1 Water Samples

4.5.1.1 Sampling Procedure

Once a borehole is installed and developed, a method of removing the water from the borehole must be selected. There are a large number of different devices commercially available for this task. The method selected for sampling should not alter the chemistry of the sample from when it is taken till it reaches the laboratory. This may occur if the sampler (pump, bailer etc.) is manufactured from materials that could either leach compounds into the sample or absorb compounds from the sample.

Taking the above considerations into account a semi transparent bailer manufactured of inert materials was selected. The bailer consists of a disposable polyethylene tube, which has a valve at both ends. This feature allows water to pass through the bailer as it is lowered down the borehole. Once the tube is at the desired sampling depth and is withdrawn from the borehole, the upper valve prevents water from entering the tube and the lower valve prevents water inside the tube from exiting.

To prevent cross contamination of samples, a bailer and rope was designated to each borehole that formed part of the routine monitoring network.

4.5.1.2 Storage

Jet fuel comprises of compounds that degrade relatively rapidly in the presence of oxygen and medium to high temperatures. For this reason airtight glass bottles were used to store and transport samples. No space was left in the cap of the bottle, which limited contact of the sample with air. The samples were stored and transported in a cooler box filled with ice and taken to the laboratory within 24 hours of being taken.

4.5.2 Water Quality

4.5.2.1 Organic Chemistry

Two pollution plumes are present within the aquifer, namely a free phase and dissolved phase plume. The free phase plume consists of immiscible free product on top of the ground water as well as in the capillary zone, while the dissolved phase plume consists of dissolved pollutants migrating in the ground water. Extremely high levels of organic pollutants are present in the ground water below the free phase. Levels of pollution decrease rapidly further from the free phase plume. Sampling has determined that ground water pollution is restricted to within the boundaries of the AFB. This is due to the low hydraulic conductive properties of the aquifer in the immediate area where the leak occurred. The results of the organic analysis on samples are listed in Appendix G.

The organic compounds from petroleum in the contaminated samples can be grouped into three groups according to certain chemical properties. These are:

(i) Aromatic compounds. This group includes volatile compounds such as benzene, toluene, ethyl benzene and xylene. Not all of these compounds were found in all contaminated samples, but all contaminated samples contained at least some of these compounds

(ii) Petroleum hydrocarbons. This group includes single and double bonded paraffins and olefins with chain lengths varying from 10 to 25 carbon atoms. These compounds were present in the contaminated samples to varying degrees. They have an oily nature and their boiling points are higher than that of water, with the result that they are not volatile at normal physiological temperatures. They are soluble in organic solvents and certain detergents. Upon contact with plants, insects and other animals, these compounds will coat the organism with an oily layer that will result in the eventual death of the organism. Under dry conditions these compounds will cover the soil particles, thus changing the water dispersion and holding capacity of the soil as well as the ion exchange capacity of the soil particles. Soils become fatty and unsuitable for

normal plant growth. Many soil microorganisms will be affected negatively by the presence of these compounds.

(iii) PAH's. This group include compounds such as naphthalene and naphthalene derivatives. Naphthalene is a volatile compound with insecticidal properties. These compounds are toxic to insects and animals.

The presence of these organic compounds in the soil water is a clear indication of petroleum pollution. Contaminated water is unsuitable for human and animal consumption and cannot be used for irrigation purposes (Whitehead, 2002).

Risk assessment

In order to determine the risk posed by the organic pollutants to human health a Risk Based Corrective Action (RBCA) Tier 1 assessment was conducted. The water quality from BR06 and BR11 was used for the assessment as these boreholes were being used for domestic purposes on the AFB. The results are summarised in Table 5.

The risk assessment uses measured contaminant concentrations and site specific information to calculate the numerical risk that the pollutants pose to human health. The carcinogenic risk is unacceptable if it exceeds 1:100 000 (>1.0E-05). The results indicate that the water poses an unacceptable health risk with carcinogenic values greater than 1.0E-04.

The hazard quotient is calculated for non-carcinogenic contaminants, which may induce a negative effect in sensitive populations if they are exposed to that specific concentration. A hazard quotient of larger than 1 indicates a non-carcinogenic risk. The results indicate an unacceptable risk through inhalation during showering for a resident child (VNM & Ass., 2002).

The numerical risk posed due to the domestic use of water from BR06 and BR11 is difficult to determine for the following reasons:

- The water from these two boreholes was supplemented with uncontaminated water from boreholes adjacent to the Sand River.
- The boreholes were drilled and water quality samples were taken during December 1998. The water quality samples indicate similar inorganic results as that obtained during 2002 and 2003. No analysis was conducted for organic compounds.
- The origin of contamination in these two boreholes is uncertain, as previous spills have occurred on the AFB.

TABLE 5: Summary of RBCA Tier 1 analysis (VNM & Ass., 2002).

SUMMARY OF CARCINOGENIC RISK For Ground Water					
CASE 1: Child Resident - Typical					
	Ingestion of Ground Water	Dermal Contact Shower	Inhalation During Shower	Ingestion of Irrigation Water	Total
Benzene	3.10E-04	1.10E-05	2.20E-04	1.80E-07	5.40E-04
TOTAL	**3.10E-04**	**1.10E-05**	**2.20E-04**	**1.80E-07**	**5.40E-04**
CASE 2: Adult Resident - Typical					
	Ingestion of Ground Water	Dermal Contact Shower	Inhalation During Shower	Ingestion of Irrigation Water	Total
Benzene	2.20E-04	9.20E-06	7.00E-05	5.70E-08	3.00E-04
TOTAL	**2.20E-04**	**9.20E-06**	**7.00E-05**	**5.70E-08**	**3.00E-04**
SUMMARY OF HAZARD QUOTIENTS For Ground Water					
CASE 1: Child Resident - Typical					
	Ingestion of Ground Water	Dermal Contact Shower	Inhalation During Shower	Ingestion of Irrigation Water	Total
Naphthalene	8.50E-02	9.60E-03	9.20E-01	4.90E-05	1.00E+00
TPH Aromatic C10 – 12	6.30E-01	8.90E-02	2.80E-01	3.60E-04	1.00E+00
TOTAL	**7.10E-01**	**9.90E-02**	**1.20E+00**	**4.10E-04**	**2.00E+00**
CASE 2: Adult Resident - Typical					
	Ingestion of Ground Water	Dermal Contact Shower	Inhalation During Shower	Ingestion of Irrigation Water	Total
Naphthalene	4.00E-02	5.60E-03	2.00E-01	1.00E-05	2.40E-01
TPH Aromatic C10 – 12	3.00E-01	5.20E-02	6.00E-02	7.70E-05	4.10E-01
TOTAL	**3.40E-01**	**5.70E-02**	**2.60E-01**	**8.70E-05**	**6.50E-01**

4.5.2.2 Inorganic Chemistry

Water samples were analysed for a number of inorganic elements and compounds. Samples were taken on the 5th February 2002 and 8th January 2003. The samples taken on the 8th January 2003 were analysed in the field using hand held instruments. Samples were also submitted to the laboratory for analysis on the 9th January 2003. The results are presented in Appendix G. The inorganic chemistry is important in order to quantify effects that the pollutants have on the natural environment. Parameters such as pH and oxidation-reduction potential are also discussed in this section.

The hydrochemical classification of the ground water according to the piper diagram (Figure 37) indicates that for cations there is a tendency towards magnesium type, however the majority of points plot in the no dominant type area. For cations the ground water is between bicarbonate and chloride type.

High levels of iron and manganese are regularly found in aquifers contaminated with petroleum hydrocarbons. The hydrocarbons act as an organic food source for indigenous microorganisms, which utilise oxygen as the main electron receptor. With time the oxygen level in the aquifer drops and the environment changes from an oxidising to reducing. This will result in insoluble Ferric (Fe^{3+}) iron and Mn being preferred over oxygen as an electron acceptor and reduced to a more soluble oxidation state (Fe^{2+}). Elevated levels of iron and manganese is expected in and down stream of the organic pollutants. This is what is observed at L.T.AFB (Figure 38 to 41). The elevated levels of iron were not from the casing of the boreholes as the casing never intersected the water or free phase levels and all the boreholes were fitted with the identical type of casing. The average pH for both contaminated and uncontaminated samples is 7.65 which indicates slightly alkaline ground water.

Aerobic degradation or the organic pollutants is probably taking place, however as the oxygen content decreases anaerobic degradation may take over. The anaerobic degradation of organics is less effective than aerobic degradation.

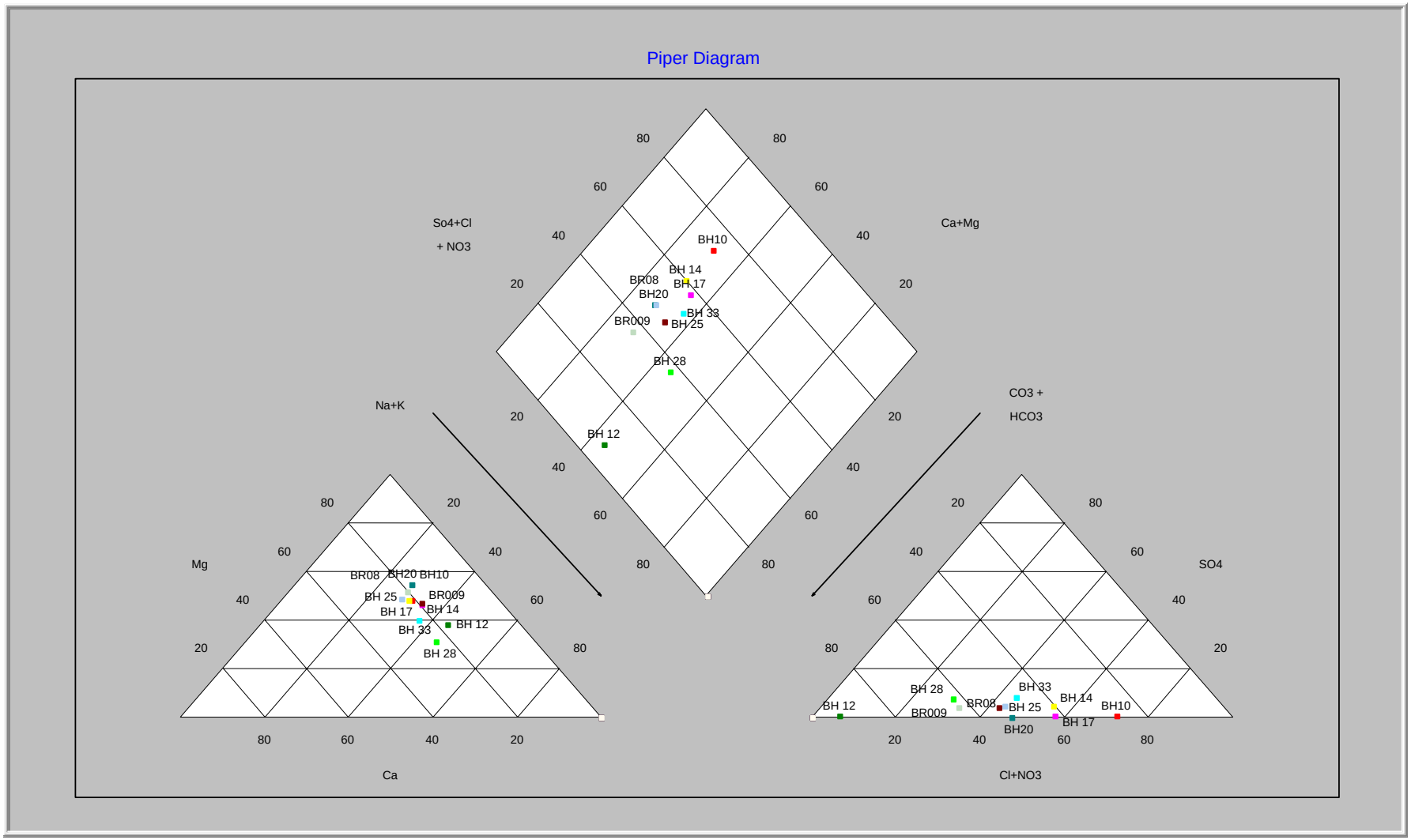

FIGURE 37: Piper diagram of inorganic chemical constituents.

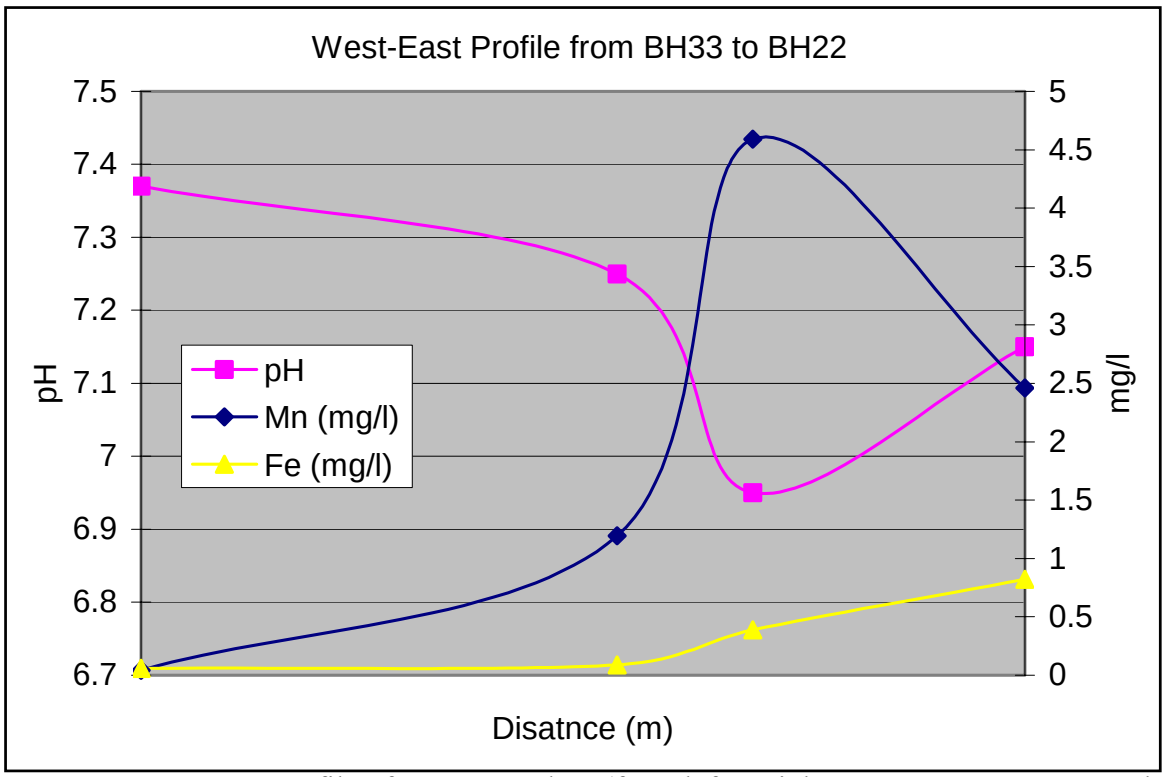

FIGURE 38: West to East profile of pH, Mn and Fe (from left to right BH33, BH12, BH17 and BH22).

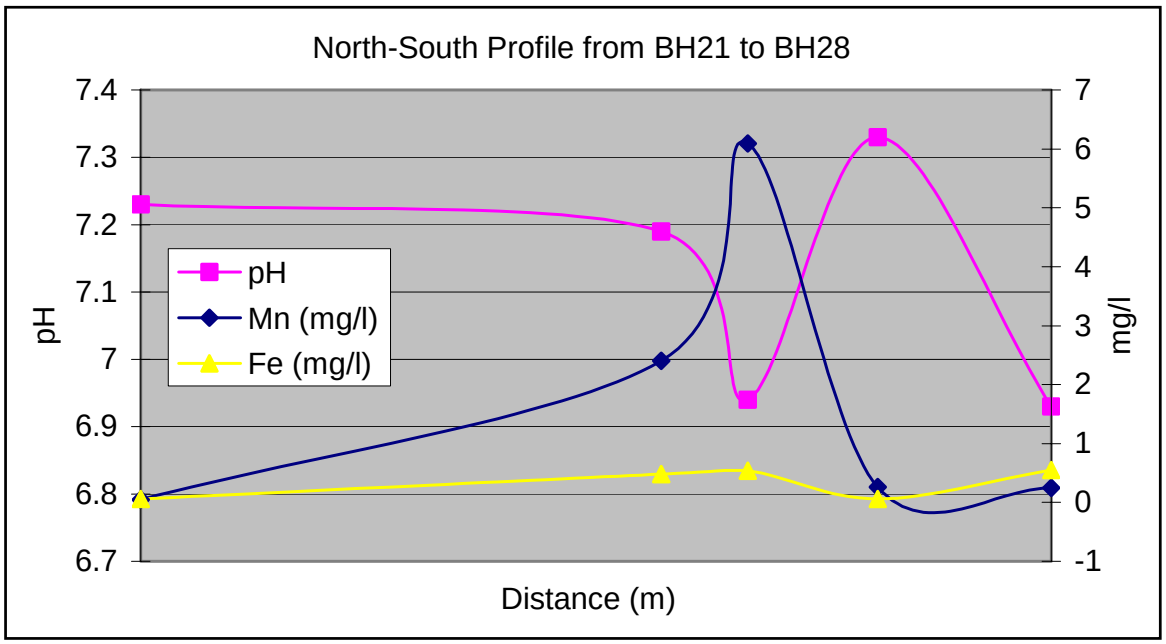

FIGURE 39: North to South profile of pH, Mn and Fe (from left to right BH21, BH13, BH10, BH25 and BH28).

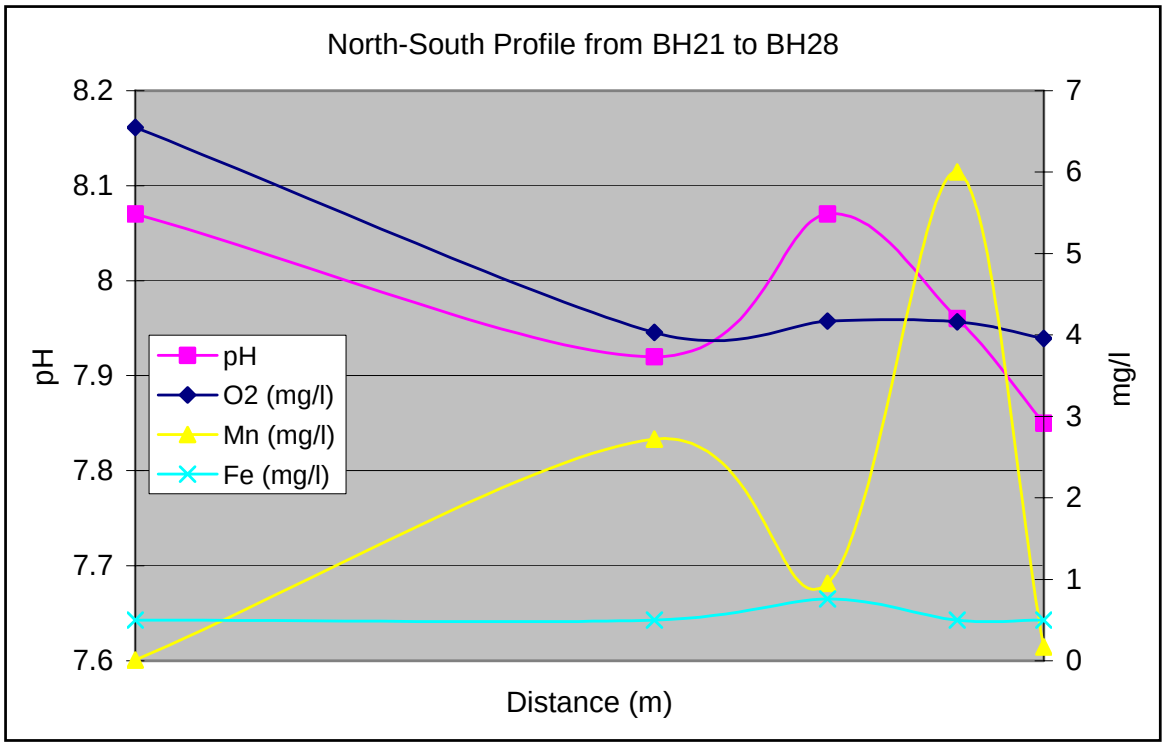

FIGURE 40: North to South profile of pH, O2, Mn and Fe (from left to right BH21, BH13, BH12, BH24 and BH28).

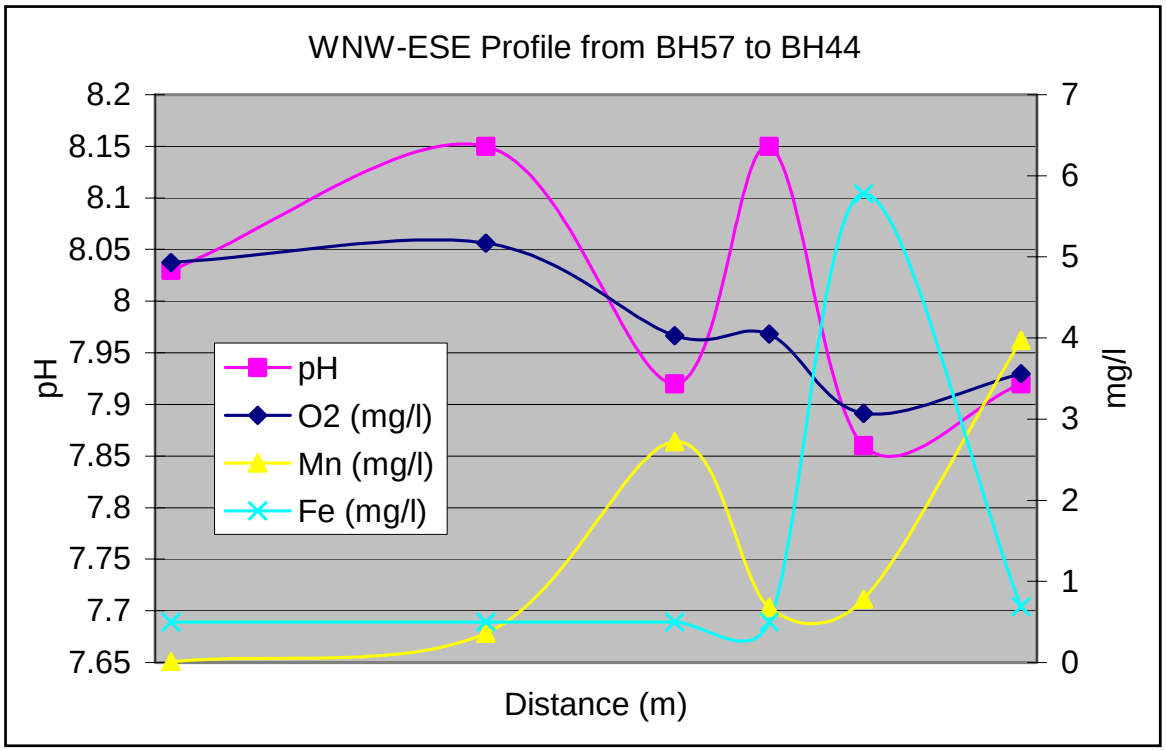

FIGURE 41: West-Northwest to East-Southeast profile of pH, O2, Mn and Fe (from left to right BH57, BH04, BH13, BH20, BH42 and BH44).

The BR boreholes which are at a considerable distance from the pollution plume have a similar inorganic chemical signature (Figures 42 to 45). These boreholes represent background values for the aquifer. Polluted boreholes are either enriched or depleted in cations and anions. Boreholes BH09 and BH10 are enriched in Ca and Mg, while BH28 is depleted in Ca, Mg and HCO_3. The trends of Na versus HCO_3 is similar to that of Ca + Mg versus HCO_3. Boreholes BH09 and BH10 are enriched in Cl by a factor of 2, compared to background values.

Figure 44 indicates BH09, BH10 and BH32 are enriched in chlorine, while BH12 and BH28 are depleted in comparison to the BR boreholes which represent background. Similar trends are observed for Na versus Cl (Figure 45).

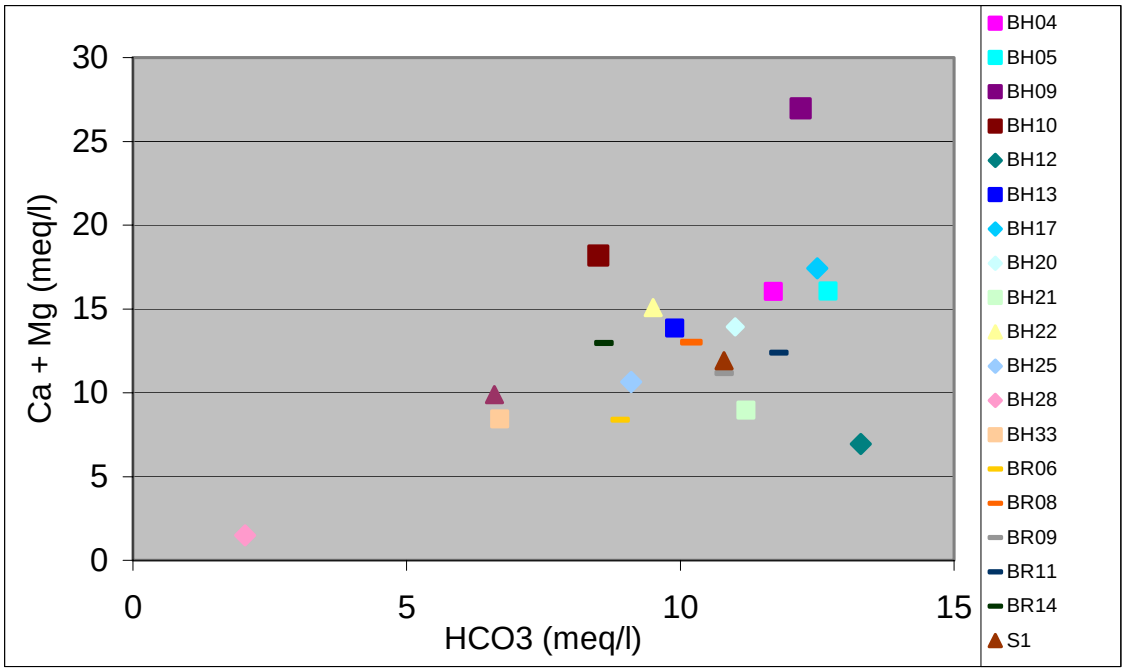

FIGURE 42: Plot of Ca + Mg versus HCO3 in milli equivalents per litre (meq/l).

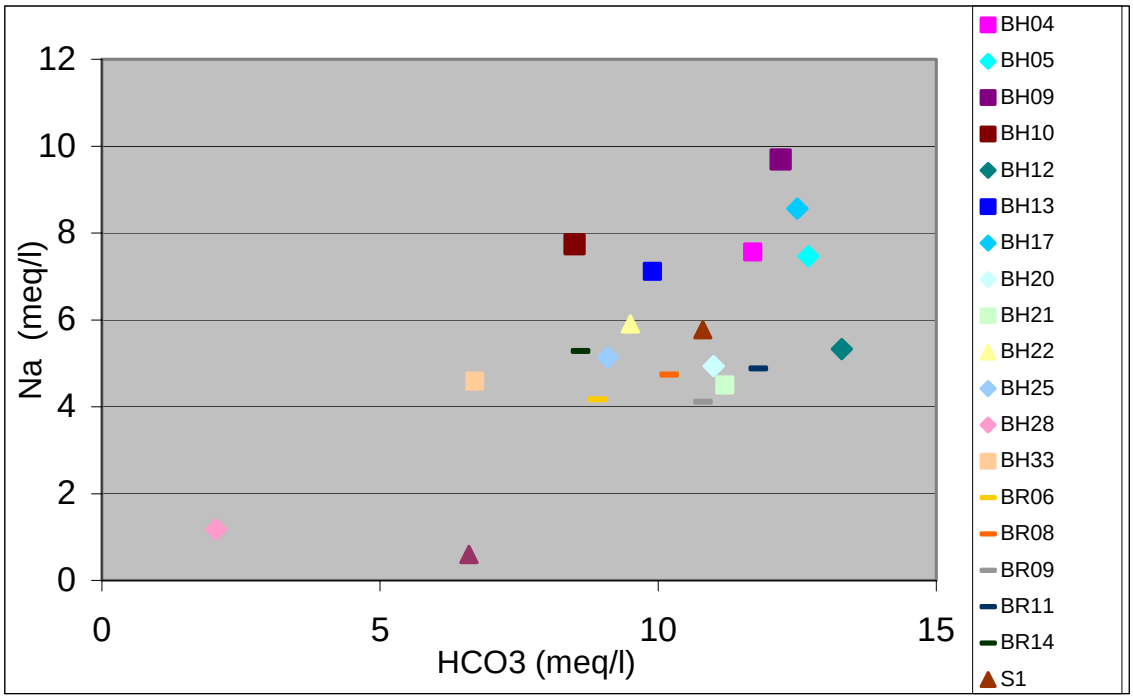

FIGURE 43: Plot of Na versus HCO3 in milli equivalents per litre (meq/l).

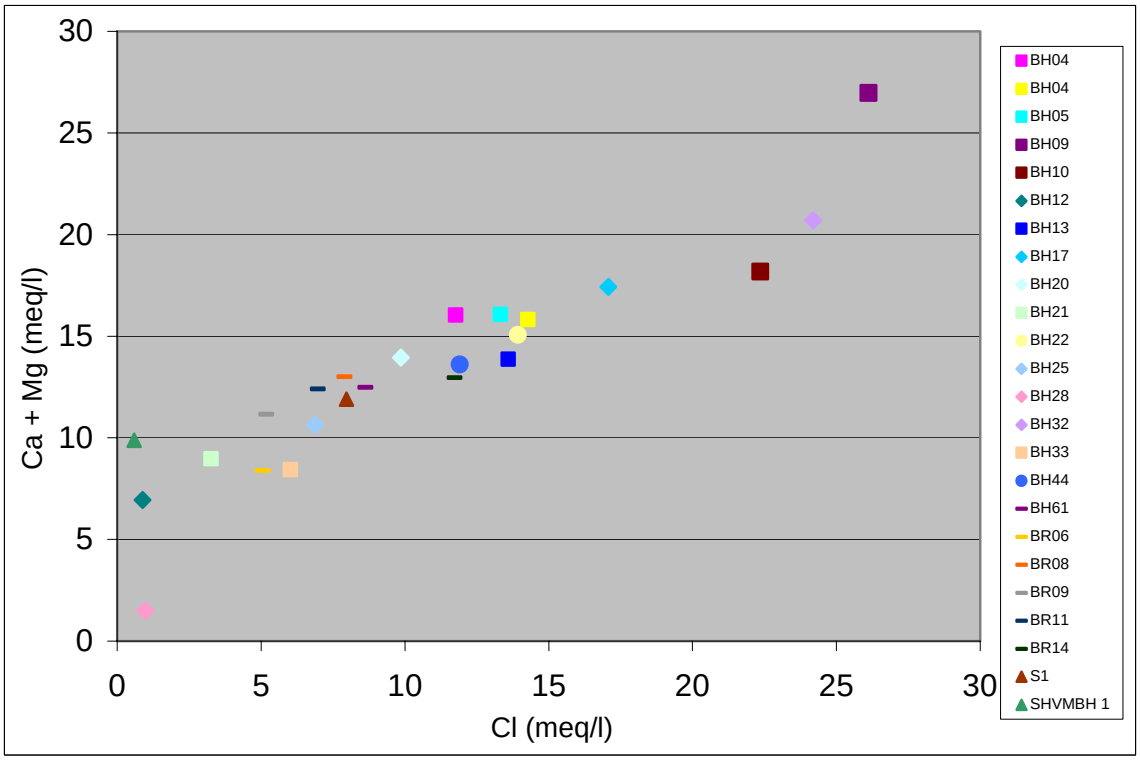

FIGURE 44: Plot of Ca + Mg versus Cl in milli equivalents per litre (meq/l).

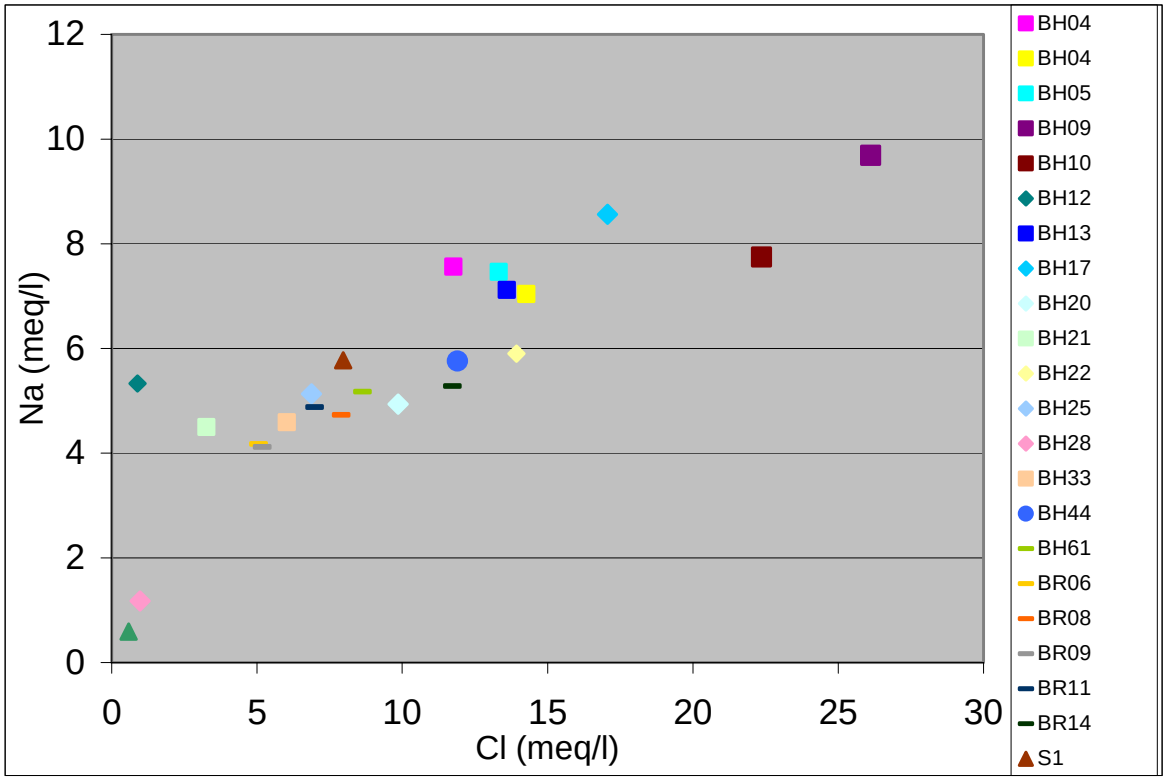

FIGURE 45: Plot of Na versus Cl in milli equivalents per litre (meq/l).

Discussion

The presence of hydrocarbon pollutants have effected the inorganic chemical composition of the ground water. The pH is slightly alkaline for both contaminated and uncontaminated samples. The highest levels of iron and magnesium were present in contaminated samples while the lowest dissolved oxygen levels were also present in these samples. The low levels of oxygen are presumably caused by high concentrations of living organisms in the polluted ground water. The organisms use oxygen in the degradation of organic constituents to form CO_2, water and energy. The environment tends from oxidising to reducing as more oxygen is used. Under aerobic conditions oxygen is used as the electron acceptor, however under anaerobic conditions other elements/compounds are used. At L.T.AFB iron and manganese are presumably under going reduction. The oxidation number of the metal decreases during biodegradation, which renders them more soluble in water; resulting in the high dissolved concentrations.

The unique inorganic chemical composition of BH09 and BH10 suggests that the origin of the water is from an external source, possibly a leaking water pipe at movements 2.

5. Numerical Model

5.1 Introduction

It is imperative to have a computer-generated simulation of the aquifer system and pollutants in order to successfully manage such a rehabilitation project. Such a model can be used as a tool for many applications, however probably the most important of these is to quantify the risk associated with health threatening pollutants reaching water resources presently being utilised. Other almost equally important applications include the implementation of the most effective remedial measures as well as the time frame to achieve water quality goals. The model can be refined as more data is collected with time to increase its accuracy and confidence with the predictions.

5.2 Assumptions and Limitations

The real world system is extremely complication. To develop a ground water model which simulates this system a number of assumptions have to be made. The following conclusions were made to develop this model:

- The aquifer may be represented as a 2-dimensional system due to its large lateral extent in comparison with the vertical extent. Horizontal flow dominates the system.
- No abstraction boreholes were used in the model. Abstraction from boreholes BR06 and BR11 was stopped following the detection of unacceptable levels of pollutants. No abstraction occurred for at least six months prior to the measurement of water levels used to calibrate the model.
- The water levels used to calibrate the model were measured on 15th January 2003. The bailing operation was stopped from the middle of December 2002 until the measurements were taken. The system was assumed to be in equilibrium and therefore in steady state.
- The model simulates saturated single-phase flow; therefore corrected water levels were used to calibrate the model. The effect of free phase on the ground water system was not considered as it constitutes a separate phase.

- Data limitations. The level of confidence in any model is dependent on the available data. This includes both the spatial and time dependant data.
  - Although a high density of observation points are located around the spill site, data on the aerial distribution of both free phase and dissolved phase is limited.
  - The organic chemical data show low levels of contamination outside the free phase plume. The data varies with orders of magnitude between sample events and does not follow trends.
- No recharge calculations were done for the site. The recharge was estimated using the results of a study conducted near the AFB. The value was adjusted during calibration of the steady state model.
- Transport parameters were estimated according to documented values.

5.3 Model Design

5.3.1 Code

The modelling software package GMS4.0 was used for this study for both flow and transport simulations. The Department of Defense Groundwater Modeling System (GMS) was created using interface software developed by the Environmental Modeling Research Laboratory (emrl) of Brigham Young University. The GMS program consists of a number of analysis codes. The following codes were used during this study MODFLOW, MODPATH and MT3DMS.

GMS4.0 utilises MODFLOW2000, which is a cell centred 3D finite difference computer model used for flow calculations. MODPATH is a particle tracking code that runs in conjunction with MODFLOW. MODPATH simulates the route pollutants will follow from a user defined source. MT3DMS is a three-dimensional transport model. It is used to simulate advection, dispersion and chemical reactions in the saturated zone.

5.4 Conceptual Model

5.4.1 Introduction

Conceptual models are developed to describe the present conditions of a ground water system. It is used to make predictions of future behaviour by converting the conceptual model to a dynamic model. A conceptual geohydrological model was created using borehole logs and information contained in reports from previous investigations conducted in the area.

A conceptual model was created using the Map Module in GMS4.0. This is a GIS based module that consists of layers for each aquifer parameter, such as recharge, hydraulic conductivity, etc. Polygons and arcs are created within each layer to form zones where the aquifer properties are similar. Attributes are assigned to each polygon/arc for the various layers to represent the aquifer properties. The map is then converted to a numerical code, which can be read by MODFLOW.

5.4.2 Boundaries and Recharge

5.4.2.1 Regional Boundary

A regional model was initially created to model the ground water system. The boundaries were chosen at hydrological features such as drainage lines and watersheds. However due to the uncertainty of the effect these hydrological features would have on the aquifer, the flat topography as well as limited spatial information, it was assumed reasonable to specify the boundaries as constant head boundaries. The boundaries were chosen at a distance of more than 3.5km from the leakage site. This was to ensure that the boundary conditions would have a negligible impact on the area of interest, i.e. the spill site (Figure 46).

The regional model was converted to a local model. Contours of piezometric head elevation from the regional model were used for the local model boundaries. Boundaries were assigned constant head boundary conditions (Figure 47).

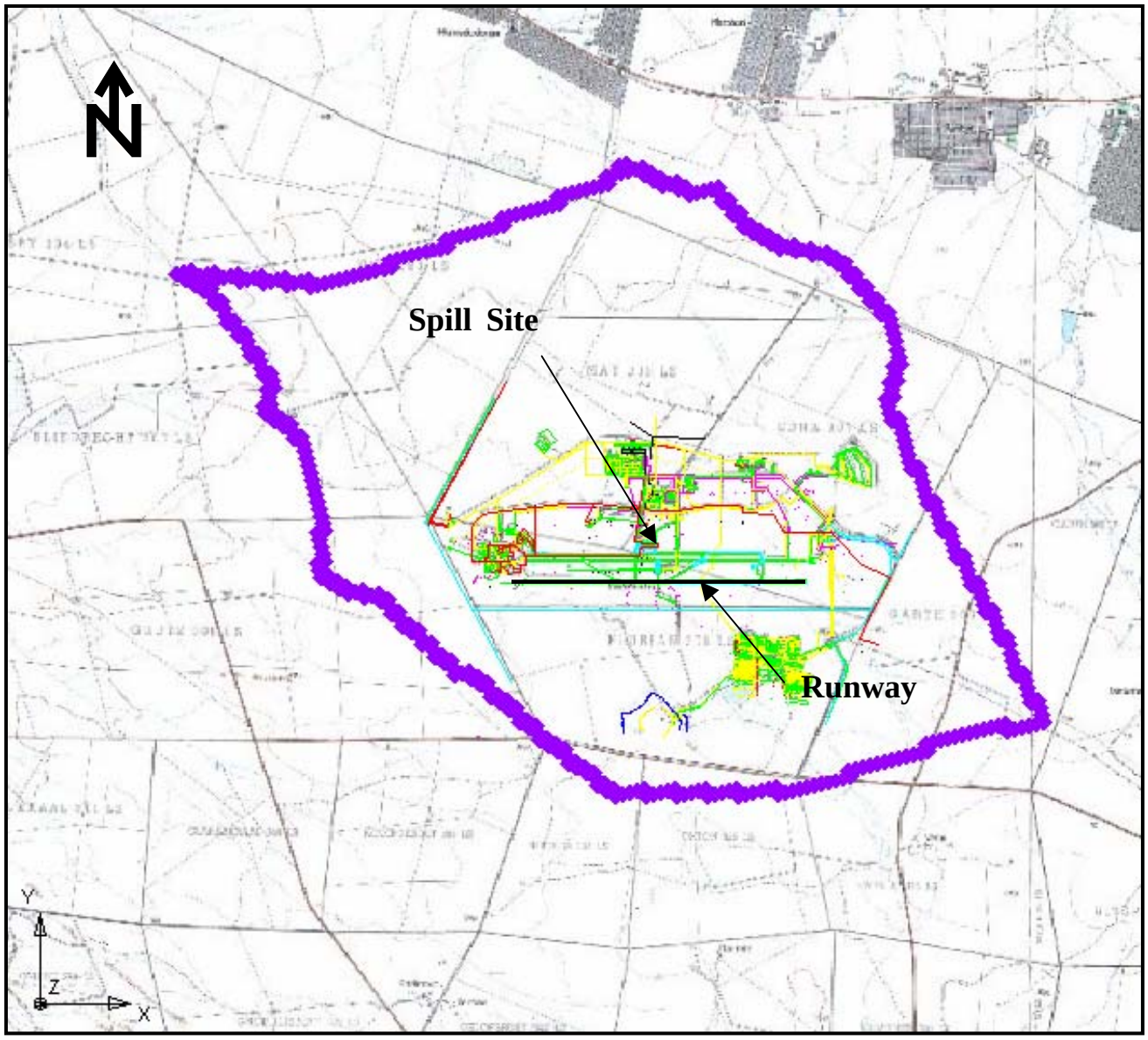

FIGURE 46: Regional model boundary.

5.4.2.2 Local Boundary

The northern and southeastern boundaries are parallel to the regional model contours and have a constant piezometric elevation of 883mamsl and 904mamsl respectively. These boundaries represent equipotential lines and ground water flow is therefore perpendicular to them. The northeastern and southwestern boundaries are perpendicular to the regional piezometric head elevation contours. Ground water flow is therefore parallel to the

boundary as they represent flow lines. Constant head elevations were specified where the boundary intersected a regional ground water elevation contour (equipotential line).

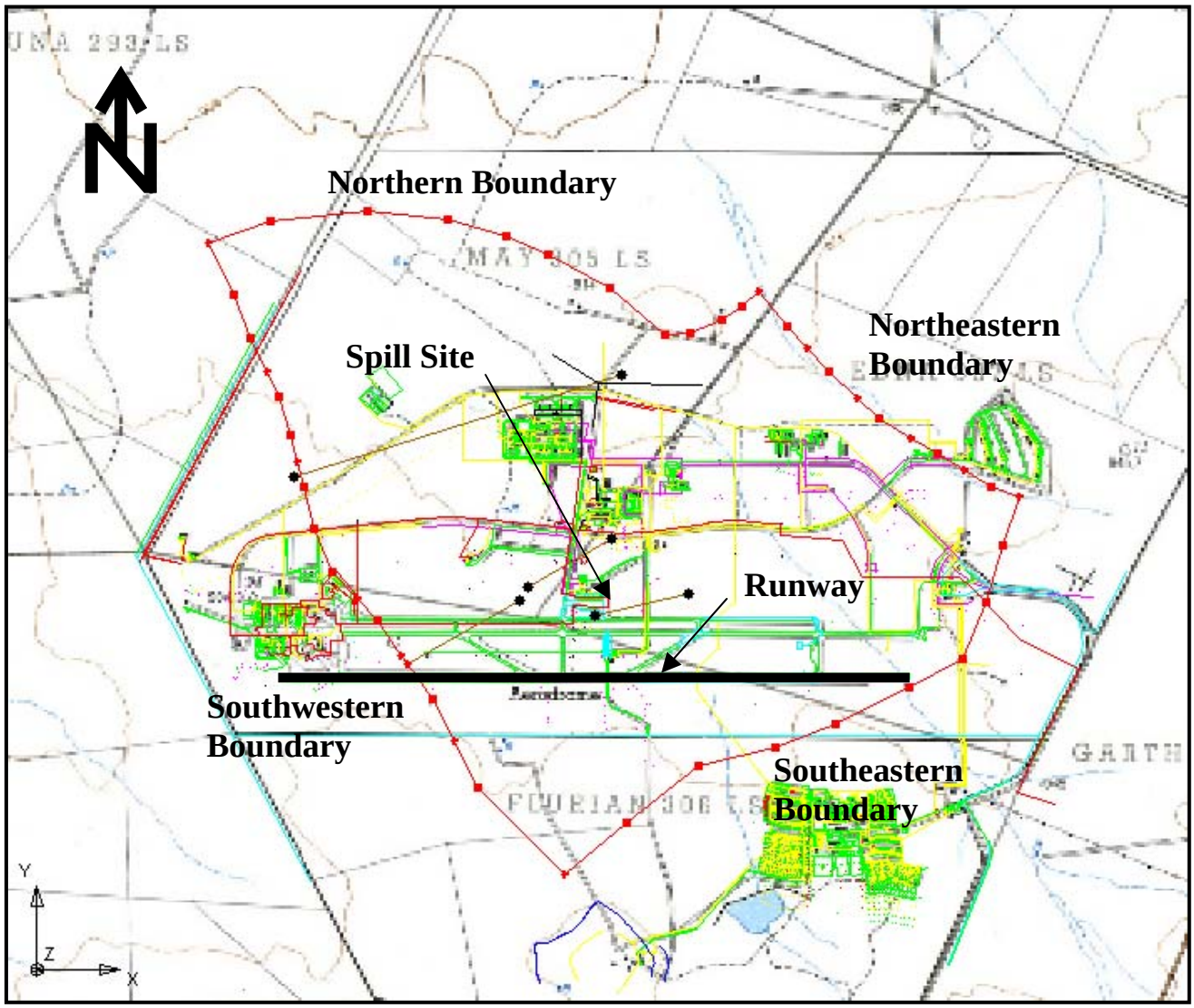

FIGURE 47: Local model boundary.

5.4.2.3 Recharge

The recharge was calibrated using hydraulic conductivity values obtained from slug tests and piezometric levels from observation points. The only available information on recharge was a study conducted 35km south west of the AFB which estimates an annual recharge of 6.78mm/a or 2% of MAP.

When calibrating the model using a value of 2% of MAP for the AFB the calculated values were significantly higher than observed values. The model was run numerous times with different values until a minimum error was obtained. This was achieved by using a value of 1% of MAP.

The two options available for modelling the drainage lines were either as rivers with a low conductance or zones of higher recharge. Both scenarios were considered during the calibration of the model. The best representation of the real system was obtained by modelling the drainage features as zones of higher recharge rather than river cells with a very low conductance. This is due to the intermittent flow nature of the drainage features and lack of flow data for the AFB.

The piezometric levels vary significantly from west to east through the free phase pollution plume. Figure 31 indicates a localised peak in both observed and corrected ground water levels at borehole BH10. Observation boreholes BH10, BH03, BH09, BH27 and BH11 (descending order of magnitude) have the highest piezometric levels in the modelled area. Boreholes BH09, BH10 and BH11 were drilled through asphalt which forms a large impermeable cover around Movements 2. The inorganic chemistry for BH09 and BH10 indicate they are enriched in Ca, Mg and Cl when compared to the BR boreholes, which represent background aquifer values (Figure 44). It therefore seems reasonable to assume that ground water in that area originates from an external source e.g. leaking sub surface water pipe. When recharge values 2 orders of magnitude larger were assigned to that area the model fit increased significantly.

5.4.3 Hydraulic zones

A three layer grid was used to simulate the ground water system. The model was based on the topography and the 3-D grid is illustrated in Figure 48. The grid was rotated to the same orientation as the measured foliation strike. Horizontal anisotropic values of 2 were assigned to cells representing matrix and 1 for cells representing fractures. This is due to the preferential flow direction parallel to the foliation strike obtained during the constant rate

pump test in borehole BH35. The top cells of the grid have a vertical height of 70m while the lower two cell layers both have a vertical height of 20m.

A three layer model was chosen as the aperture of the fractures presumably decreases with depth, however it was not a necessity due to; the vertical variation of hydraulic conductivity has not been determined, the hydraulic zones are sub vertical and the pollutants are LNAPL's. The second layer was assigned hydraulic conductive values an order of magnitude lower than the upper layer and the third layer an order of magnitude lower than the second.

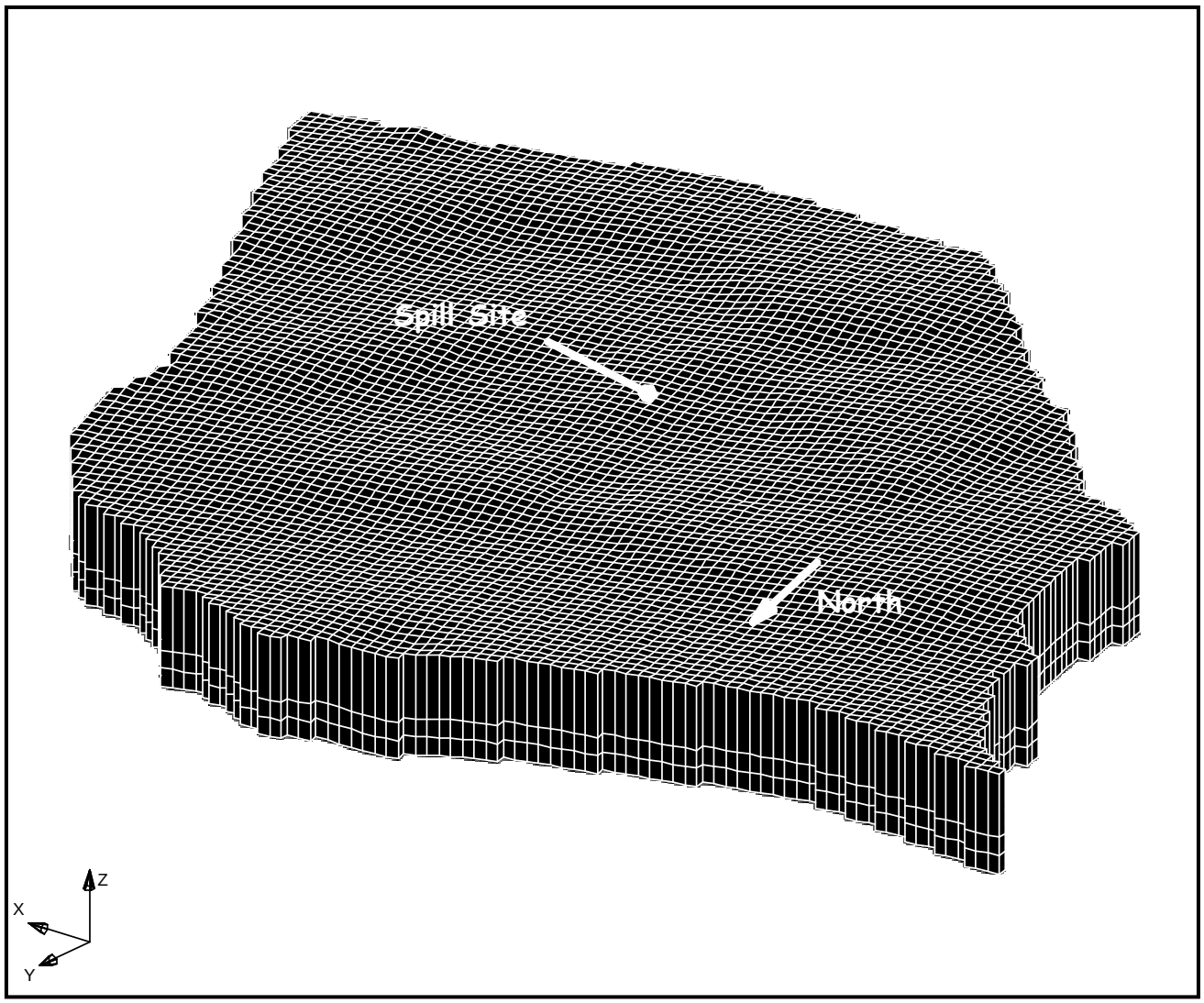

FIGURE 48: Finite difference grid.

Zones with similar hydraulic properties were created based upon the results of geophysical surveys. The slug test results were used as an indication of the hydraulic conductive value for that zone.

The fracture zones (zones with high hydraulic conductivity's) were delineated from the regional and local aeromagnetic survey and the frequency domain electromagnetic survey. Inferred faults and lineaments were only modelled as fractures when high yielding boreholes were located on them or slug test results indicated high hydraulic conductive values. The hydraulic zones used in the model are indicated in Figure 49.

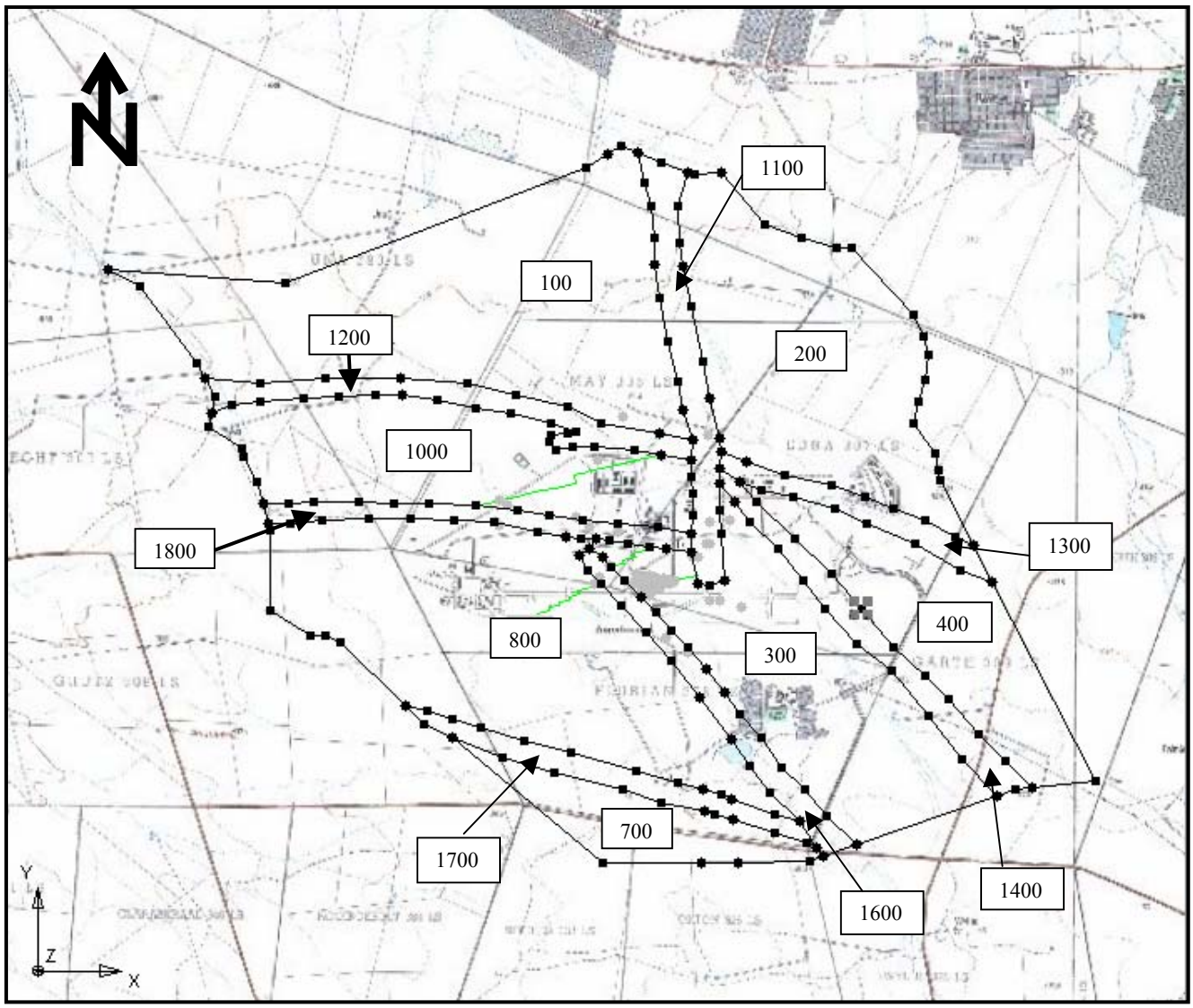

FIGURE 49: Hydraulic zones used to model the aquifer.

Hydraulic zones 1100, 1200, 1300, 1400, 1600 and 1700 were delineated from geological features identified during the Africon Inc. (1999) investigation (Appendix C). Zone 1700 was extrapolated towards the east due to magnetic lineaments identified from the aeromagnetic survey conducted by Stettler *et al* (2002). Zone 1600 was extended in a northwesterly direction to joint the inferred fault that displaced the northern dyke (aeromagnetic interpretation). Slug tests conducted in BH63 and BH64 confirmed higher hydraulic conductive values in this zone. Hydraulic zone 1800 was identified as an inferred fault from the local aeromagnetic survey. Slug tests in boreholes BH52 and BH65 indicated higher hydraulic conductivity values. Table 6 lists the hydraulic conductive values used to model the aquifer as well as values obtained from slug tests in that zone.

TABLE 6: Hydraulic conductivity values specified in the numerical model.

Hydraulic Zone	Slug test results (m/day)			Modelled Value (m/day)
	Min	Max	Average	
100	No observation points			0.001
200	No observation points			0.010
300	0.001	0.045	0.017	0.011
400	No observation points			0.0012
700	No observation points			0.0036
800	0.062	0.062	0.062	1.000
1000	0.002	0.114	0.033	0.069
1100	0.017	1.200	0.4172	2.620
1200	BR11 (pump test yield - 5l/s)			1.296
1300	No observation points			0.800
1400	No observation points			0.010
1600	0.103	0.803	0.3102	0.100
1700	No observation points			1.250
1800	0.041	0.611	0.239333	0.0412

The most important structural feature in the model is the north-south fracture (zone 1100). The presence of the fracture is confirmed by; a regional aeromagnetic survey conducted by Africon Inc. (1999), three EM34 traverses and boreholes with higher yields were drilled on the structure. This structure is responsible for creating a piezometric gradient in an easterly direction. Figure 31 illustrates the piezometric elevation from west to east through the plume.

The steep gradient in piezometric levels to the east is due to a change in hydraulic conductivity. The average hydraulic conductivity obtained from slug tests to the east of the leakage site (phase 4 boreholes) is 0.054m/day in comparison with 0.017m/day for zone 300. A number of cells were selected in this area and the model was run numerous times with different hydraulic conductivity values. A value of 0.069m/day produced the lowest RMSE value. A zone was not created in the map module due to the uncertainty of the extent of the zone of higher hydraulic conductivity.

The diabase dykes intersected by boreholes were unweathered to slightly weathered and no water strikes were encountered within the diabase. The dykes therefore restrict flow across them except where fractured. The location and orientation of dykes were obtained from the local aeromagnetic survey and modelled as flow barriers with a low conductance. The conductance value is given as:

$$C = \frac{k}{t}$$

where: C = conductance
k = hydraulic conductivity
t = thickness of barrier

5.4.4 Model Calibration

The model was calibrated by comparing observed and calculated values of piezometric levels at observation points. Corrected levels were used for calibration as MODFLOW solves the flow equation for single-phase fluids in a saturated media. The suppression of the piezometric surface by free phase therefore cannot be modelled with MODFLOW. PEST was used to estimate the values for the hydraulic zones. The model is calibrated against the Root Mean Square Error (RMSE) between observed and calculated values at 95% confidence. The RMSE is given by the following expression:

$$RMSE = \left(\frac{\Sigma (O_i - P_i)^2}{n} \right)^{-1/2}$$

where P_i is the predicted value and O_i the observed, with the sum divided by n observation points.

Unknown hydraulic parameters were varied until the RMSE reached a minimum value. The comparison between observed and calculated values is illustrated in Figure 50.

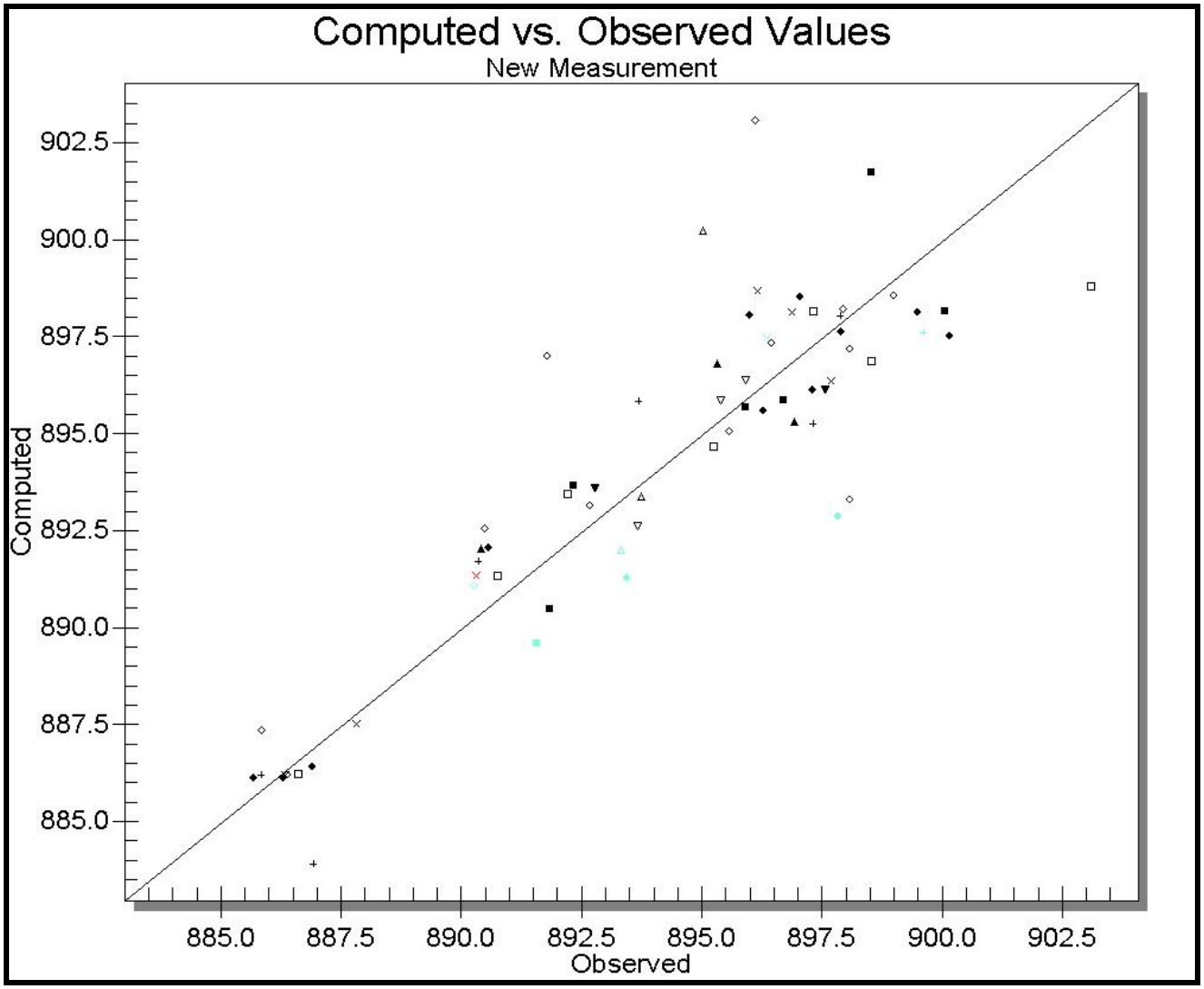

FIGURE 50: Diagram of computed versus observed values.

5.5 Transport Model

High levels of ground water contamination are present in boreholes within the free phase plume. Levels of contamination decrease rapidly beyond the boundary of this plume.

The transport simulation was created to simulate the migration of dissolved contaminants in the saturated zone. Only the dissolved contaminants migrating as a single phase with the ground

water were modelled. The areal extent of free phase was modelled as a constant source of pollution. The aim of the model is to predict the extent of dissolved contaminants with time. The MT3DMS program is utilised by GMS4.0 for the transport simulation.

5.5.1 Transport Mechanism

The transport process of dissolved contaminants can be described by the migration of pollutants as a single phase in the upper saturated zone of the ground water. Mechanisms that were used to simulate the migration of pollutants include advection, dispersion and chemical reactions.

The modified method of characteristics (MMOC) is used in this simulation, as advection is the dominant mechanism of transport. The longitudinal dispersivity was estimated as 10% of the length of the plume and assigned a value of 70. A value of 0.1 was used for the ratio of transverse to longitudinal dispersivity and 0.01 for vertical to longitudinal dispersivity. Sorption was modelled using the linear isotherm method with a 1st order sorption constant of 0.019.

A tracer was used to simulate the direction and extent of pollutant migration. The transport model was not calibrated against observed contamination levels in observation boreholes. This is due to low contaminant concentrations beyond the boundary of the free phase plume. The aerial extent of the free phase plume is modelled as a constant source of pollution. The boundary of the free phase plume between BH44 and BH45 is unknown and estimated.

5.6 Results of Numerical Modelling

A number of scenarios were considered and the model was run for different time periods. The extent of pollution is illustrated in Figures 51 to 54. A number of cells were selected around the spill site and modelled as a constant concentration of pollution. The model was run for 100years to illustrate the movement of pollutants from the spill site. A movie file is inserted on the CD on the cover to illustrate the results.

Scenario 1: Extent of pollution after 10 years.

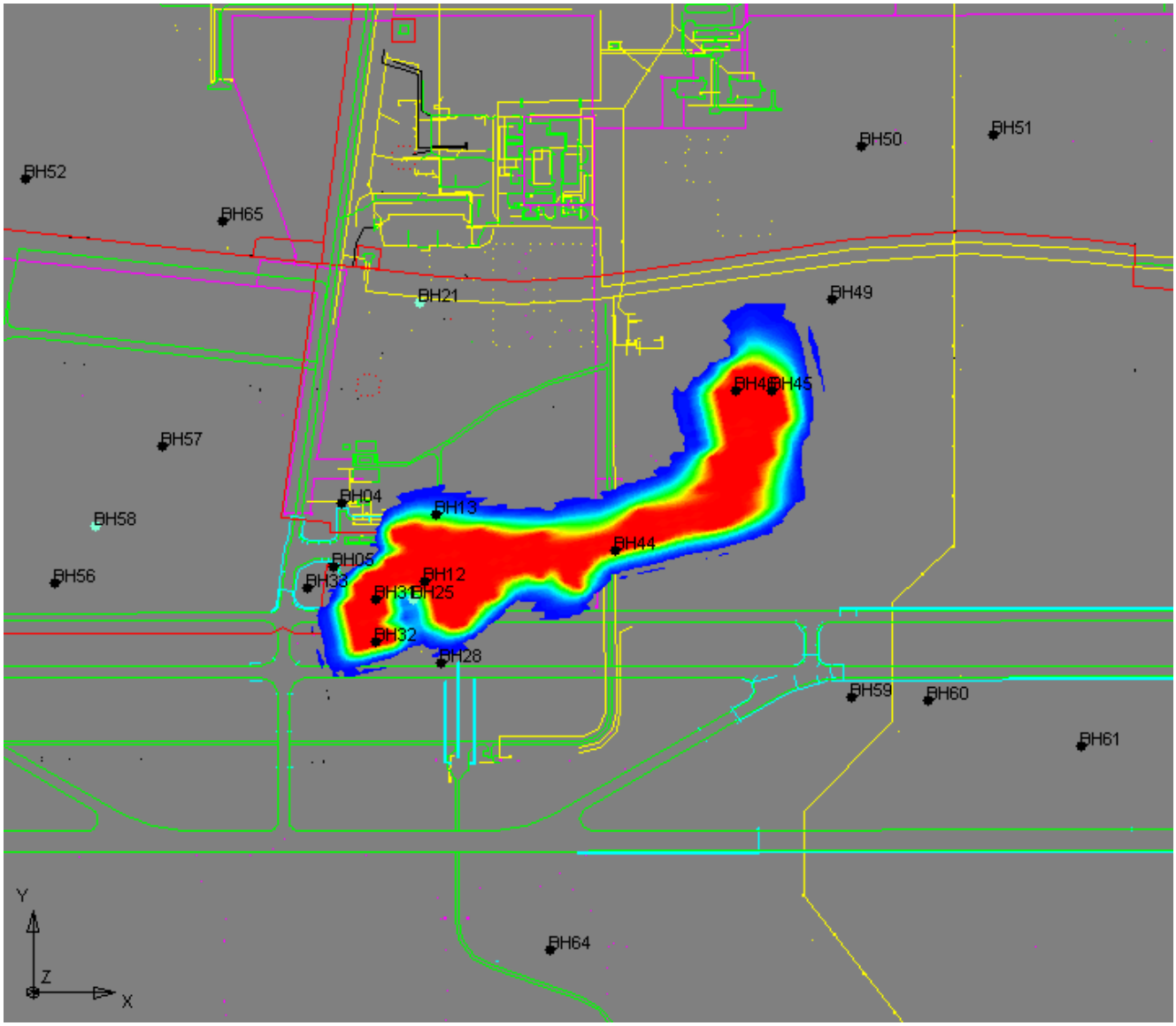

FIGURE 51: Distribution of hydrocarbons after 10 years.

Scenario 2: Extent of pollution after 20 years.

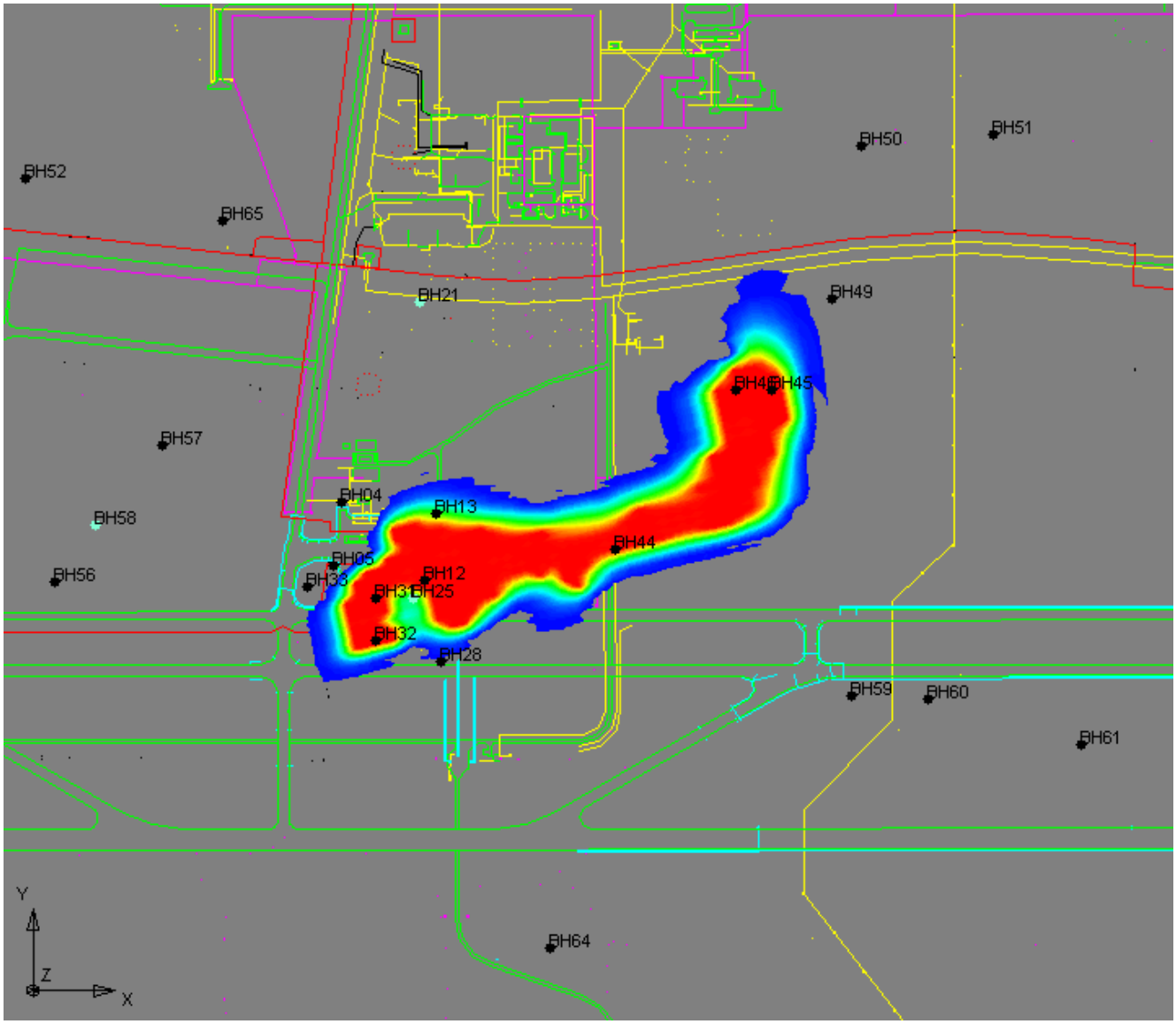

FIGURE 52: Distribution of hydrocarbons after 20 years.

Scenario 3: Extent of pollution after 50 years.

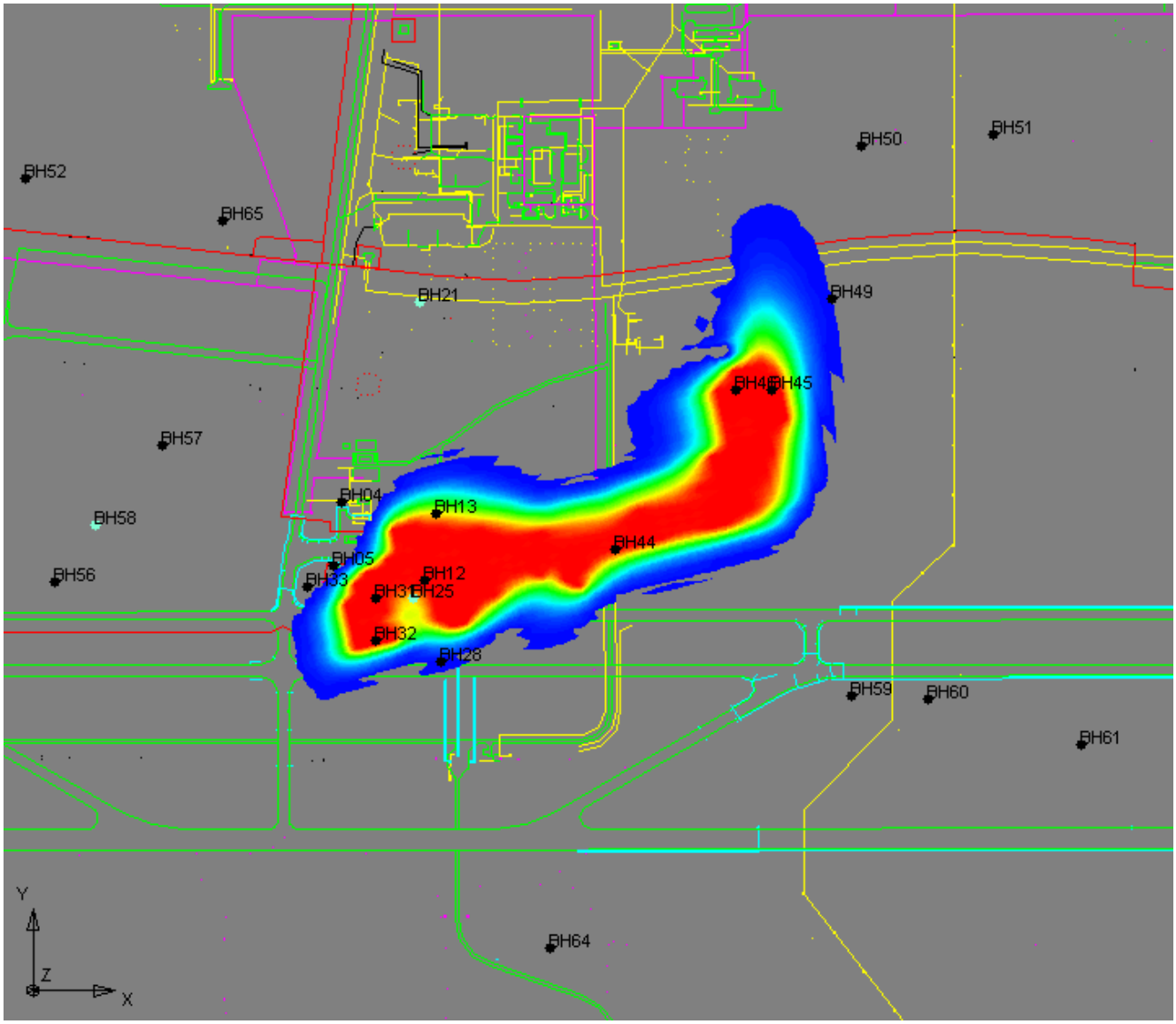

FIGURE 53: Distribution of hydrocarbons after 50 years.

Scenario 4: Extent of pollution after 20 years when simulating abstraction from BR06.

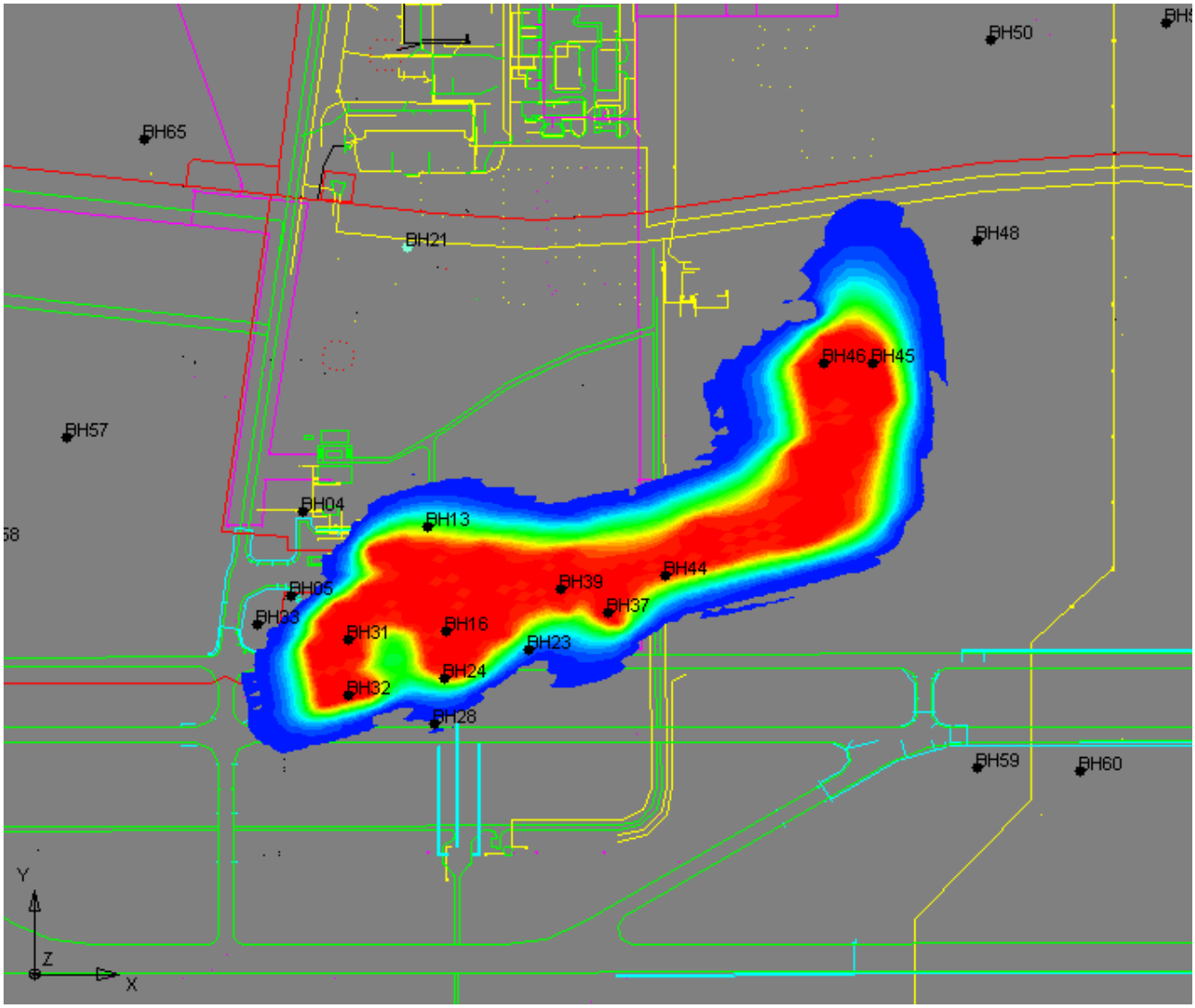

FIGURE 54: Distribution of hydrocarbons after 20 years following abstraction of water from BR06.

5.7 Conclusion

The predicted extent of pollution after 50 years was less than anticipated, however the concentration of dissolved organic pollutants have been monitored for 3 years and indicate limited evidence of migration. The inorganic chemical data indicates that biodegradation of organic constituents is occurring. The pollutants have been in the environment for over a decade during which time the aerial extent of the plume has increased. However this increase results in a larger surface area of pollutants being exposed to biodegradation. With time this will result in an

surface area of pollutants being exposed to biodegradation. With time this will result in an equilibrium developing between the mechanisms spreading and retarding the migration of pollutants. The model suggests that the environment at L.T.AFB is tending towards an equilibrium which quells fears of possible regional ground water contamination.

6. Remediation

6.1 Introduction

A study by Smith (2002) was conducted into the suitability of various remediation options for L.T.AFB. Both in situ and ex situ options were considered. Advantages and disadvantages of the remediation options considered are listed in Appendix H. After evaluating all the available site-specific information and budgetary requirements the most appropriate treatment technology (or a combination of technologies) was selected. Pump-and-treat technology was chosen for the final remediation option. At the time of writing this thesis the pump-and-treat remediation option was accepted by the regulators and was in the design phase. It however had not been implemented due to a delay in available funds. Prior to the installation of the pump-and-treat system the fuel was removed by a bailing procedure as part of an emergency remediation plan. Details of both remediation options are discussed in the following section.

6.2 Emergency Measures

6.2.1 Bailing

A-1 Jet fuel was bailed from a number of boreholes as part of an emergency remediation plan. Only fuel was bailed and bailing was stopped once the water level was reached. The boreholes were bailed daily and left to recover over night and during weekends. Boreholes were only bailed if the apparent free phase thickness recovered to more than 0.5m. The free phase level and water level was measured each day prior to the commencement of bailing.

The fuel was bailed over a period of over two and half years from 30th April 2001 to the present with over 380 000 litres removed from the aquifer. The total volume of fuel bailed from each borehole is indicated in Figure 55. The removal of fuel through bailing has resulted in a reduction of apparent free phase thickness (Figure 56).

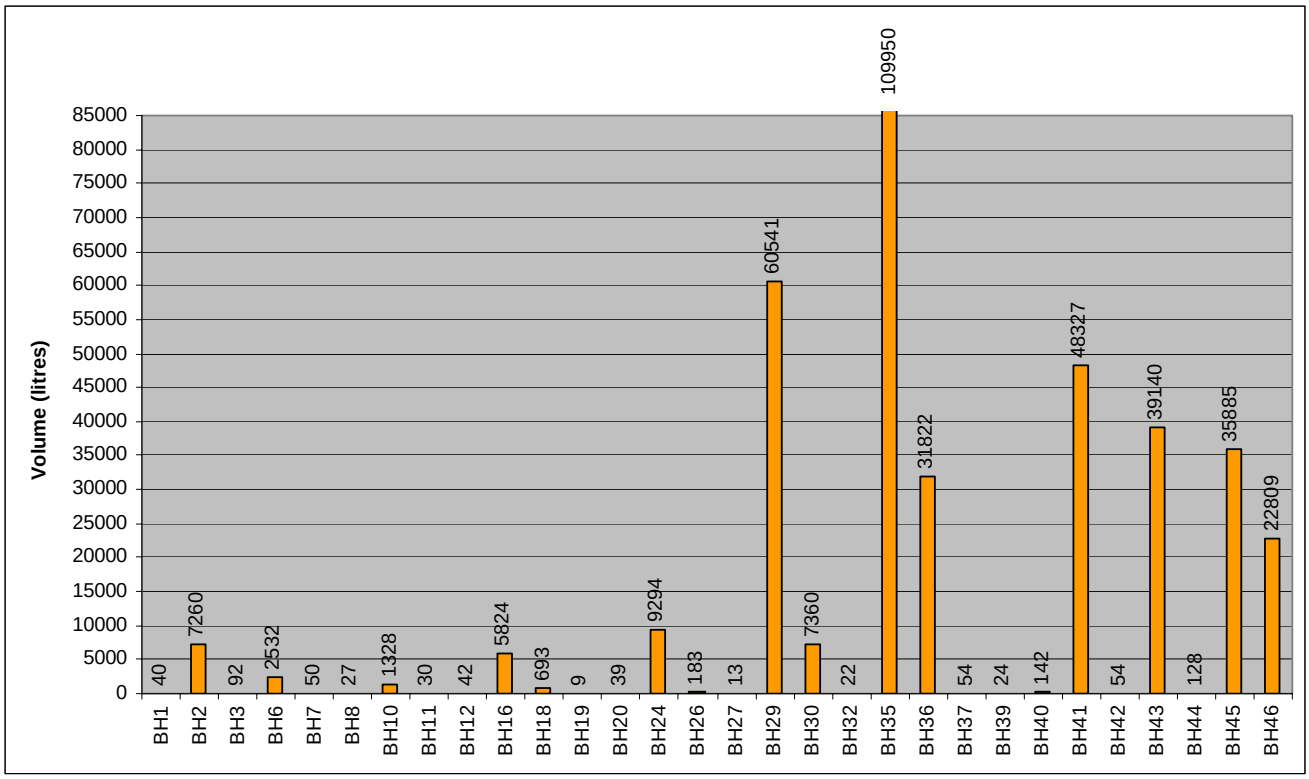

FIGURE 55: Volumes of fuel bailed from 30th April 2001 to 21st November 2003.

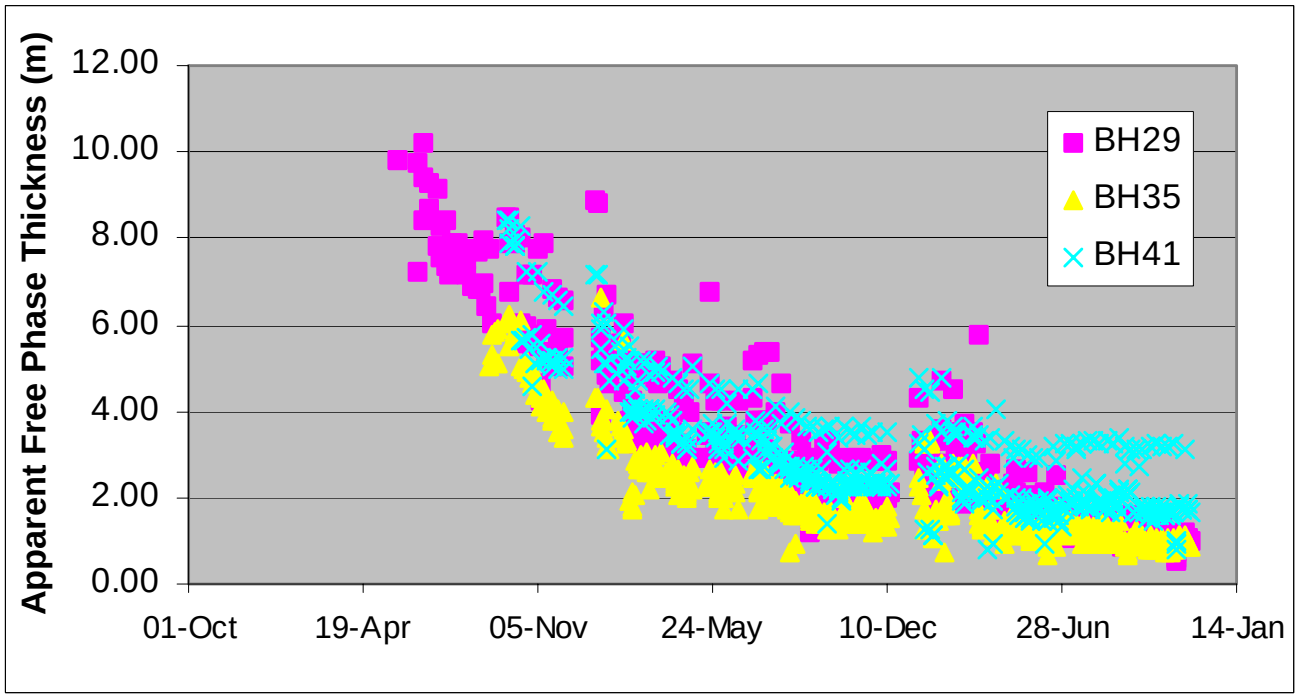

FIGURE 56: Apparent free phase thickness trend (30 April 2001 to 21 November 2003).

6.2.2 Disposition of fuel

The fuel is temporarily stored on the base in 5000 litre containers. It is removed once a week to a timber plant where it is used in a drying kiln. The owner of the plant registered with the Department of Environmental Affairs and Tourism in terms of The Atmospheric Pollution Prevention Act, 1965 (Act 45 of 1965). This is to ensure that the removal and disposal of the fuel does not result in further environmental contamination.

6.3 Pump-and-Treat

The remediation will consist of abstracting both free phase and ground water from selected boreholes. The abstraction points will be located within the free phase plume to create a negative gradient towards the abstraction points thus preventing lateral migration of pollutants. A concern is vertical "smearing" of pollutants due to a cone of depression developing around the abstraction points. This results in residuals sorbed to the aquifer material. When the water level returns to normal - following the discontinuation of pump-and-treat remediation or recharge through precipitation - the sorbed contaminants will become dissolved. This phenomenon is called "rebound".

The polluted water and free phase will be pumped to a separator. The free phase is separated from polluted water and stored in temporary storage tanks from where it will be disposed of in a suitable manner. The contaminated water is pumped from the separator into a reservoir where it is aerated. The remediated water will be used for irrigation purposes in the nature reserve if the water quality meets standards set by the regulators (DWAF & DEAT).

Volatile compounds will be stripped by bubbling air through the contaminated ground water in a reservoir. A forced air blower and a distribution manifold will be designed to ensure maximum air-water contact without the need for any packing materials.

For the designing of an efficient aerator it was necessary to calculate the chemical oxygen demand (COD) and its variation with aeration time. An experiment was conducted to determine the

optimal aeration time with respect to pH, dissolved oxygen, COD, EC, Fe and Mn. The experiment is discussed below.

Experiment:

A representative contaminated water sample was taken from the Air Force Base and kept under anaerobic conditions. The sample was split into 10 smaller samples with a volume of one litre each. All the samples except one were aerated with a normal air pump at a pump rate of 2.8ℓ/min. Every half-hour a sample was removed for up to three hours. There after a sample was removed every hour up to five hours. One sample was left overnight for twelve hours. With the removal of each sample, the dissolved oxygen (DO) content was measured. The DO of the sample not aerated was measured to obtain a value against which the aerated samples could be compared.

The samples were sent to Waterlabs (Pty) Ltd in Pretoria to be tested for chemical oxygen demand (COD), total iron and manganese content, pH and electrical conductivity (EC). The analytical results are included in APPENDIX G.

Discussion of laboratory results

The following comments can be made from the results:

- The pH and the DO of the water in the samples increased with increased aeration times (Figures 57 & 58). The EC decreased with increased aeration time (Figure 59).
- The COD data illustrates (Figure 60) a decrease from 196mg/ℓ to 132mg/ℓ after 30 minutes of aeration. Then the values varied between 124mg/ℓ and 148mg/ℓ after which the values remained constant up to five hours. After 12 hours the COD was measured as 100mg/ℓ.
- The experimental data for Fe show an almost negligible constant decrease from 10mg/ℓ to lower values varying between 8.16mg/ℓ and 8.84mg/ℓ (Figure 61). Even the 12-hour sample did not show a marked decrease in Fe concentrations.
- The manganese values also showed an erratic decrease in Mn values from 2.89mg/ℓ to concentrations varying between 1.33 mg/ℓ and 1.78 mg/ℓ (Figure 62). The 12-hour sample did not show a significant decrease in Mn values.

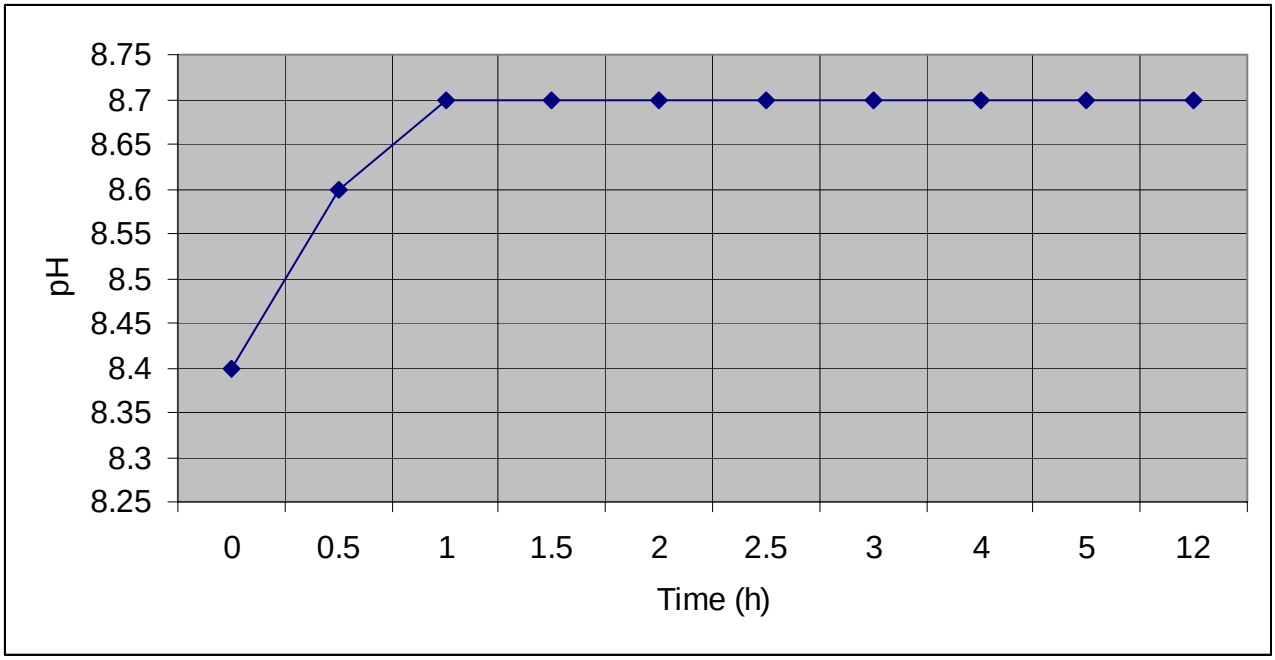

FIGURE 57: pH Variations with Increased Aeration Times.

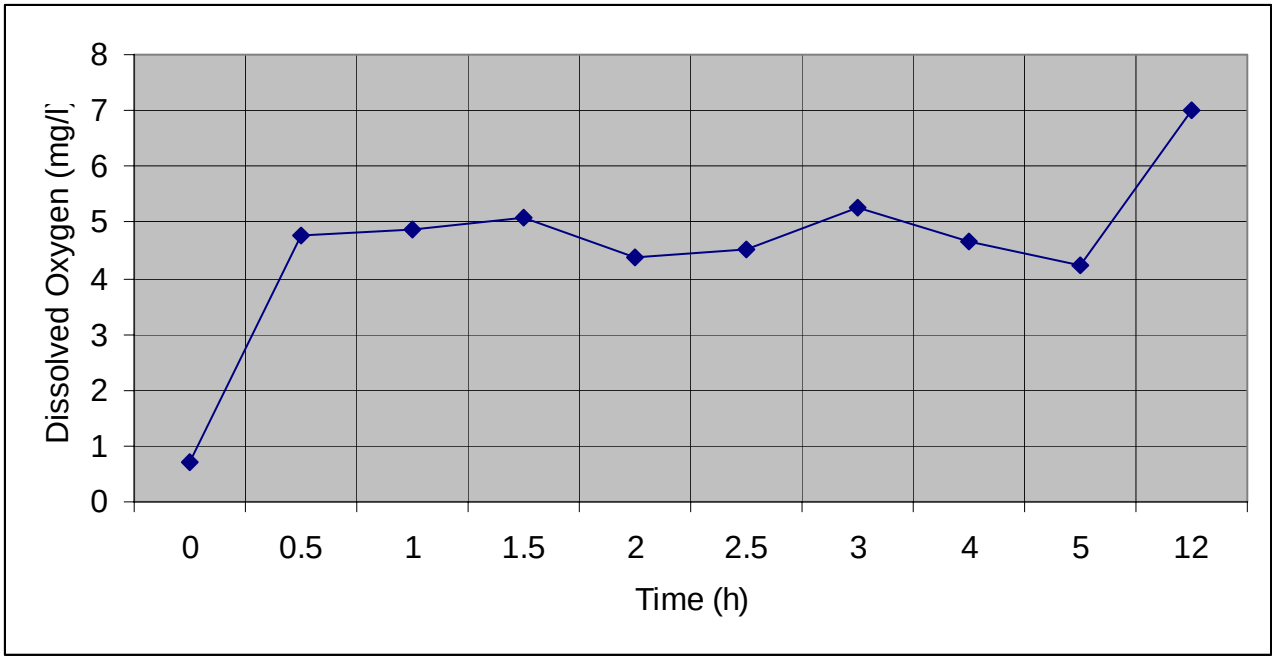

FIGURE 58: DO Variations with Increased Aeration Times.

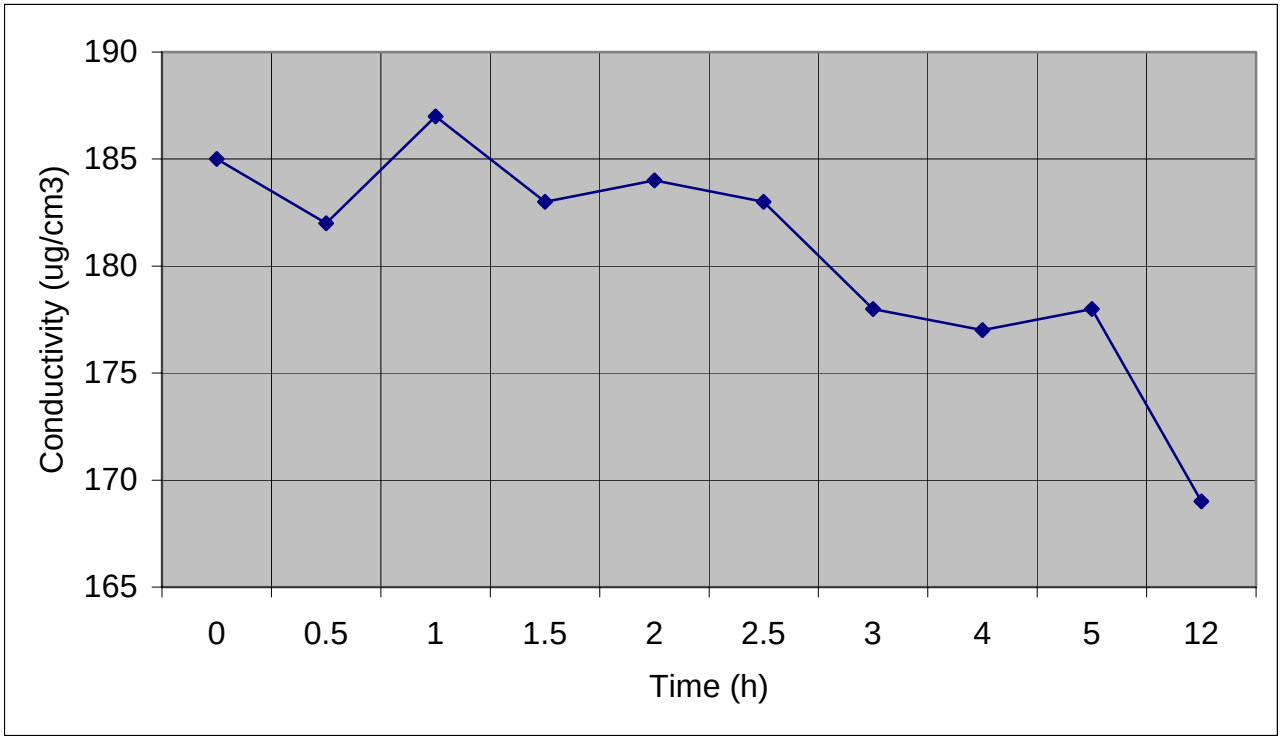

FIGURE 59: Electrical conductivity with Increased Aeration Times

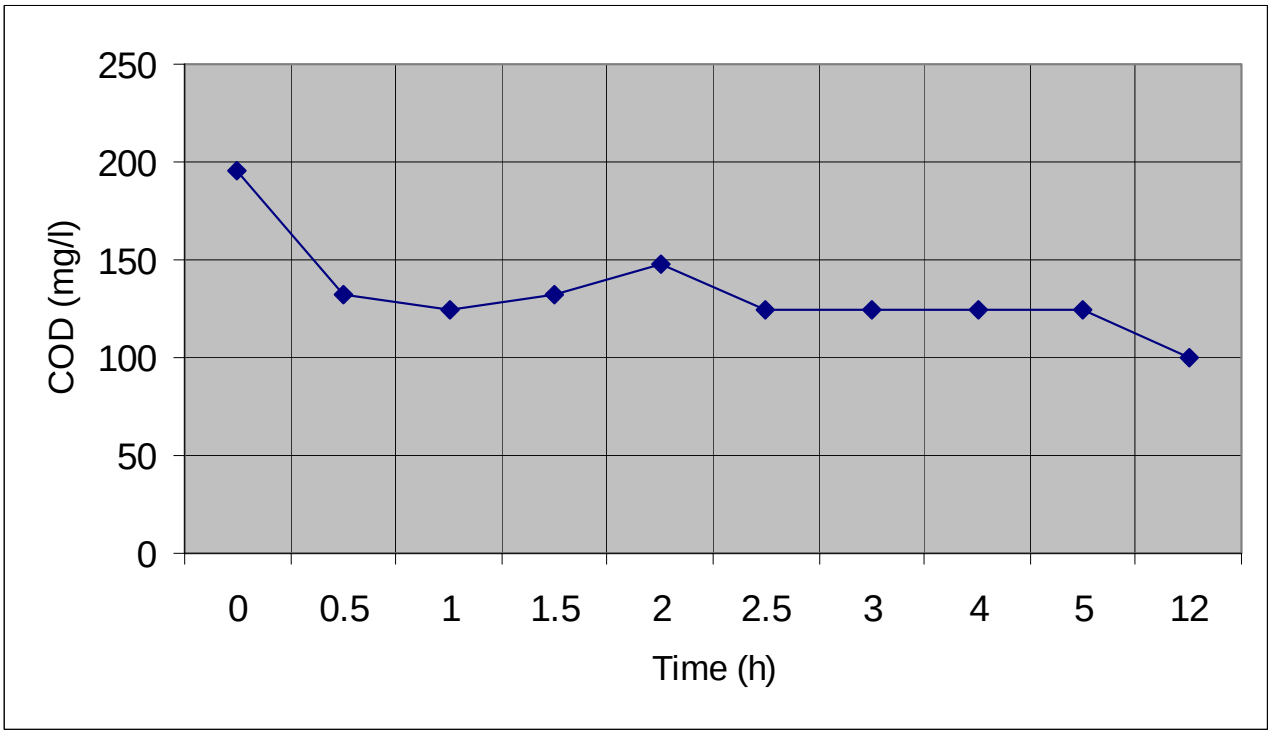

FIGURE 60: COD Variations with Increased Aeration Times

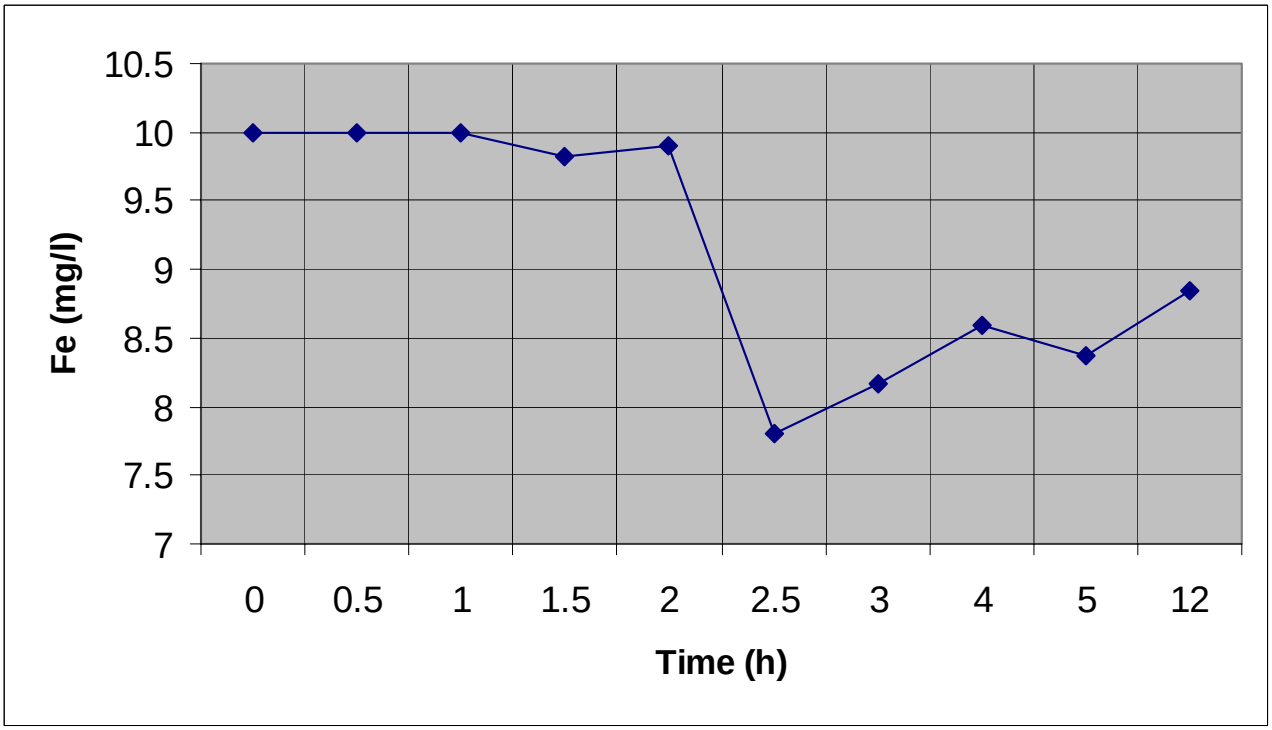

FIGURE 61: Iron Variations with Increased Aeration Times

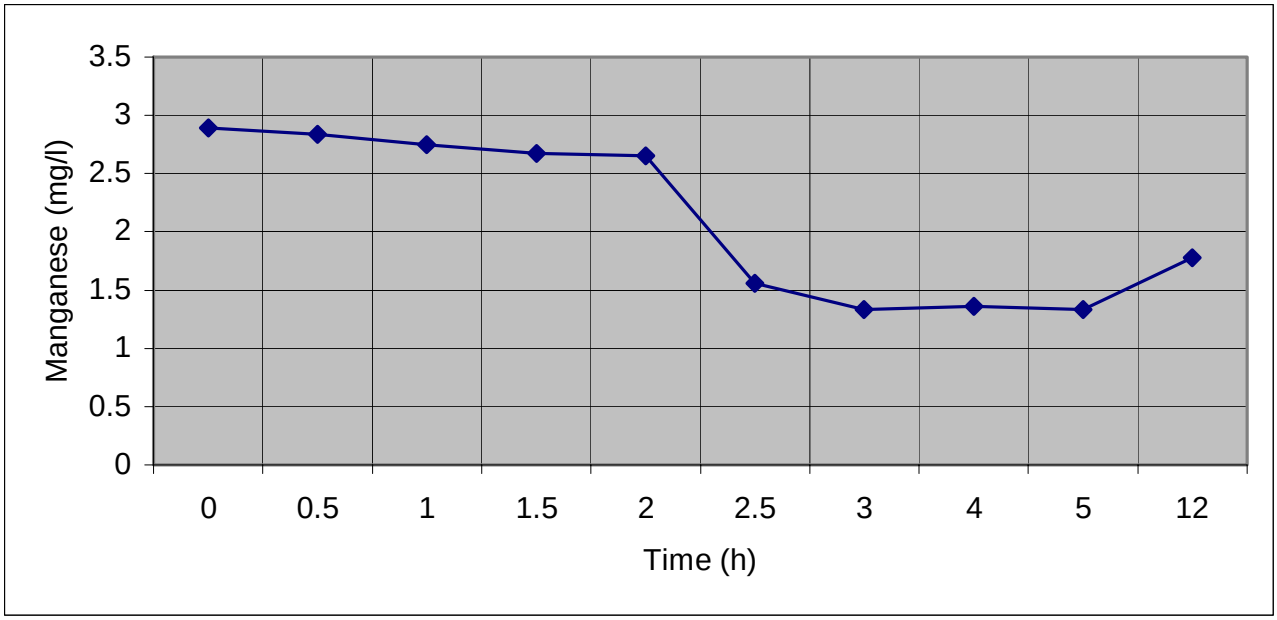

FIGURE 62: Manganese Variations with Increased Aeration Times

Conclusions

- A reduction of the COD showed a marked decrease within the first 30 minutes after which the values decreased very little over a long period of aeration. This indicates that more than 60% of the COD deteriorates within the first 30 minutes. Longer aeration will increase project costs and have a minimal effect.
- Increasing the oxygen content in the aeration process may speed up the COD deterioration but will result in increased aeration costs.

7. Conclusion

The low hydraulic conductivity of the aquifer in the vicinity of the fuel leak restricted the migration of pollutants. The available data indicates that both the dissolved and free phase contaminants are contained within the boundary of the AFB.

The study area comprises a flat undulating topography typical of basement complex lithologies. Due to limited outcrops the subsurface geology was delineated through geophysical surveys and percussion boreholes. The Time Domain and Frequency Domain EM surveys proved extremely useful as well as airborne magnetic surveys.

The local piezometric surface does not follow the topography. This is due to a large north-south structure to the east of the spill site. The structure forms a zone of high hydraulic conductivity and acts as a conduit taking water out of the system. Pump tests indicate an east-northeast preferential flow direction which corresponds with local foliation strike direction and the regional geological structural framework.

The pollutants are LNAPL's and their migration is primarily governed by the piezometric surface. The dominant transport mechanism of dissolved pollutants is through advection. The presence of the north-south structure and the orientation of the foliation has resulted in a local piezometric gradient in an east-northeast direction. The plume majority of pollutants have migrated in a similar direction. The geological control on the aquifer hydraulics that resulted in this is not completely understood and the extent of contamination in an easterly direction is unknown due to limited observation boreholes.

The numerical model is a simplified representation of the aquifer. It however creates a better conceptual understanding of the aquifer system. This is the key to successfully remediating contaminants within an aquifer. The model fits the observed data well considering the variation of piezometric elevation and hydraulic parameters over the modelled area. The model indicates that the plume initially migrates in an easterly direction until it reaches a north-south structure. The pollutants migrate in a northerly direction following the structure.

The model presented in this dissertation should ideally be used to monitor the effectiveness of the short term remediation process and conceptualise the long term aquifer response. The model indicates a limited extent of dissolved pollution resulting from the free phase plume. This is validated by the organic chemical data which indicates low levels of pollution in close proximity to the free phase plume. The inorganic chemistry indicates that organisms are present resulting in biodegradation of organic constituents.

The bailing operation is effective when a large apparent free phase thickness is present. However due to the exponential decrease in apparent free phase thickness with time, this option is impractical due to the time frame and costs involved before suitable water quality goals can be achieved. Pump-and-treat remediation is expected to achieve better results over a shorter time period. A concern is the vertical smearing of contaminants, which may prolong the remediation process. However one of the most important aspects is monitoring the plume through well positioned monitoring points and the analysis of representative water quality samples.

8. References

- 1:250000 Geological Series., 1985. 2328 Pietersburg. Printed by State Printer, Pretoria, 1985.
- Acocks, J.P.H., 1975., Veld Types of South Africa.
- AFRICON Inc., 1999., Bulk Water: The Availability of Ground Water Sources for the Louis Trichardt Air Force Base Report 1 & 2.
- Andersen, N, J, B, Less, C, W., 1992. A structural analysis of the Swartwater area – A technique for improving water borehole siting. Atomic Energy Corporation of SA, report GEA-1027.
- Beekman, H.E, Gieske, A.S.M, Selaolo, E.T., 1996. GRES: Groundwater recharge studies in Botswana 1987-1996. Botswana Jnl. of Earth Sci., Vol. III, pages 1-17.
- Bredenkamp, D.B, Botha, L.J, van Tonder, G.J, van Rensburg, H.J., 1995. Manual on Quantitative Estimation of Groundwater Recharge and Aquifer Storativity. Water Research Commission. Report No. TT73/95.
- Bucknam, P.C., 2000. Jet Fuel A/A-1, www.hess.com/about/msds/JetA 0325 cir.pdf.
- Combrinck, M., 2001. Louis Trichardt Air Force Base, Movements 2 EM34 Geophysical survey (unpubl.).
- Deming, D., 2002. Introduction to Hydrogeology. McGraw-Hill Companies, New York.
- Dippenaar, M.A., 2002. Determination of Actual Free Phase Product Thicknesses through comparison of various techniques at Louis Trichardt Air Force Base, Limpopo. Honours Thesis (unpubl.), University of Pretoria, Pretoria.
- Domenico, P.A, Franklin, W.S., 1990. Physical and Chemical Hydrogeology.
- EPA. 1984. Protecting Ground Water, the Hidden Resource, EPA 1.67/a:W29. United States Environmental Protection Agency.
- EPA. 1996. How to Effectively Recover Free Product at Leaking Underground Storage Sites, EPA 510-R-96-001, September 1996. United States Environmental Protection Agency, Washington, www.epa.gov/swerust1/pubs.
- Fetter, C.W., 1994. Applied Hydrogeology 3rd Edition. Prentice Hall, New Jersey.
- Fetter, C.W., 2001. Applied Hydrogeology 4th Edition. Prentice Hall, New Jersey.
- Hallbauer-Zadorozhnaya, V, Bessonov, A., 2002. The IP effect as indicator of Hydrocarbon Pollution in Ground Water. 16th EM Induction Workshop, Santa Fe, USA, 17th to 22nd June 2002.
- Internet. What is the difference between gasoline, kerosene, diesel etc.? http://auto.howstuffworks.com/question105.htm.

- Maclean, G.L., 1993. Roberts' Birds of Southern Africa 6th edition.
- McBride, D., 1999. Chemicals in Jet Fuel Emissions (Question 8 of August 1998 Work Plan). Washington State Department of Health, Olympia.
- National Water Act, 1998 (Act No. 36 of 1998) as published in the Government Gazette No 19182 (26 August 1998).
- Parsons, R, Conrad, J., 1998. Explanatory Notes for the Aquifer Classification Map of South Africa. Water Research Commission. Report No. KV 116/98.
- Pretorius, S.J, Wiegmans, F.E., 1994. The Establishment of Additional Production Boreholes along the Sand River for the Pietersburg City Council, November 1994. GeoCon in association with VSA Earth Science Consultants.
- Smith, P., 2002. Evaluation and Application of Alternative Cleanup Technologies for the Remediation of a Jet Fuel leak at the Louis Trichardt Air Force Base. Honours Thesis (unpubl.), University of Pretoria, Pretoria.
- Smithers, R.H.N., 1986. Land Mammals of Southern Africa.
- Sole, M.D., 2001. The Remediation up of a Hard Acid Crystalline Rock Aquifer due to a Jet Fuel Leak in the Louis Trichardt AFB. Honours Thesis (unpubl.), University of Pretoria, Pretoria.
- South African Weather Service, cell phone number +27(0)822338484.
- Smit, C.A, Roering, C and Van Reenen, D.D., 1992. The structural framework of the southern margin of the Limpopo Belt, South Africa, *Precambrium Research, 55 (1992)* pages 51-67.
- Spitz, K, Moreno, J,. 1996. A Practical Guide to Groundwater and Solute Transport Modeling.
- Stettler, E.H, Zadorozhnaya, V, Smit, J.P and Cole, J., 2002. Detection of Hydrocarbon Contamination by Analysing the IP effect in TDEM Soundings on Louis Trichardt Airforce Base. (unpubl.).
- Testa, S.M, Winegardner, D.L., 1991. Restoration of Petroleum-Contaminated Aquifers. Lewis Publishers, Florida.
- van Tonder, G, Bardenhagen, I, Riemann, K, van Bosch, J, Dzanga, P and Xu, Y., 2002. Manual on Pumping Test Analysis in Fractured-Rock Aquifers. Water Research Commission. Report No. 1116/1/02.
- VNM & Ass., 2002. Department of Public Works, Louis Trichardt Air Force Base Movements 2. WCS 032647 Fuel Leak Investigation Phase 1 & 2, Dated: 17 September 2002.
- Wilken, P., 1997. Pietersburg/Polokwane Transitional Council. Sand/Blood River Groundwater Development. Water Systems Management.

- Whitehead (Professor), C, S., 2002. Report of Petroleum Pollution at Louis Trichardt Airforce Base, Unpublished.
- Zadorozhnaya, V, Stettler, E.H., (2002 submitted). The detection of hydrocarbon polluted groundwater by using the IP effect in TDEM soundings. S.A. Jnl of Geol.

University of Pretoria etd – Sole, M D (2004)

9. Appendices

APPENDIX A: Half-lifes of Organics found in the ground water at L.T.AFB.

APPENDIX B: Geophysical results (magnetic and frequency domain electromagnetic surveys).

APPENDIX C: Aeromagnetic interpretation and TDEM results.

APPENDIX D: Borehole Logs.

APPENDIX E: Pumptest Results.

APPENDIX F: Comparison between direct field approaches and empirical techniques to determine actual LNAPL thickness.

APPENDIX G: Organic and Inorganic Chemical Results.

APPENDIX H: Advantages and disadvantages of remediation options for L.T.AFB.